5.0 Assessment of Batter Slope Landforms

The relationships developed in the preceding sections were used to determined the parameters implemented by SIBERIA and to approximate the nature of the batter slope. Initial surface profiles are described, with the effect of each additional component assessed individually, and cumulatively against the standard homogenous scenario.

Evaluation of the impact of these soil mechanisms involves 2 methods: visualisation of areas of erosion and deposition, together with difference between simulation time periods using contour maps. Surface landforms are illustrated below and can be considered representative of predictions from the model produced at a grid size of 0.4m with a numerical mapping package. Interpolation between computational grid points has also lead to appearance of erosion 'holes', which were purely an artifact of the modelling simulation process. Contour plots illustrated below are changes that have taken place since the previous time period, and are considered an optimal method for presentation of erosion depths using colour schemes attached to each simulation result.

Initially activity will be concentrated at the top of the batter slope, and over time as the gully develops, the relative sections of erosion and deposition will alter, as the gully extends to the base of the slope.

Erosion is represented as negative numbers on the colour scale, whilst deposition is represented on the positive scale. Areas of deposition can be visualised in the surface landform plots as smoothed areas.

The estimates of differences will highlight aspects observed on site, such as the stabilisation of the gully formation once the gully had initiated, with relatively little activity in the upper sections of the study site.

5.1 Standard

The standard case was run with all of the external erosion modules disabled. This surface is representative of a homogenous material (calibrated to represent the batter slope) and these scenarios were run for equivalent of three hours duration.

At the end of each hour, the average length of storm event, the β_3 parameter was changed to represent the next storm event and the model run again using the last generated surface as the new starting point. Figure 5.1.1 and Figure 5.1.2 give the perspective development of the gully over the monitoring period at 10, 20, 30 and 60 minutes, 1.5, 2, 2.5 and 3 hours respectively. The maximum depth of the gully after 3 hours, at the head of the fully was 5.7m, with deposition between Row G and Row H reaching 0.35m after 1 hour. It is noted that these estimates were obtained using Figure 5.1.3, the contour map of difference between consequent surface profiles.

Significant erosion occurs at the head of the gully, with eroded material from this area deposited at the change of curvature during first hour, whilst deposition between Row H and Row I occurs after 2 and 3 hours. The homogenous nature of the batter slope, combined with the relatively uniform initial surface determine the straight path adopted.

The fixed outlet point is the flume located at the base of the slope, and this can be seen as a boundary condition for the finite difference grid, with transported material surrounding it, at the end of the time period. The material deposited or eroded at each node element within the batter slope catchment influences the drainage direction of nodes, based on altered surface topography. This is apparent as governing equation is directly reliant on the drainage density, as well as the drainage direction and the gully direction changes between 1 and 1.5 hours, as the curvature change is reached, the area of significant deposition.

From Figure 5.1.3 it is apparent that initial activity of the gully on the upper sections of the slope transports considerable amounts of material with the gully developing to between Row F to Row H, within the first storm event. By the end of the first event, the change in direction of the gully is noted in Figure $5.1.3_e$ and Figure $5.1.4_f$. Although maximum erosion occurs at the head of the gully, the section below Row H at 3 hours duration is observed to establish the same nature of erosion as initially observed, with material eroded, deposited in a straight line through Row H and Row I in Figure $5.1.2_d$. This is a reflection of the homogenous nature of the material, and indicates that the investigation into the contribution of the slope component in the sediment transport equation is warranted.

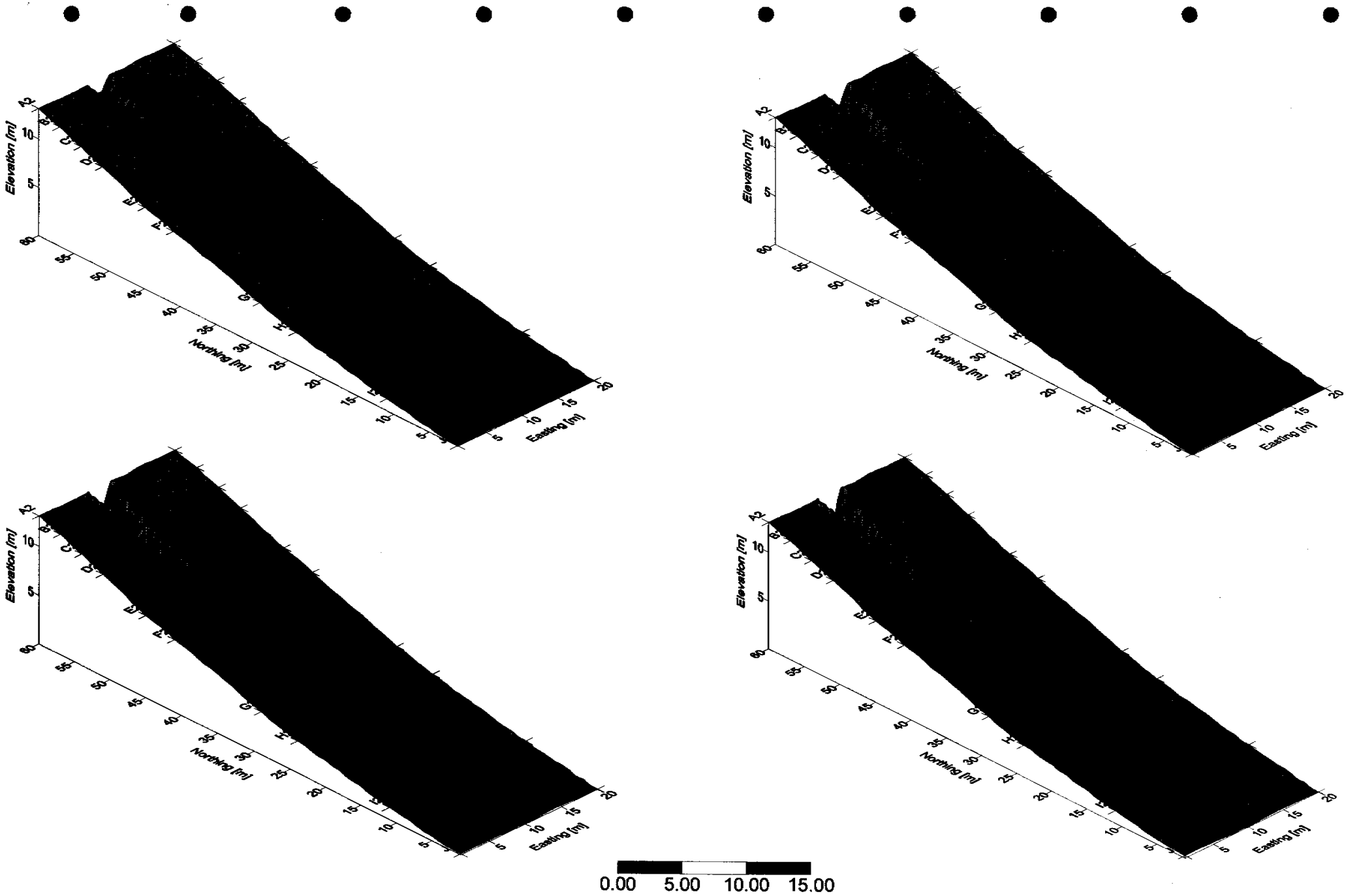

Figure 5.1.1: Simulations for STANDARD scenario at a)10 minutes, b) 20 minutes, c) 30 minutes, and d) 1 hour.

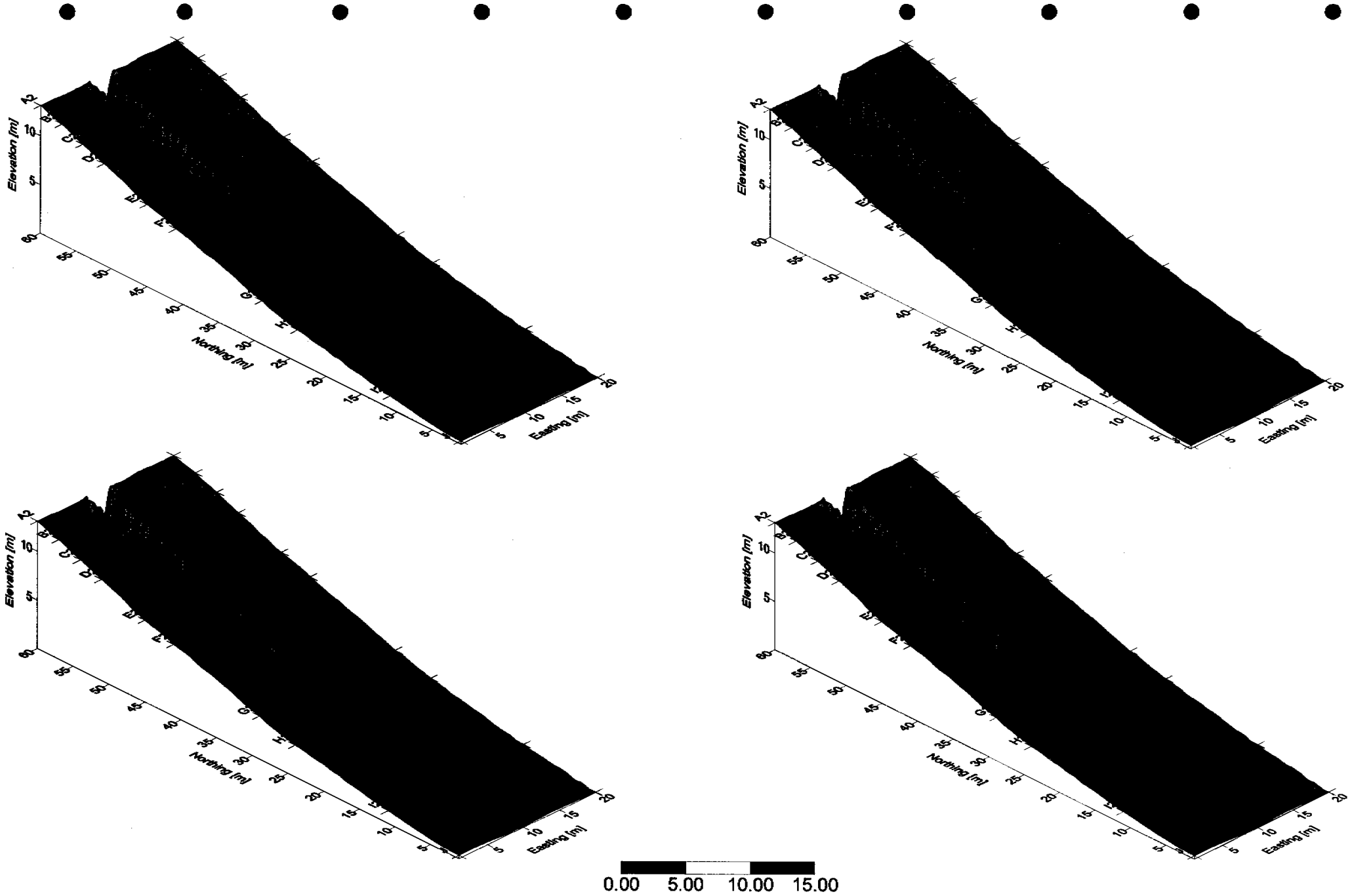

Figure 5.1.2: Simulations for STANDARD scenario at a)1.5 hours, b) 2 hours this represents the second storm event, and c) 2.5 hours and d) 3 hours representing the final storm event.

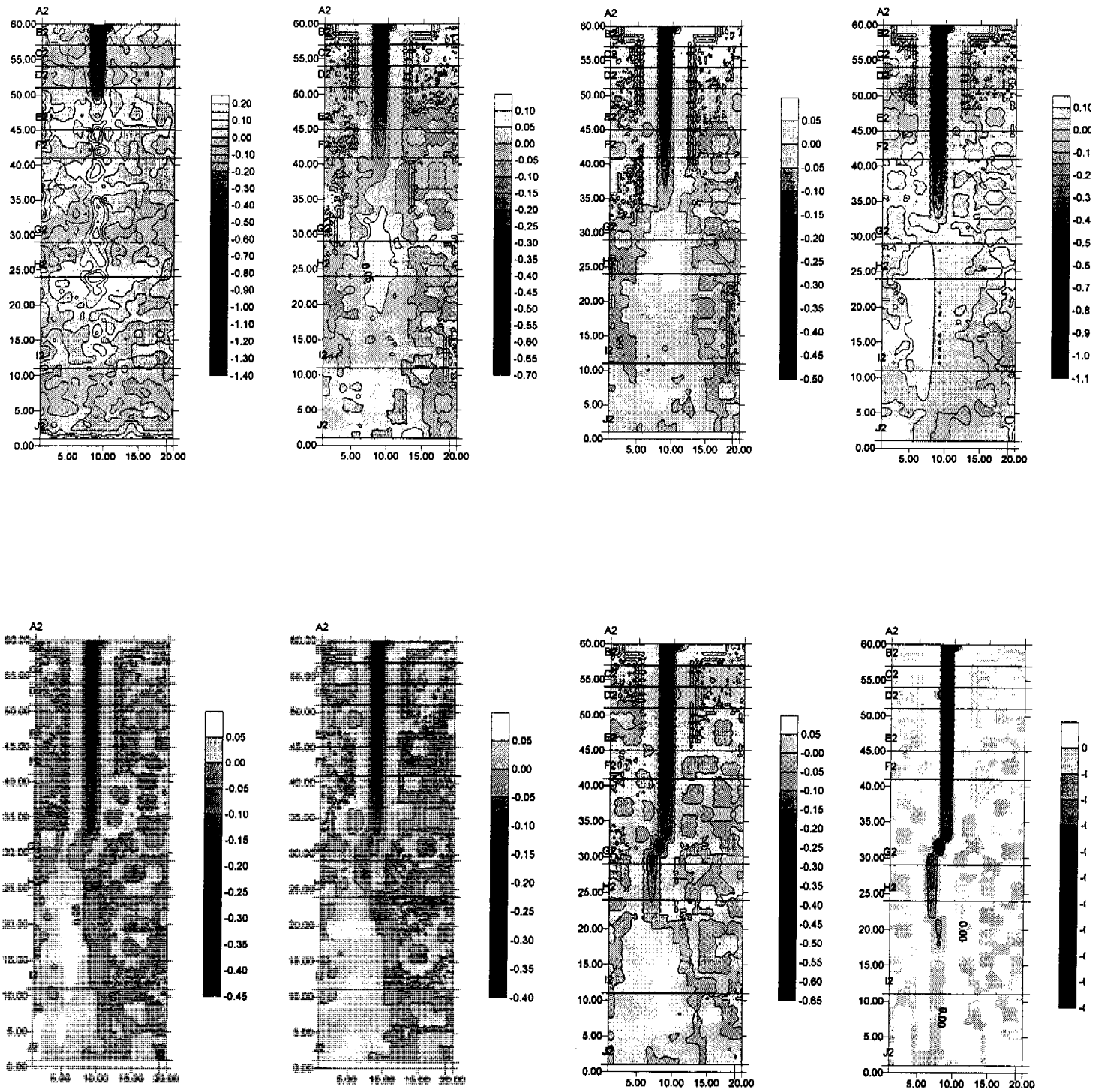

Figure 5.1.3: The initial elevations subtracted from appropriate time period (where erosion is negative, and deposition is positive) such that a) difference between initial surface and prediction at 10 minutes, b) 10 minutes and 20 minutes, c) 20 minutes and 30 minutes, d) 30 minutes and 1 hour. The difference in elevations are also calculated from the remainder of the simulations with e) difference between 1 hours and 1.5 hours, f) 1.5 and 2 hours, g) and 2.5 hours, and h) 2.5 and 3 hours.

The impact of extending the profile of the study area to include a 10m segment of the gully catchment was also investigated. Figure 5.1.4, and Figure 5.1.5 illustrate the simulation surfaces produced by the SIBERIA model for this scenario.

The gully begins to develop after about 30 minutes, with little change occurring at the transition point between the catchment and the batter slope. This point can be identified as Row A between simulations Figure $5.1.4_b$, and Figure $5.1.4_c$. The surface erodes toward the cap site, with a gully also developing onto the batter slope. Final surfaces were expected to resemble those observed in Figure 5.1.1, and Figure 5.1.2, whereas development process was slower, overall characteristics should be similar.

Once the formation reaches the inlet point of the catchment, the depth of this section increases during the remainder of the 3 hours to a maximum depth of 3 to 4 m. Noting that the depth of the gully at the top of the study area (Row A) reaches 3.4m, approximately half the depth of the previous scenario.

At the change in curvature, the path of the gully changes due to the combination between deposited material, and the contribution of the slope component in the sediment transport equation. Also noted in Figure $5.1.4_c$ and Figure $5.1.4_d$ where the path of the gully in the upper section appears to have been dictated by the random perturbations in initial elevations, a function of drainage density due to minimal contribution by slope component.

The behaviour of the gully above this transition point was observed similarly on site, due to the relatively flat nature of the gully catchment (combination of accumulated sediments compacted over time, and the construction of a flat surface initially), and the reservoir at the head of the gully which effectively raised the head of the gully about 30cm.

The initial delay in development observed in these simulations highlights the nature of sediment transport with slope component playing a considerable role. This is highlighted by comparison with previous simulations in Figure 5.1.1 and Figure 5.1.2, where after 60 minutes duration the gully has reached Row E, compared to below Row F, and the final location of the gully was about 5m above that seen for the standard case.

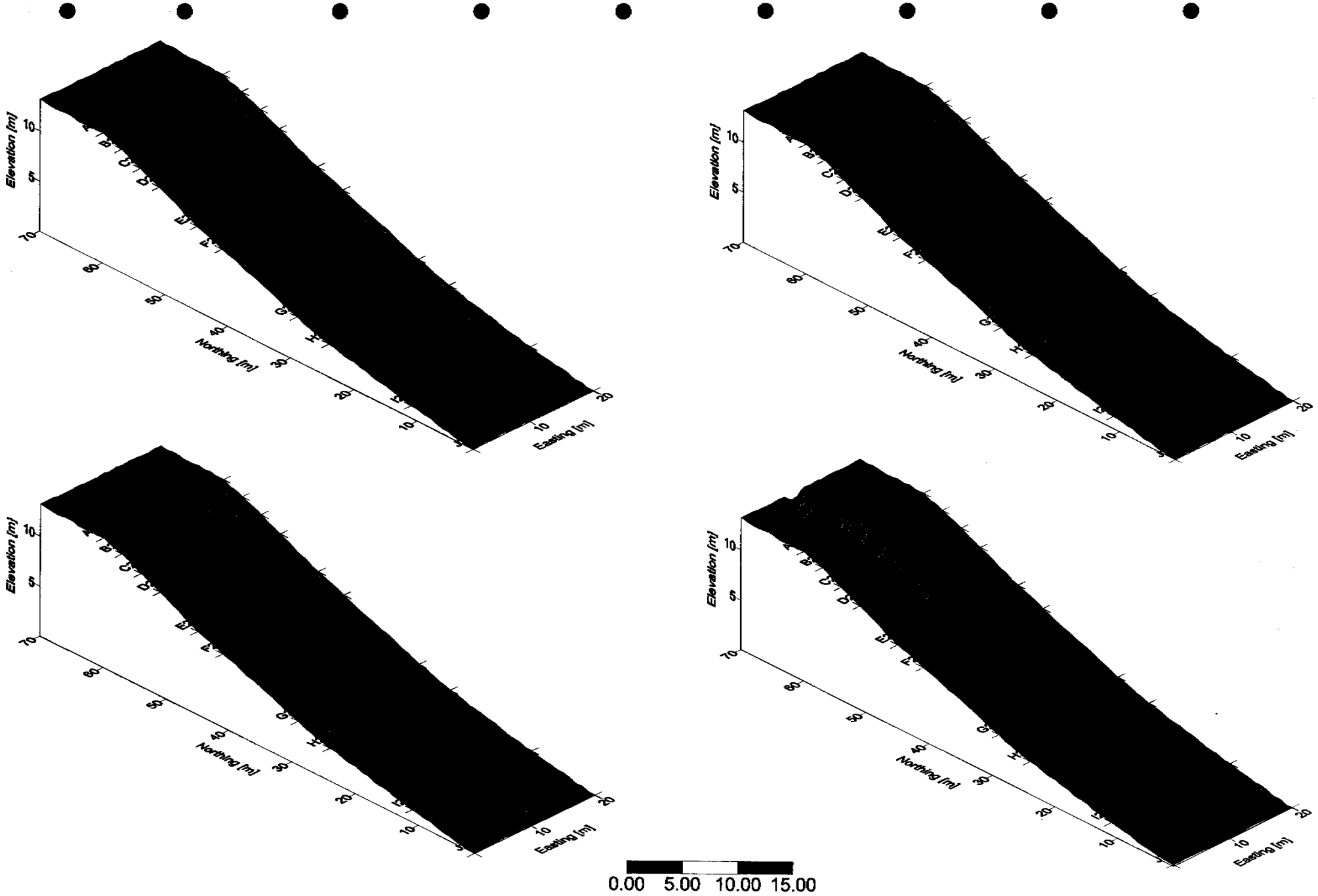

Figure 5.1.4: Simulations for extension of the batter slope to include a portion of the gully catchment, a)10 minutes, b) 20 minutes, c) 30 minutes, and d) 1 hour.

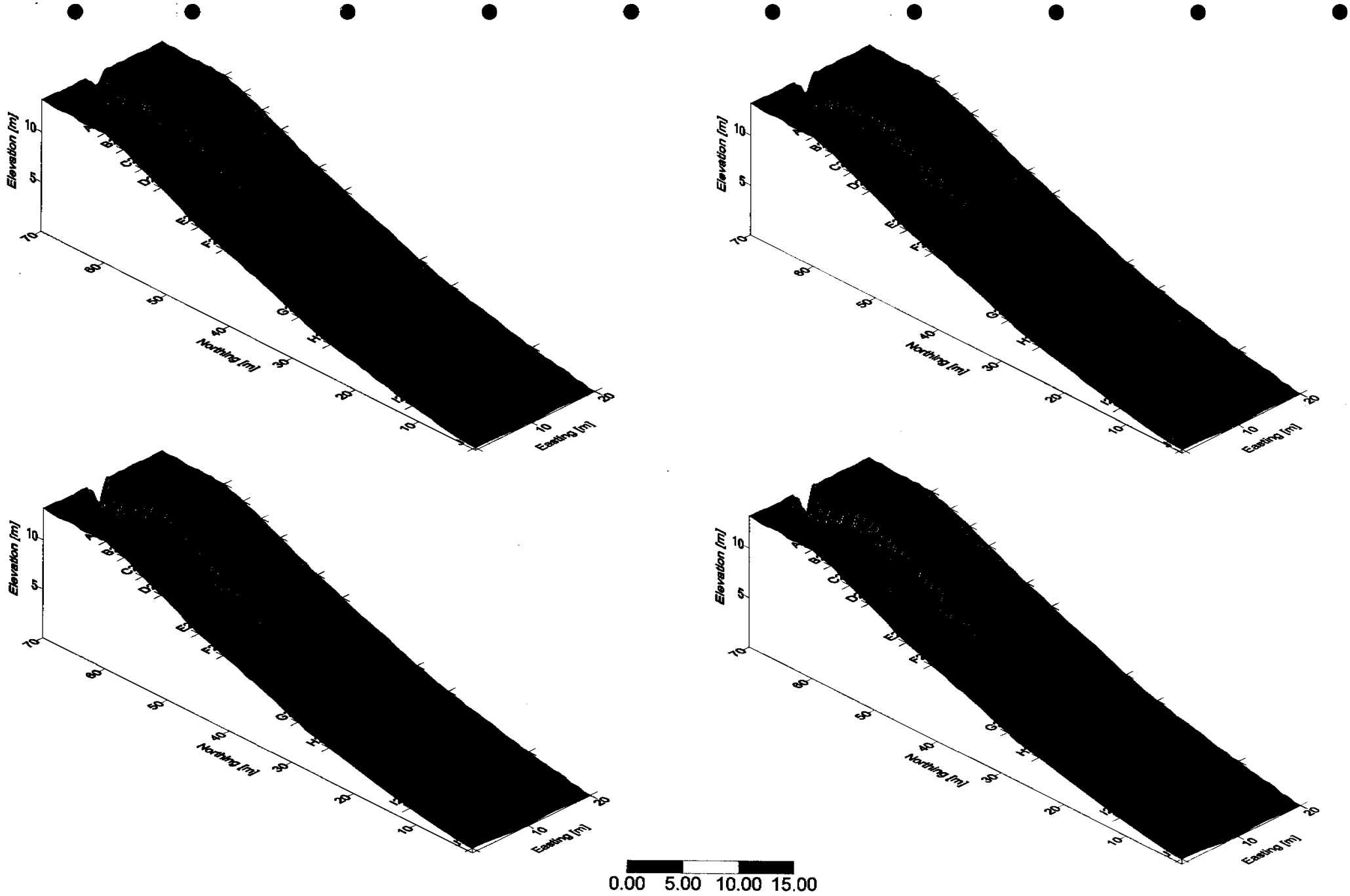

Figure 5.1.5: Simulations for extension of the batter slope to include a portion of the gully catchment at a)1.5 hours, b) 2 hours this represents the second storm event, and c) 2.5 hours and d) 3 hours representing the final storm event.

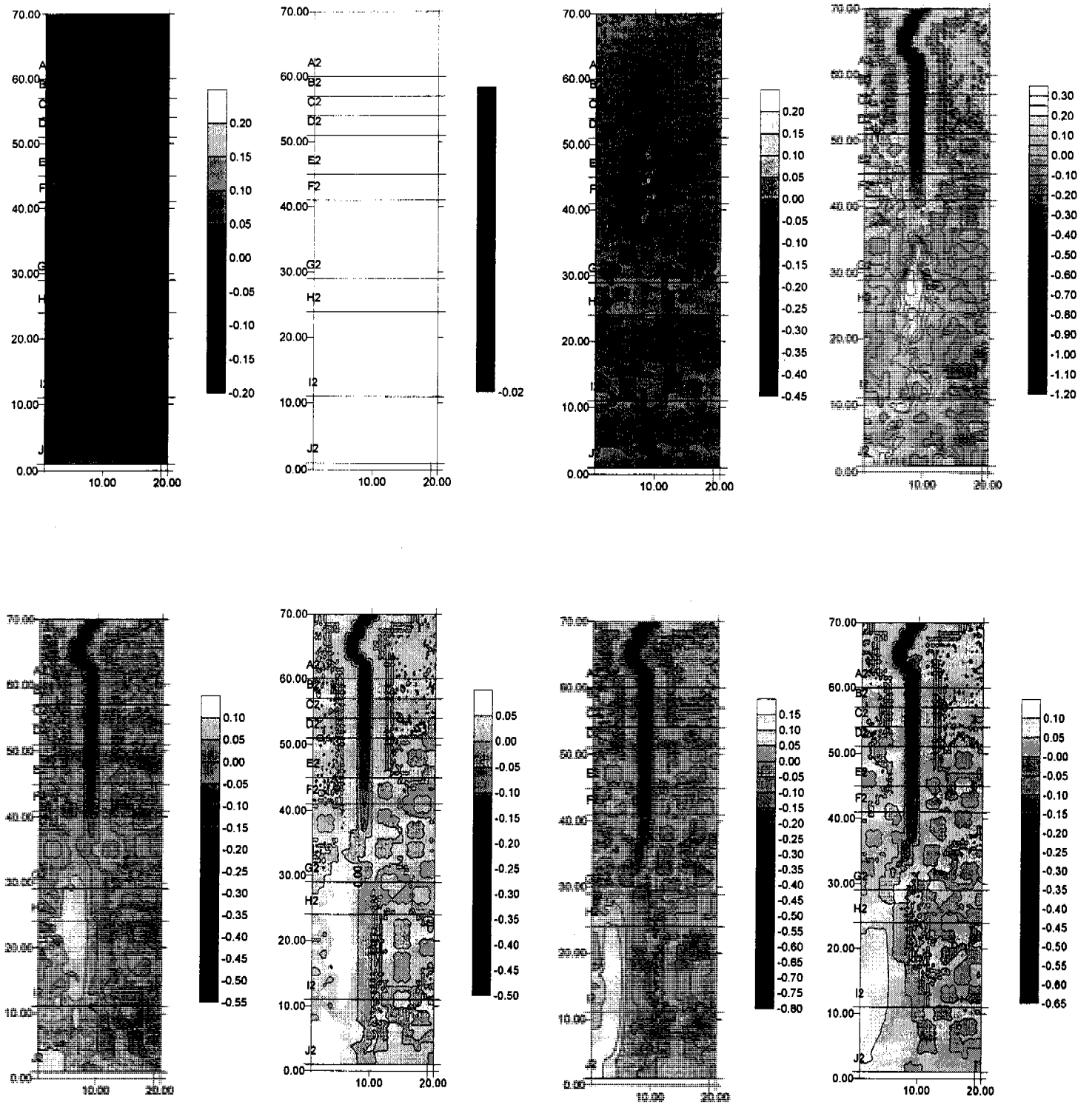

Figure 5.1.6: The initial elevations subtracted from appropriate time period (where erosion is negative, and deposition is positive) such that a) difference between initial surface and prediction at 10 minutes, b) 10 minutes and 20 minutes, c) 20 minutes and 30 minutes, d) 30 minutes and 1 hour. The difference in elevations are also calculated from the remainder of the simulations with e) difference between 1 hours and 1.5 hours, f) 1.5 and 2 hours, g) and 2.5 hours, and h) 2.5 and 3 hours.

5.2 Slope Dependence

The sediment transport equation is dependent on two major components, drainage density and slope dependent component. The exponent on the slope term n_1 has been estimated from field studies to be 0.69 (Section 4.1), however if the sediment transport equation is described according to the Einstein-Brown relationship, a value for n_1 of 2.1 is default.

The impact of the alteration of this exponent was investigated, with n_1 devised from mean particle diameter, equation 4.1.5. The standard batter slope, and the extended profile scenarios were both used to assess the implication of this alteration.

The results of this alteration were expected to be dramatic, with typical slope profiles of the batter site between 20% and 25%, compared to slope profiles of 1.5% to 2% for the gully catchment. The difference in the contribution of the slope component to total sediment transport can be seen with $0.2^{0.69} \sim 0.34$, whilst adopting the same value for the catchment yields $0.2^{2.1} \sim 0.034$, and order of magnitude difference is observed.

Figure 5.2.1, and Figure 5.2.2 illustrates the elevation profiles over the 3 hour duration, with maximum erosion depth at 3 hours reaching 11 to 12m, and erosion at 10 minutes seen to be a level of 4.5m in Figure $5.2.1_a$.

A similar scenario is observed, with the extension of the batter slope site in Figure 5.2.4, and Figure 5.2.5 respectively. The same behaviour observed in Figure 5.1.4, and Figure 5.1.5 can be seen in this case, where development of the gully is delayed with little activity initially. This can be accounted specifically by consideration of the slope of the catchment, where at 2% slope n_1 at 0.69 yields 0.067, whilst at 2.1 yields 0.00027.

When the gully reaches the inlet point, the excavation of the transition point is considerably greater. Figure 5.2.3, and Figure 5.2.6 illustrate the difference in elevations between modelling simulations using contour plots.

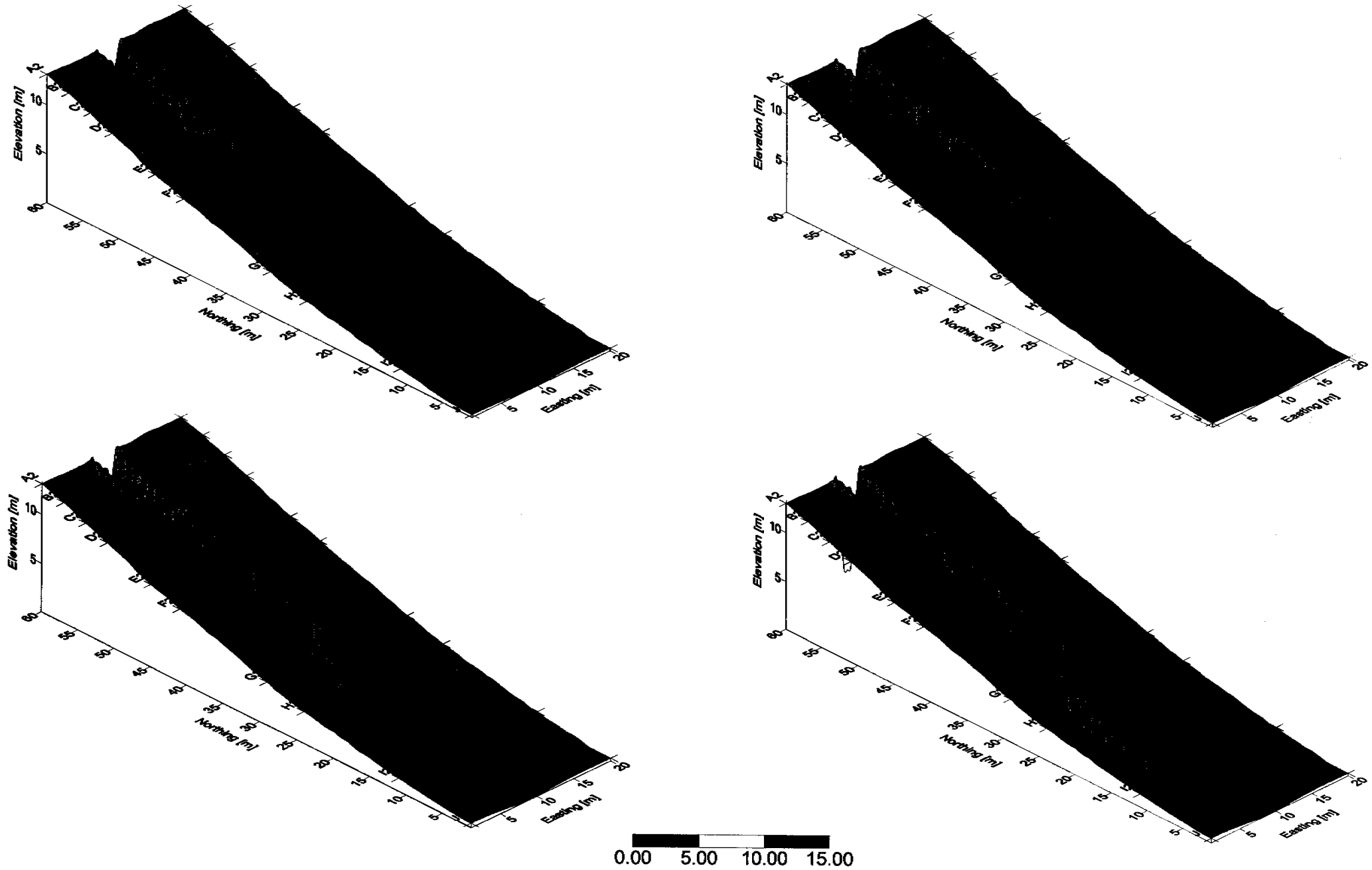

Figure 5.2.1: Simulations for standard batter slope profile with the exponent on the slope term in sediment transport equation set at 0.69, rather than 2.1, a)10 minutes, b) 20 minutes, c) 30 minutes, and) 1 hour.

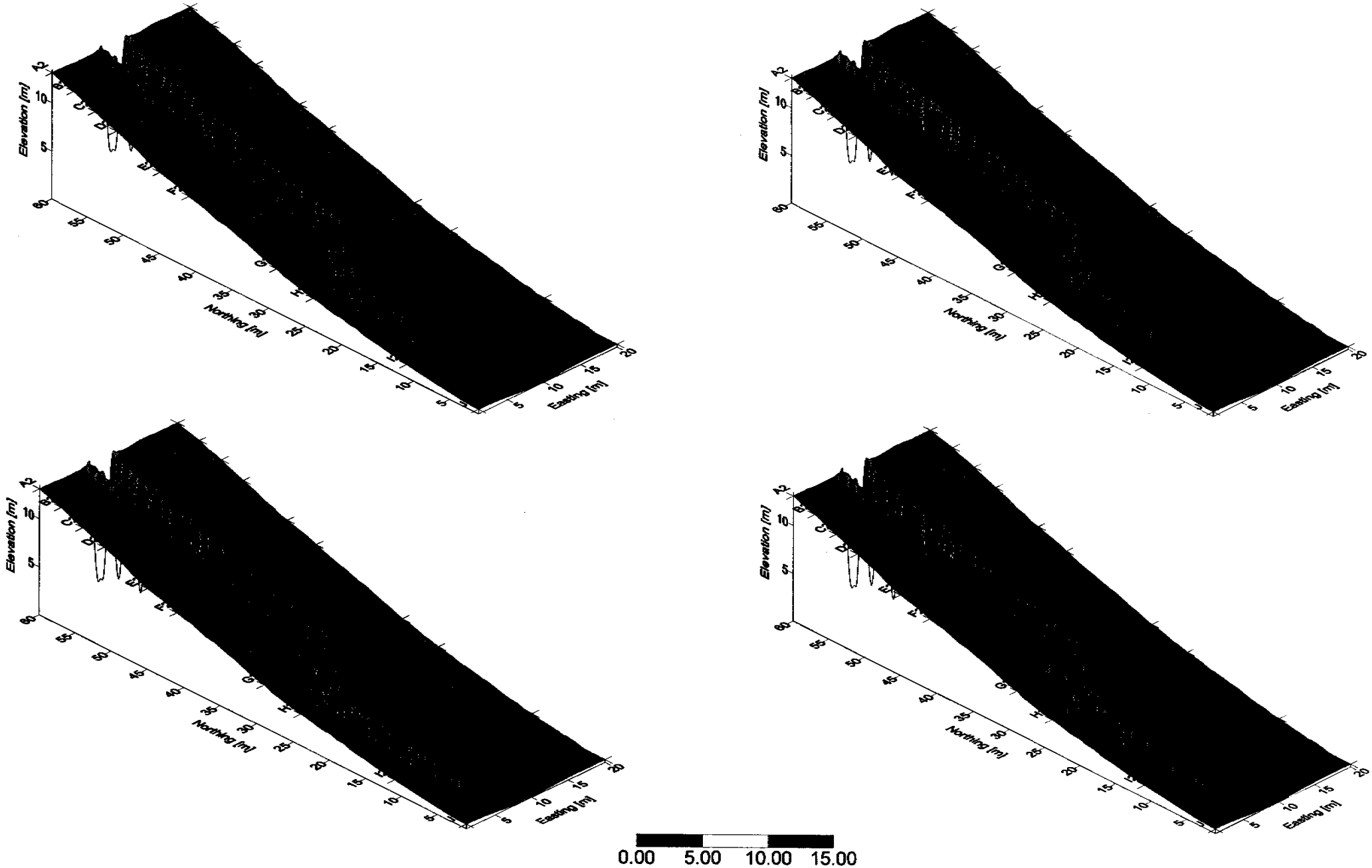

Figure 5.2.2: Simulations for standard batter slope profile with the exponent on the slope term in sediment transport equation set at 0.69, rather than 2.1, at a)1.5 hours, b) 2 hours this represents the second storm event, and c) 2.5 hours and d) 3 hours representing the final storm event.

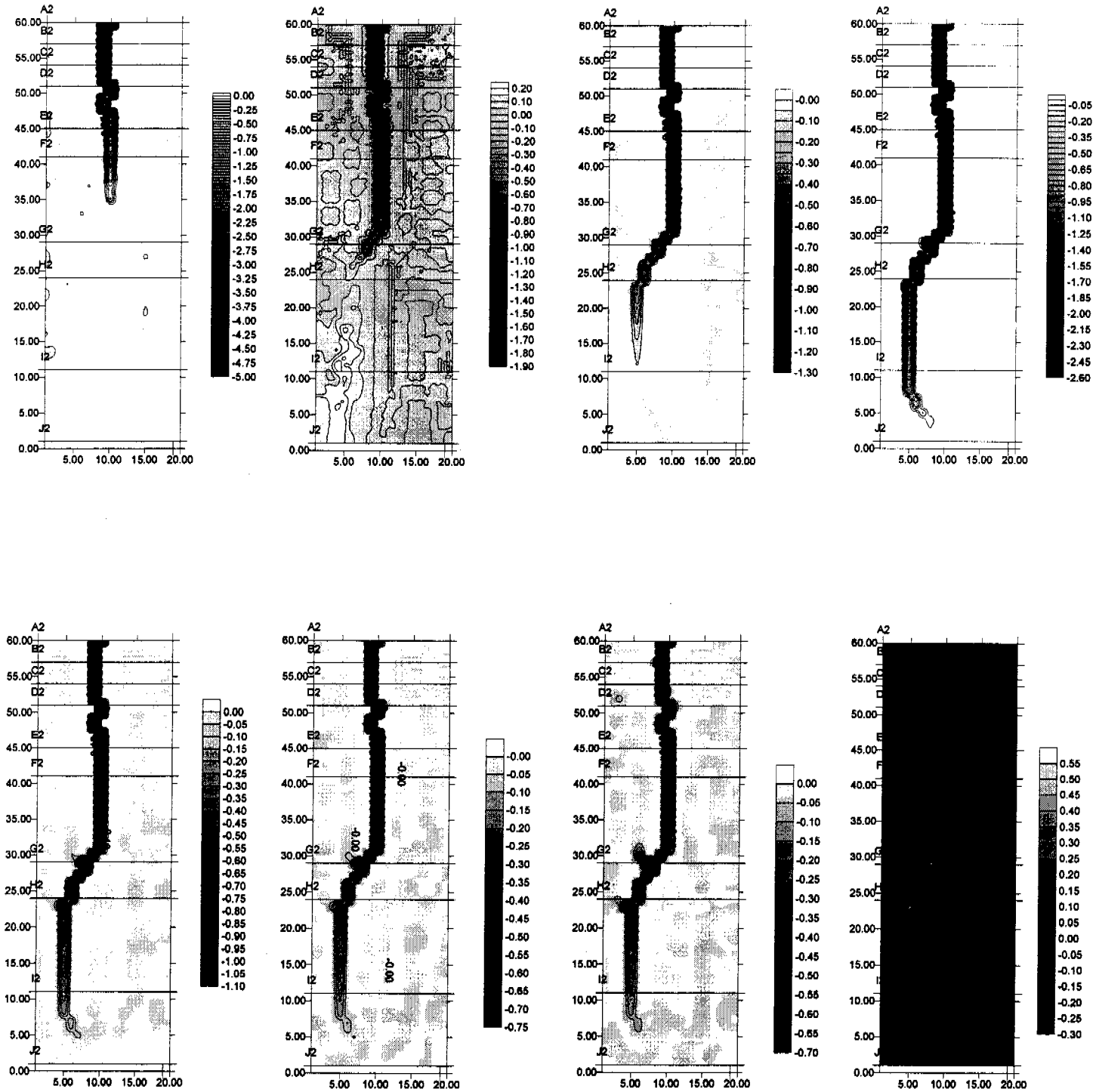

Figure 5.2.3: The initial elevations subtracted from appropriate time period (where erosion is negative, and deposition is positive) such that a) difference between initial surface and prediction at 10 minutes, b) 10 minutes and 20 minutes, c) 20 minutes and 30 minutes, d) 30 minutes and 1 hour. The difference in elevations are also calculated from the remainder of the simulations with e) difference between 1 hours and 1.5 hours, f) 1.5 and 2 hours, g) and 2.5 hours, and h) 2.5 and 3 hours.

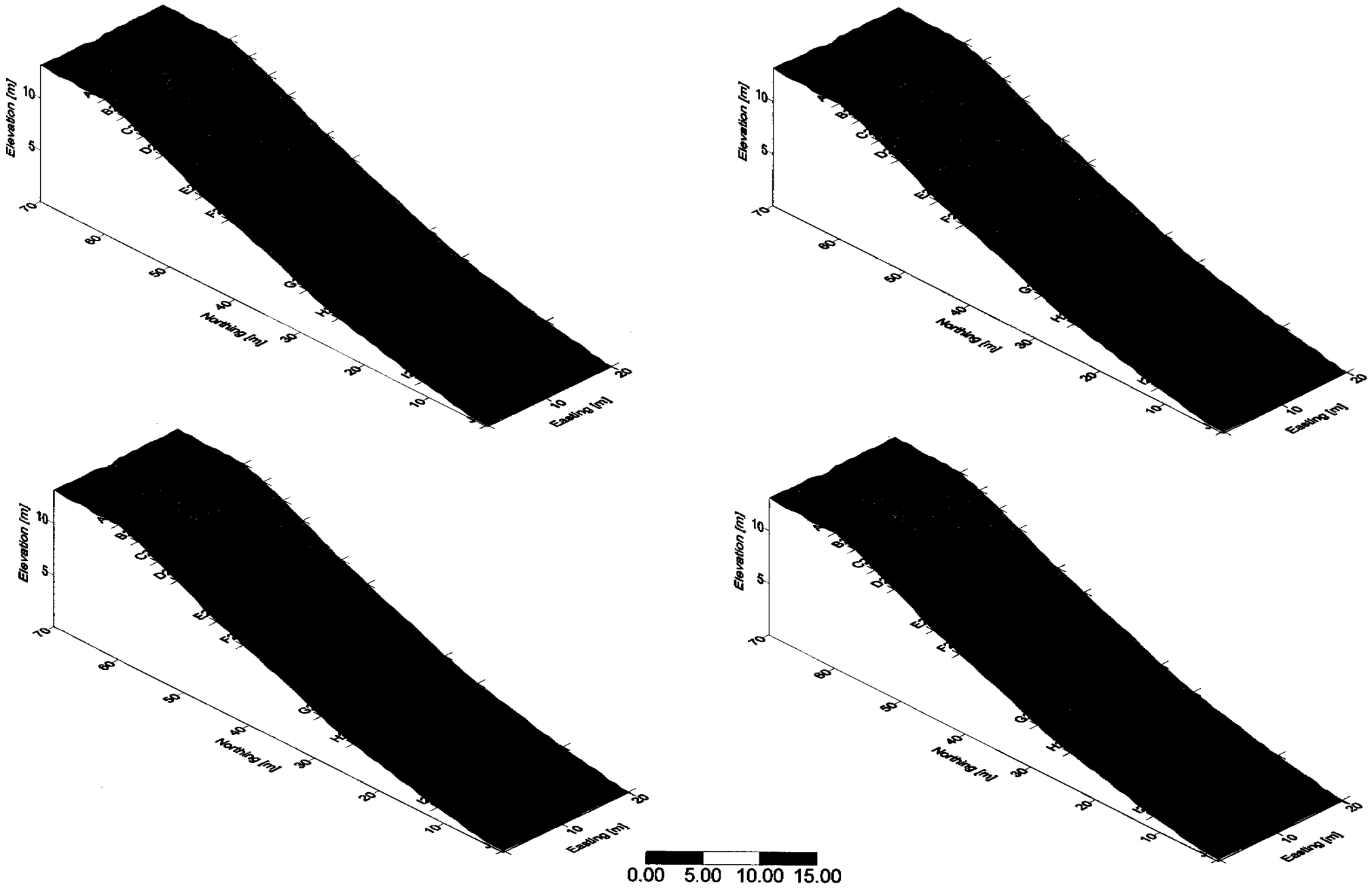

Figure 5.2.4: Simulations for extended batter slope profile with the exponent on the slope term in sediment transport equation set at 0.69, rather than 2.1, a)10 minutes, b) 20 minutes, c) 30 minutes, and d) 1 hour.

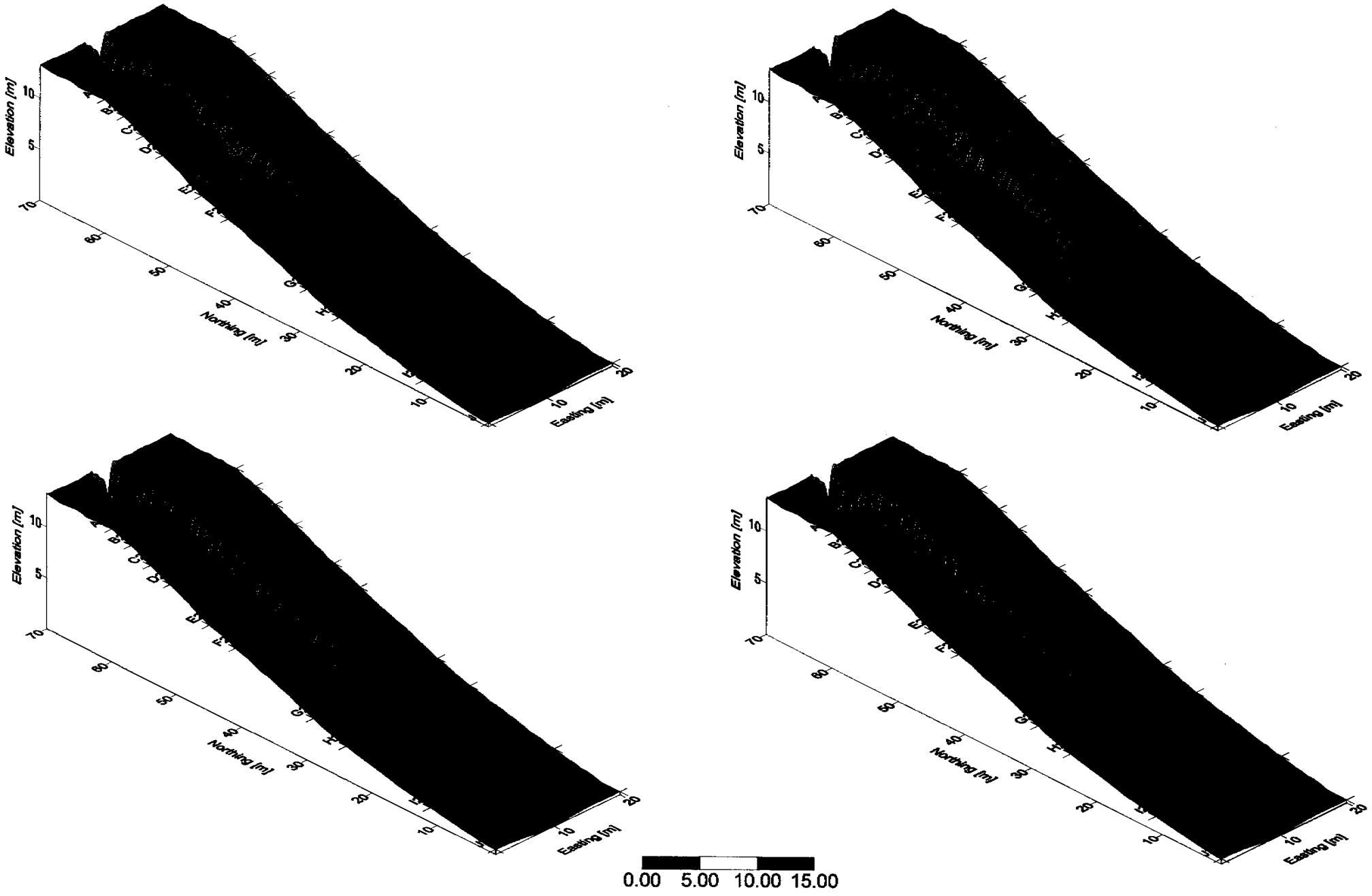

Figure 5.2.5: Simulations for extended batter slope profile with the exponent on the slope term in sediment transport equation set at 0.69, rather than 2.1, at a)1.5 hours, b) 2 hours this represents the second storm event, and c) 2.5 hours and d) 3 hours representing the final storm event.

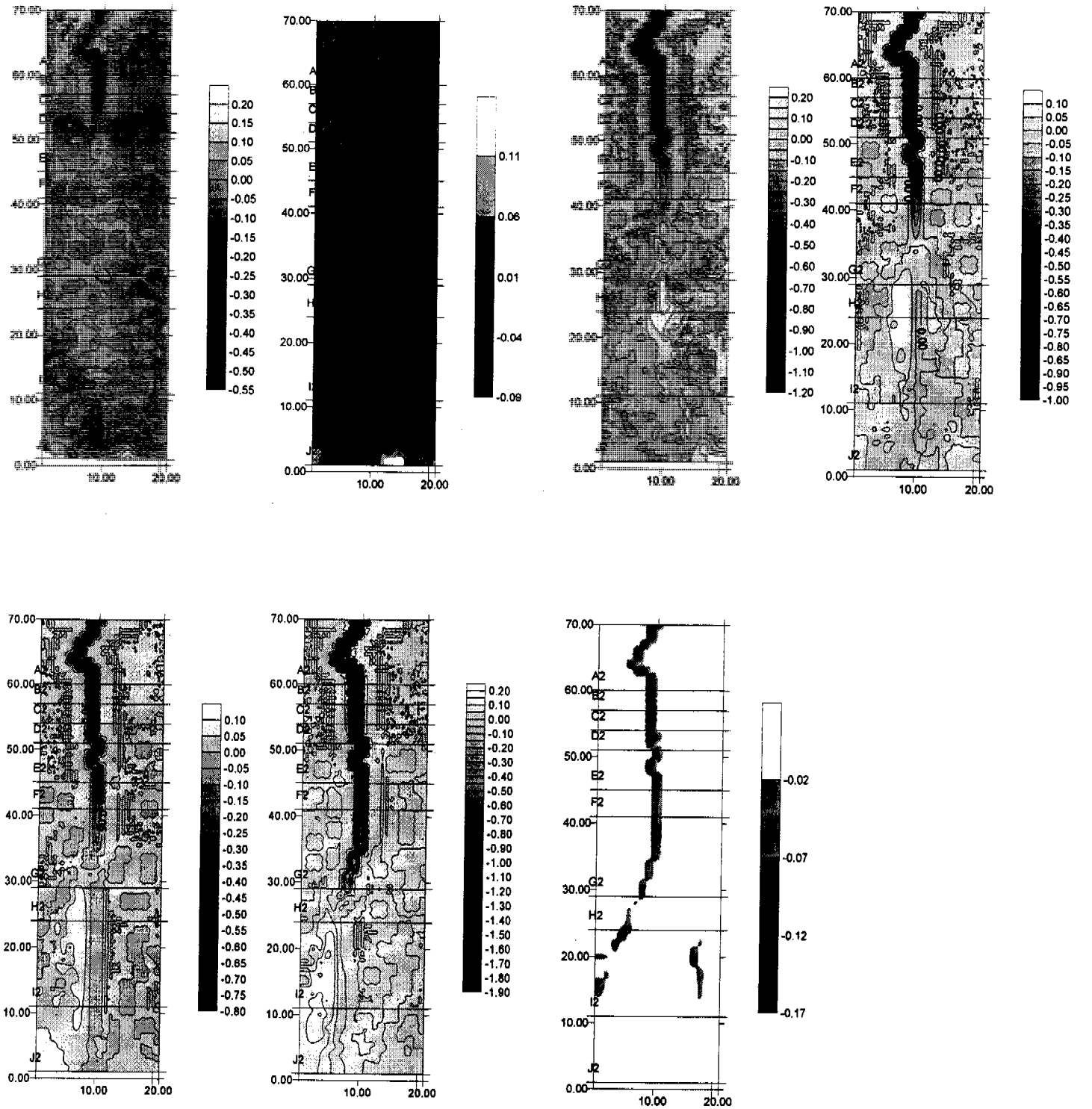

Figure 5.2.6: The morphology contour plots a) initial profile and 10 minutes, b) 10 minutes and 20 minutes, c) 20 minutes and 30 minutes, d) 30 minutes and 1 hour. The difference in elevations are also calculated from the remainder of the simulations with e) difference between 1 hours and 1.5 hours, f) 1.5 and 2 hours, g) 2 and 2.5 hours, and h) 2.5 and 3 hours.

5.3 Increased Width

The effect of increasing the number of inlet points was assessed by simulating both the standard batter slope, and also the extended batter profile. The overall discharge was maintained at the same level, with each inlet node, 1800 equivalent nodes instead of 3600 nodes for the standard narrow two feed point scenario.

Gully formation observed in Figure 5.3.1, and Figure 5.3.2, is more widespread at the top of the batter slope with maximum depth of erosion 2.5m for the standard scenario. Whilst in Figure 5.3.4, and Figure 5.3.5 similar behaviour observed in Figure 5.1.4, and Figure 5.1.5, except that the gully does not proceed onto the batter slope.

The rate of development of the gully is considerably slower for the standard profile scenario, with less pronounced regions of deposition, recognised by smoothed areas at the base of the slope (Row G to Row I), with the depth of gully ranging between 0.8 to 1.5m between Row E to Row K.

The erosion depth profiles begin to resemble those observed on site, with excavation of material in some sections to a level of 60cm. Figure 5.3.3 illustrates the spatial distribution of erosion for the wide inlet.

When the same scenario was simulated using the extended profile, considerably different results were predicted. From Figure 5.3.4, and Figure 5.3.5, the development of the gully does not reach the high wall transition point and so the large formations generated above are not predicted to occur. Further investigation including the inclusion of wide inlet point with randomised erodibility of the waste rock material yielded similar behaviour for this extended profile.

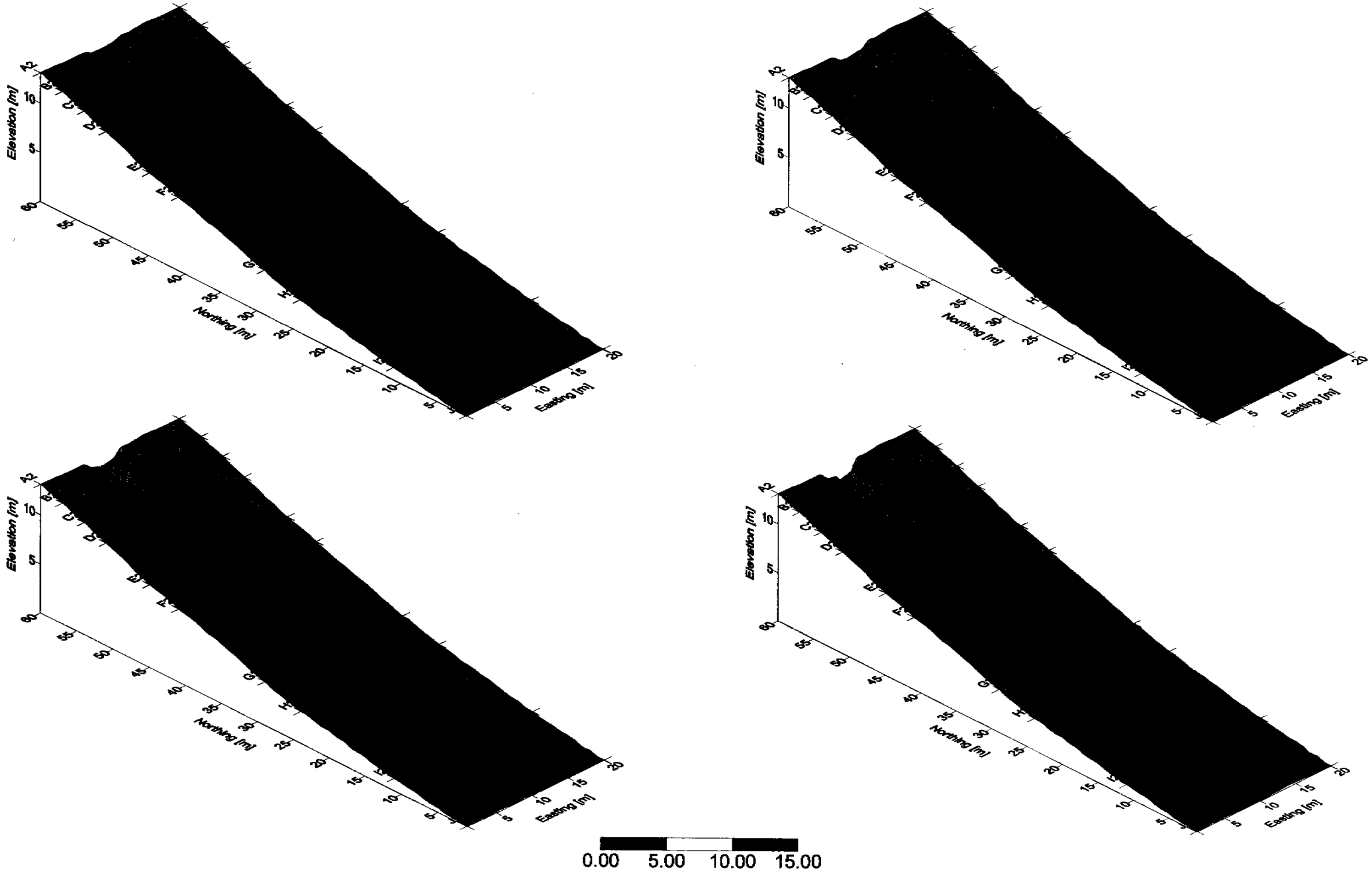

Figure 5.3.1: Simulations for standard batter slope profile with increased width inlet point to four points instead of only two, at a)10 minutes, b) 20 minutes, c) 30 minutes, and d) 1 hour.

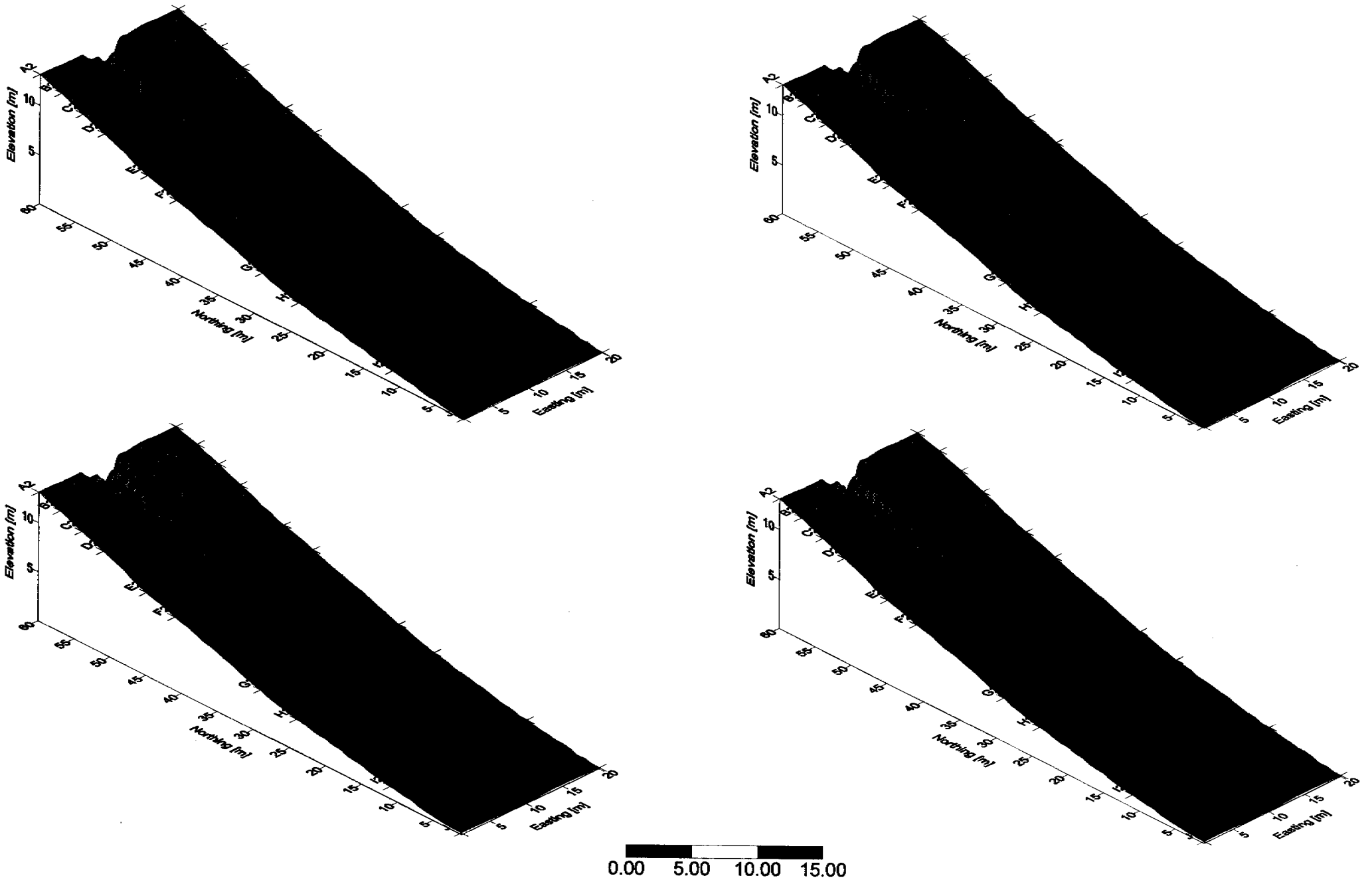

igure 5.3.2: Simulations for standard batter slope profile with increased width inlet point to four points instead of only two, at a)1.5 hours, b) 2 hours this represents the second storm event, and c) 2.5 ours and d) 3 hours representing the final storm event.

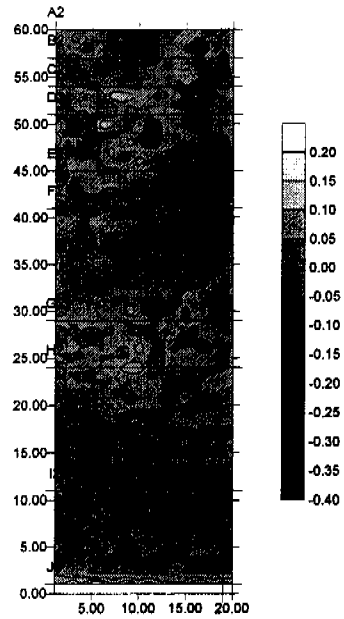

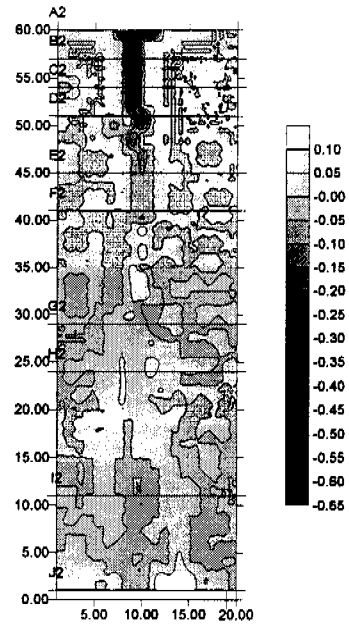

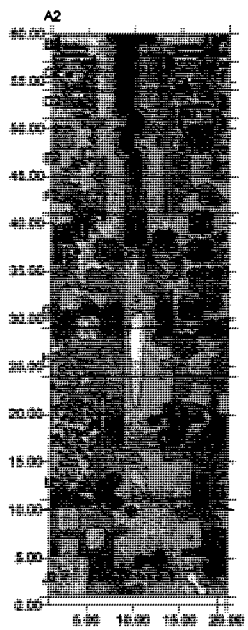

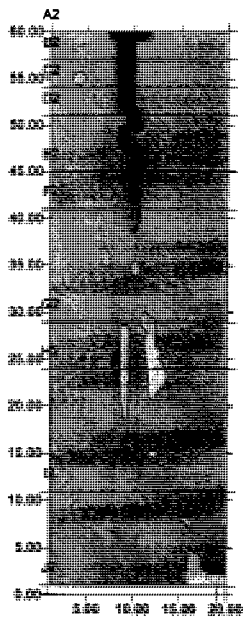

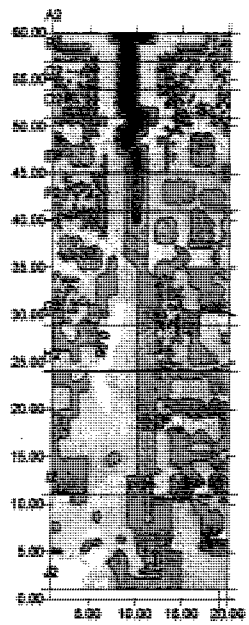

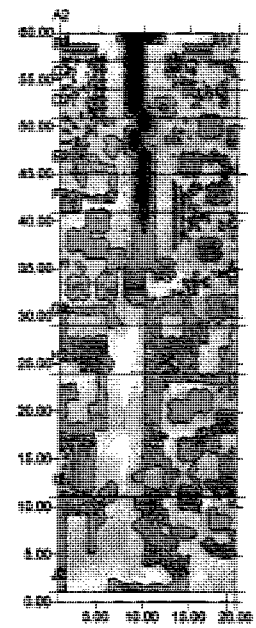

Figure 5.3.3: The morphology contour plots a) initial profile and 10 minutes, b) 10 minutes and 20 minutes, c) 20 minutes and 30 minutes, d) 30 minutes and 1 hour. The difference in elevations are also calculated from the remainder of the simulations with e) difference between 1 hours and 1.5 hours, f) 1.5 and 2 hours, g) 2 and 2.5 hours, and h) 2.5 and 3hours.

5.4 Randomised Erodibility

The erodibility factor $beta_i$ was multiplied by a randomly generated number between 0 and 5, with a mean of 1.0 to introduce a random perturbation to the surface erodibility.

By the introduction of some degree of heterogeneity, the formation of the gully was expected to follow those regions more susceptible and the straight line paths characteristic of Sections 5.1 should not be observed.

The sensitivity of the slope to erodibility will have been increased in some sections although the overall erodibility, representative of the actual site, has not been changed, leading to deeper gullies observed where they occur.

This synopsis seems somewhat reasonable, as illustrated in Figure 5.4.1, and Figure 5.4.2 with gully formation across the slope from almost in front of the inlet zone.

The pathway adopted, as discussed above, is dependent on the drainage direction, as well as the surface elevation of the nodes lying around the current node under calculation and ultimately the erodibility of this point, this influences the nature of gully formation with reduced amounts of deposition observed in Figure 5.4.3.

Although the quantity of deposition observed in each of the time periods is reduced, the dynamic nature of the pathway of erosion observed in these simulations is similar to standard scenario in Section 5.1. Inherently the overall erosional characteristic of the slope has not been altered, and predictions indicate similar maximum depths of erosion, although areas of deposition will be more widespread. The maximum depth of erosion at the head of the gully network at 5.5m, indicating that overall nature of gully development has not altered, but merely the pathway adopted. This conforms to the hypothesis that the erodibility of the material had not been significantly changed.

Figure 5.4.4 and Figure 5.4.5 illustrate the same design scenario incorporating the extended profile of the batter slope. Comparison of these simulations with Figures 5.1.4, and 5.1.5 reveal a similar behaviour with initial delay in gully development, until the 30 minute mark, where development initiates at the transition point between

the batter slope and gully catchment. Similarities in the development process also included the maximum depth of erosion at Row A at 4.5m, as can be observed in Figure 5.4.4.

The assessment of the inclusion of wide inlet point with the standard profile combined with randomised erodibility was also conducted, as illustrated in Figure 5.4.7 and Figure 5.4.8. The continuity of transported material in these cases, can be compared to Figure 5.4.4, and 5.4.5 respectively. The depth of erosion ranges between 0.5m and 1.0m for Row E to Row G, whilst more extensive excavation sections between Row B to Row D. It also noted that cross-sectional profile at Row B in Figure $5.4.7_d$ is almost identical to that observed in Figure $5.3.1_d$ Row B, with similar observations for all except just below the inlet zone in Row A.

The pathway adopted, mimics that of Figure 5.4.1, and Figure 5.4.2, whilst this is not observed when comparing standard scenario and addition of increased width component (Figure 5.1.1 and 5.1.2 against 5.3.1 and 5.3.2), with a reduction in depths of erosion observed.

A similar comparison can be drawn between the standard extended profile and randomised erodibility scenario, with depth of erosion of similar magnitude, with path dominated by developing process, rather than random perturbations in material characteristic. Once the gully extends past Row D in this figure, the dominant process changes as expected.

Another important observation from Figure 5.4.7, and Figure 5.4.8 where 2 independent erosion paths have developed. By further increasing inlet width, and increasing grid discretisation, modelling simulations can yield predictions similar to the 2 main gully pathways observed on site.

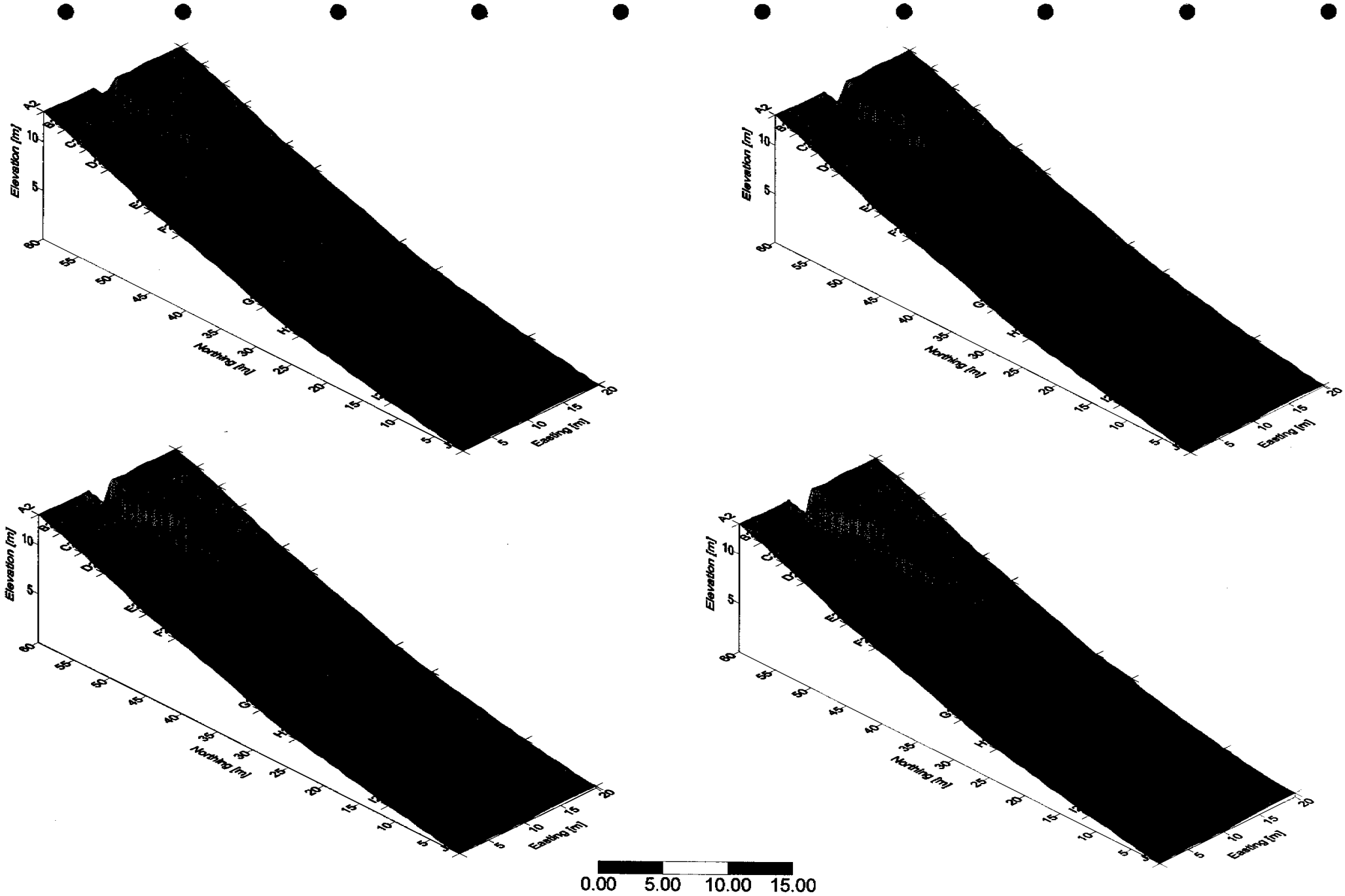

Figure 5.4.1: Simulations for standard batter slope profile with randomised erodibility at a)10 minutes, b) 20 minutes, c) 30 minutes, and d) 1 hour.

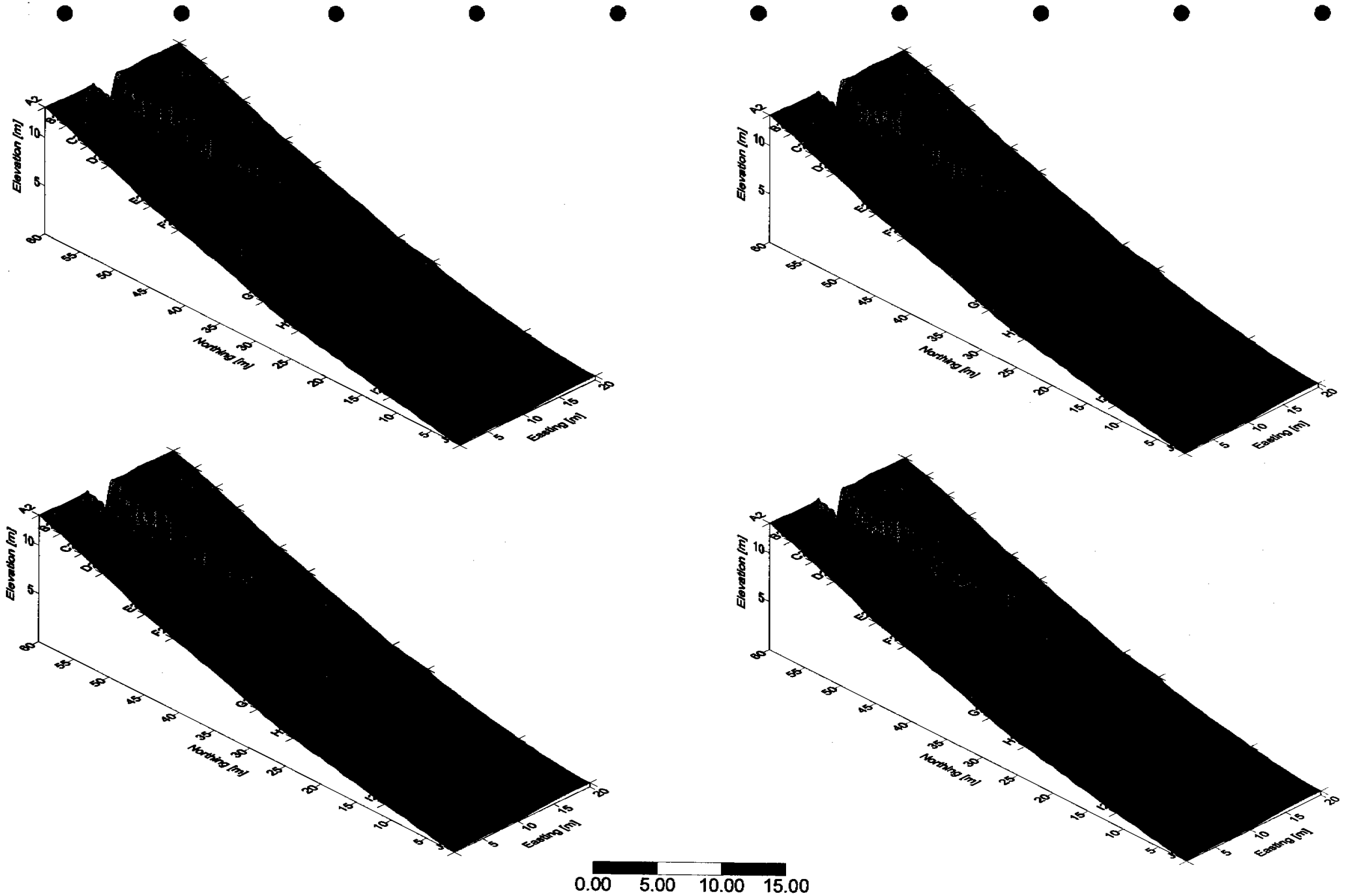

Figure 5.4.2: Simulations for standard batter slope profile with randomised erodibility, at a)1.5 hours, b) 2 hours this represents the second storm event, and c) 2.5 hours and d) 3 hours representing the final storm event.

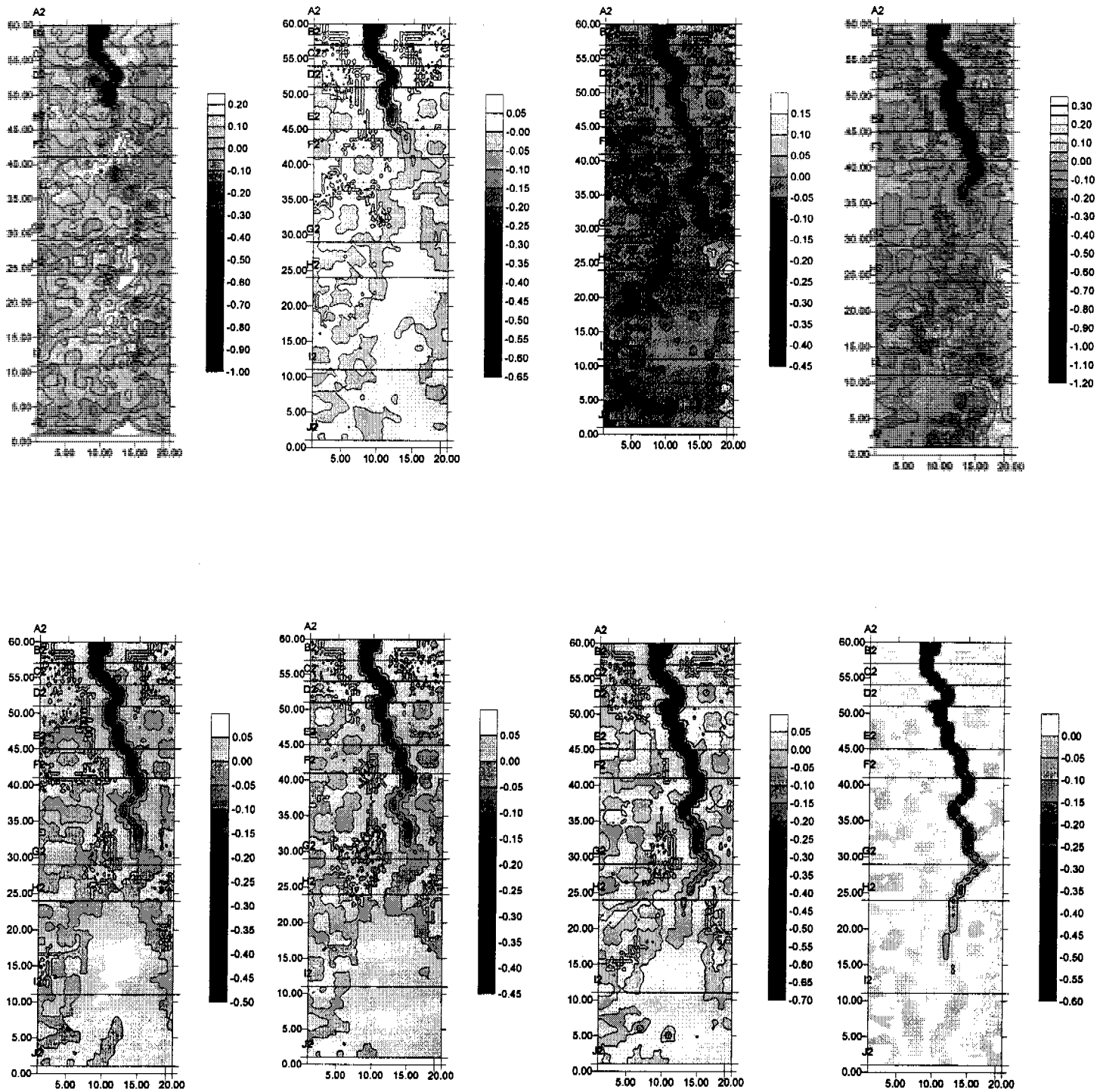

Figure 5.4.3: The morphology contour plots a) initial profile and 10 minutes, b) 10 minutes and 20 minutes, c) 20 minutes and 30 minutes, d) 30 minutes and 1 hour. The difference in elevations are also calculated from the remainder of the simulations with e) difference between 1 hours and 1.5 hours, f) 1.5 and 2 hours, g) 2 and 2.5 hours, and h) 2.5 and 3 hours.

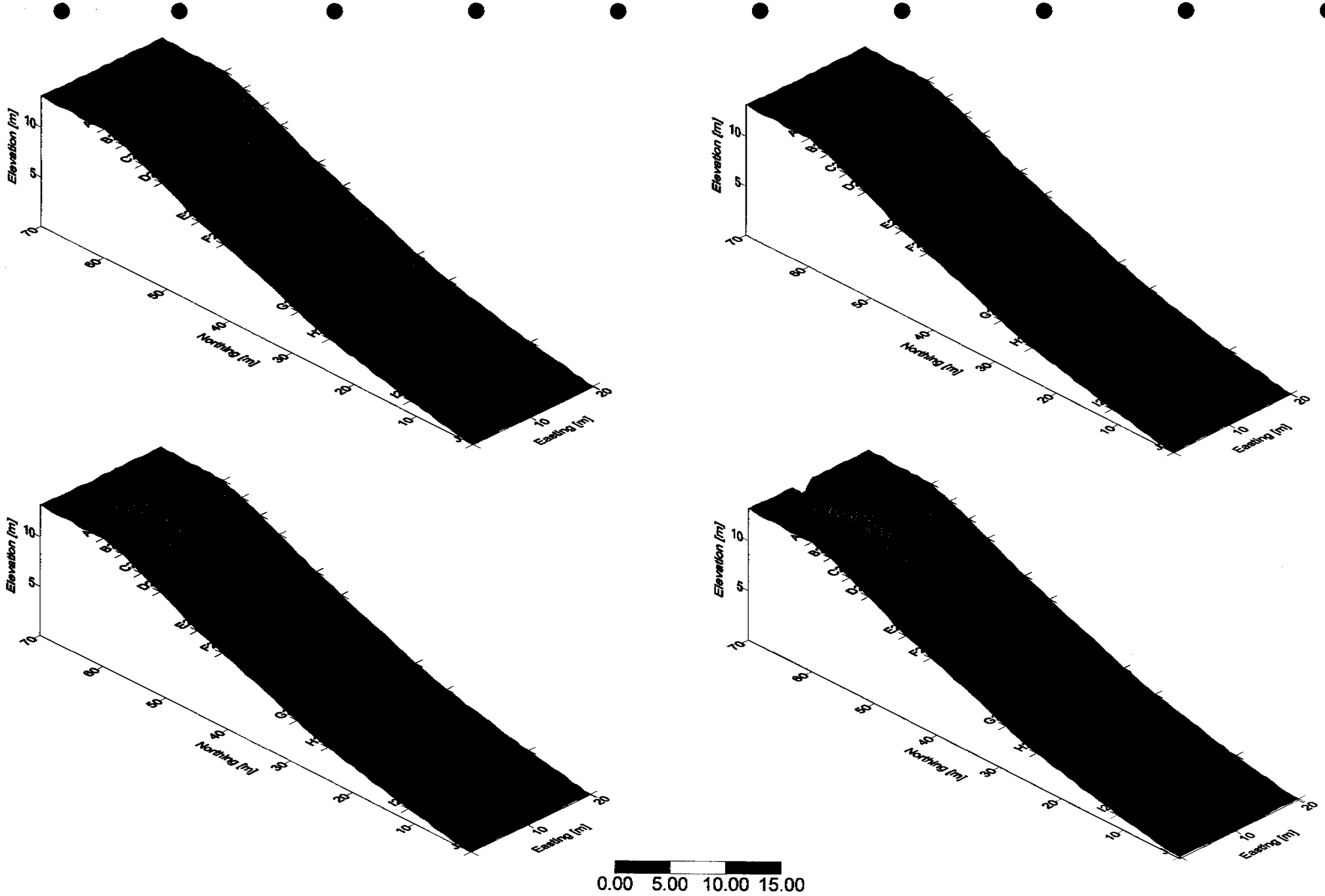

Figure 5.4 Simulations for ~~standard~~ Extended batter slope profile with randomised erodibility at a)10 minutes, b) 20 minutes, c) 30 minutes, and d) 1 hour.

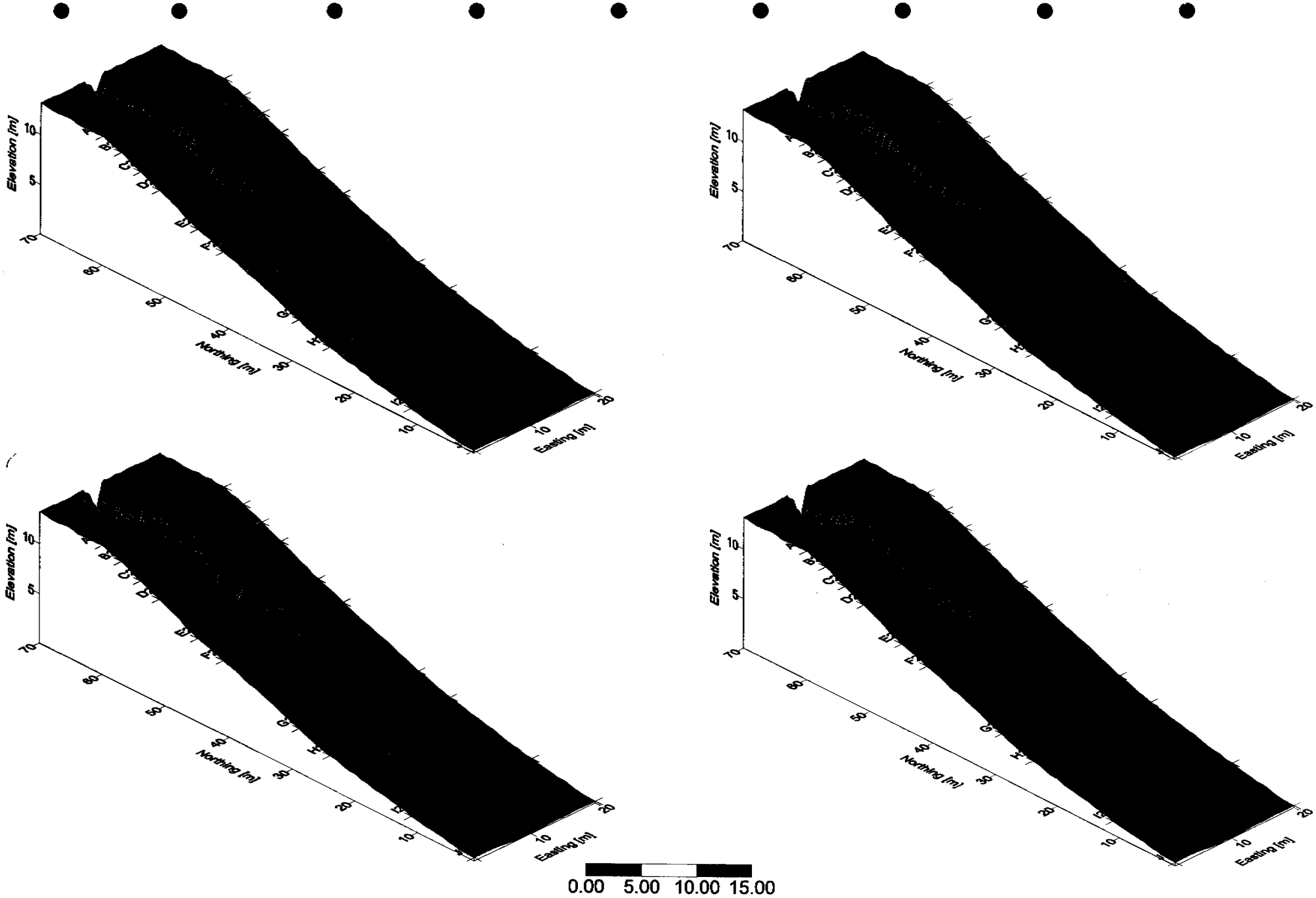

Figure 5.4.8: Simulations for standard batter slope profile with randomised erodibility, at a)1.5 hours, b) 2 hours this represents the second storm event, and c) 2.5 hours and d) 3 hours representing the final storm event.

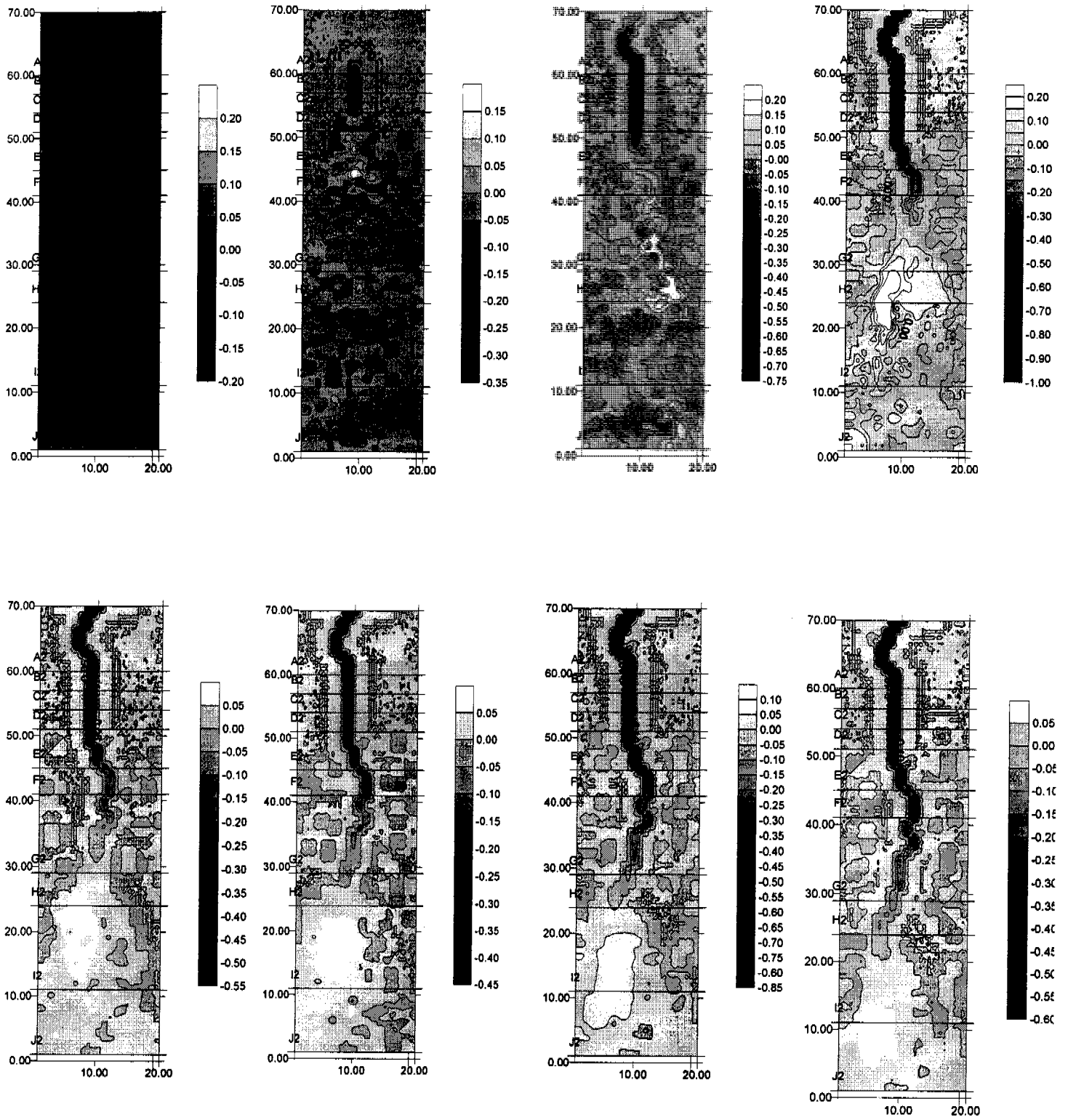

Figure 5.4.6: The morphology contour plots a) initial profile and 10 minutes, b) 10 minutes and 20 minutes, c) 20 minutes and 30 minutes, d) 30 minutes and 1 hour. The difference in elevations are also calculated from the remainder of the simulations with e) difference between 1 hours and 1.5 hours, f) 1.5 and 2 hours, g) 2 and 2.5 hours, and h) 2.5 and 3 hours.

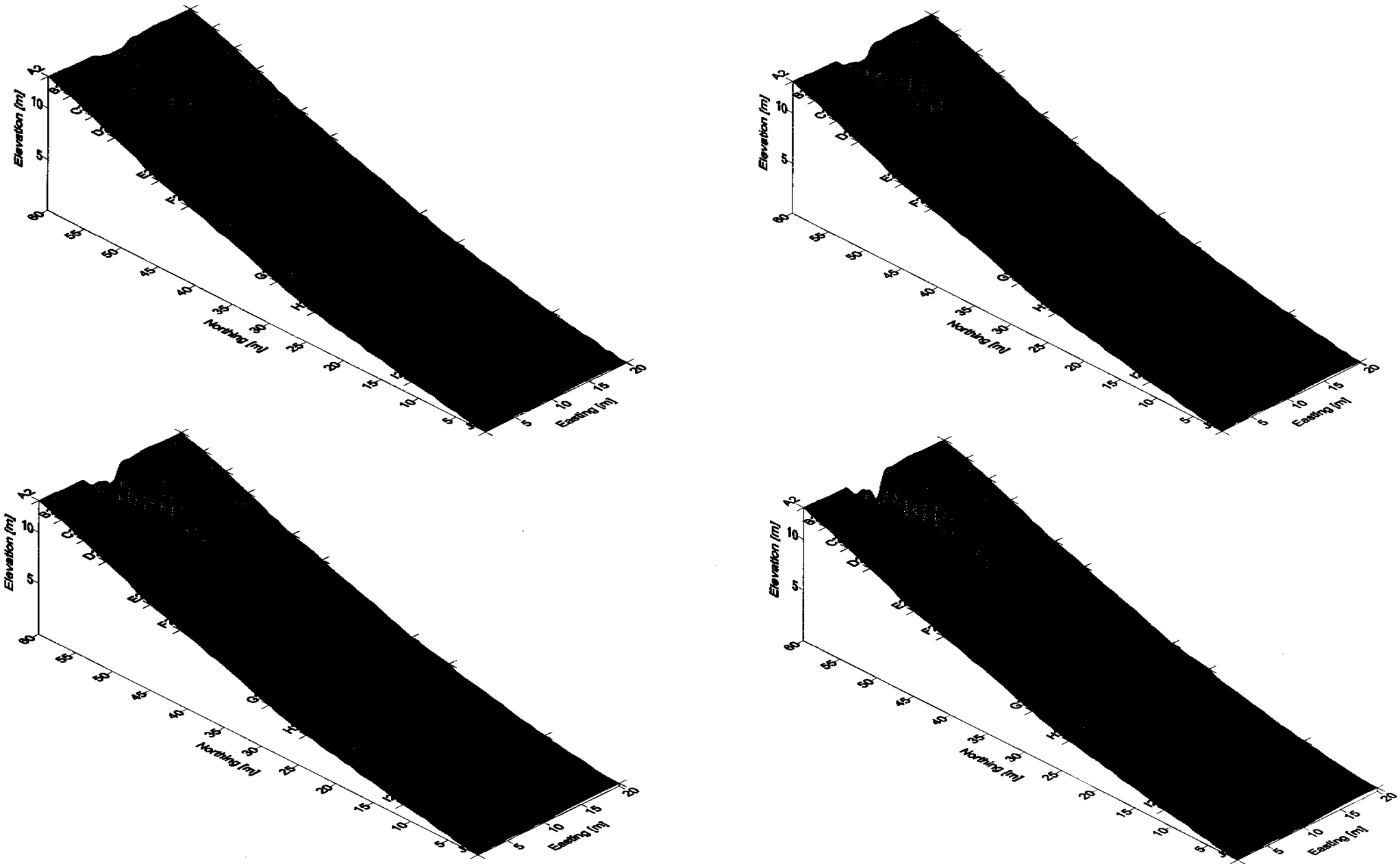

Figure 5.4.7: Simulations for standard batter slope profile with increased width inlet point to four points instead of only two, combined with randomised erodibility, a)10 minutes, b) 20 minutes, c) 30 minutes, and d) 1 hour.

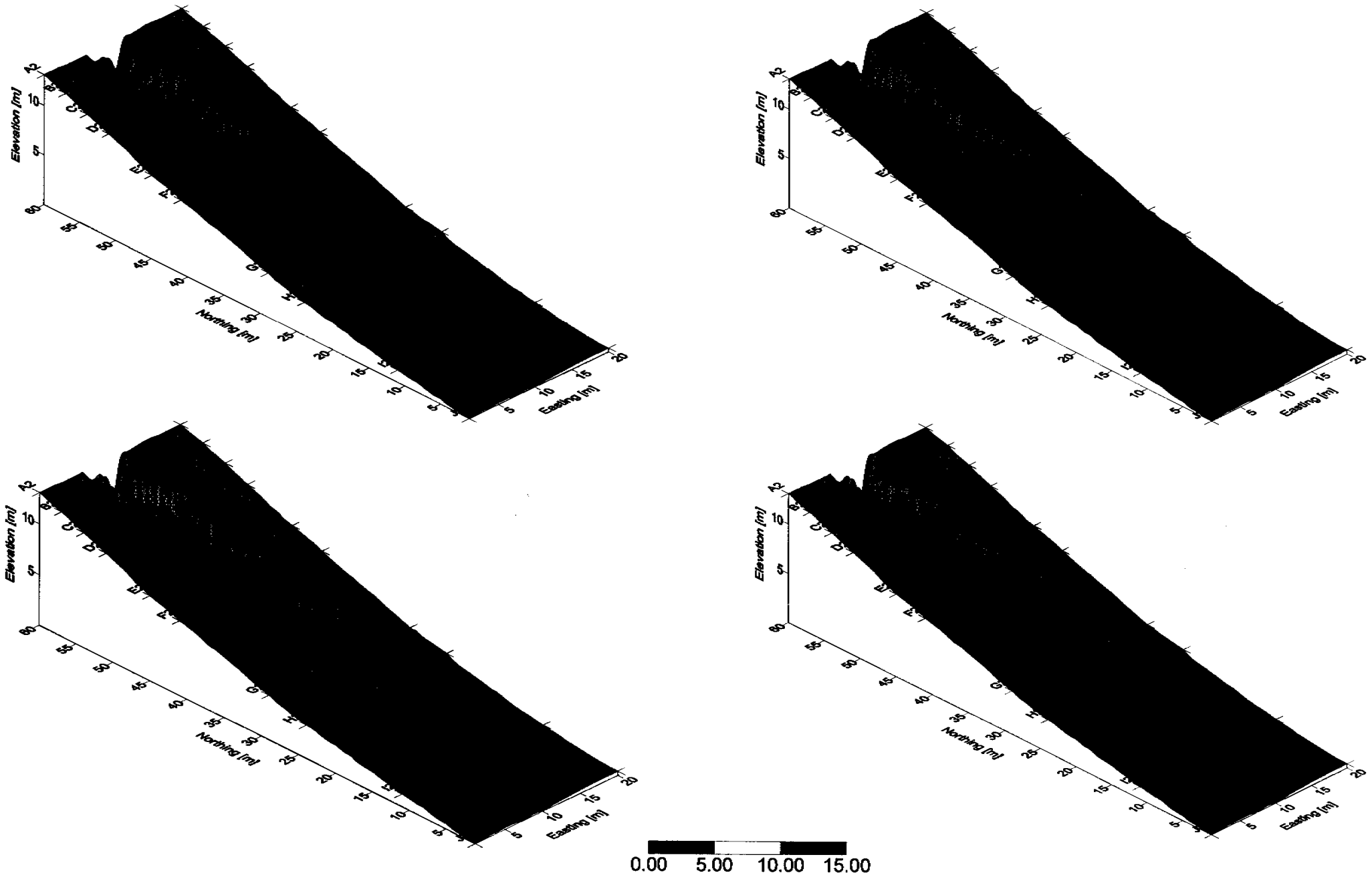

Figure 5.4.8: Simulations for standard batter slope profile with increased width inlet point to four points instead of only two, combined with randomised erodibility, at a)1.5 hours, b) 2 hours this represents the second storm event, and c) 2.5 hours and d) 3 hours representing the final storm event.

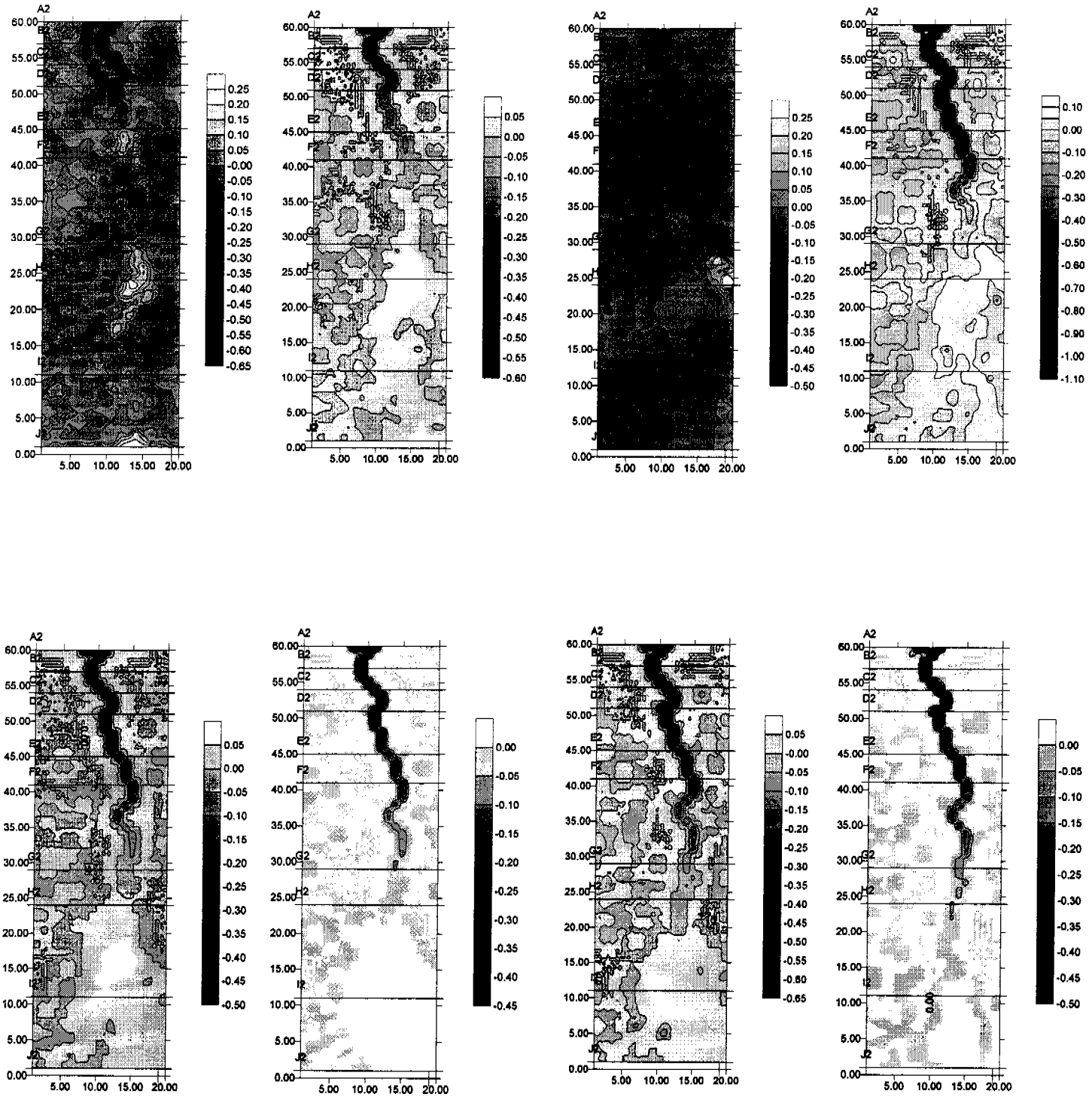

Figure 5.4.9: The morphology contour plots a) initial profile and 10 minutes, b) 10 minutes and 20 minutes, c) 20 minutes and 30 minutes, d) 30 minutes and 1 hour. The difference in elevations are also calculated from the remainder of the simulations with e) difference between 1 hours and 1.5 hours, f) 1.5 and 2 hours, g) 2 and 2.5 hours, and h) 2.5 and 3 hours.

5.5 Differential Erodibility with Depth

The next component of this investigation involved alteration of the nature of surface material from randomised erodibility (somewhat heterogeneous) to include differential erodibility with depth function.

By approximating erodibility using mean grain diameter basis, an increase in d_{50} from 2mm to 20mm over 2m depth equated to a reduction in erodibility of 30 fold. This represents a conservative estimate, as illustrated in Figure 4.3.5, with these ratios considered very conservative over a differential depth of only 20cm. However, as noted once the armouring rock layer was breached and the soft earthen material extracted from above the mined ore is exposed and this erodibility factor will change dramatically. Further work currently being conducted into dynamism in sediment size profile, with development over the dry season also considered important given the rate of geochemical weathering noted on the waste rock dumps.

The preliminary investigation would also involve an assessment of the impact of a change in the magnitude of this reduction factor, with modelling simulations used to evaluate the impact of decreasing this factor to 1/10, with depth coefficient set at C~2, instead of C~15.

Figure 5.5.1, and Figure 5.5.2 illustrate simulations using only the depth coefficient of C = 2. The comparison between Figure 5.1.1, and Figure 5.1.2 with these runs suggest that depth coefficient chosen reduces depth of erosion in all sections uniformly, with maximum erosion depth of 5 to 6m compared to about 4m for these predictions.

Equation 4.3.1 highlights the mechanism by which this armouring component functions. The change of elevation is calculated for each node point during a iteration and then this result is multiplied by the depth-erodibility relationship to reduce this depth by a factor of 1/10 for Figure $5.5.1_a$, to Figure$_d$. However for the next iteration representative of the consequent storm event, the same scenario is repeated, as equation is reapplied and depth of erosion is reduced by a factor of 1/10 again. This can be observed as a jump in erosion depth between Figure $5.5.1_d$ and $5.5.2_a$.

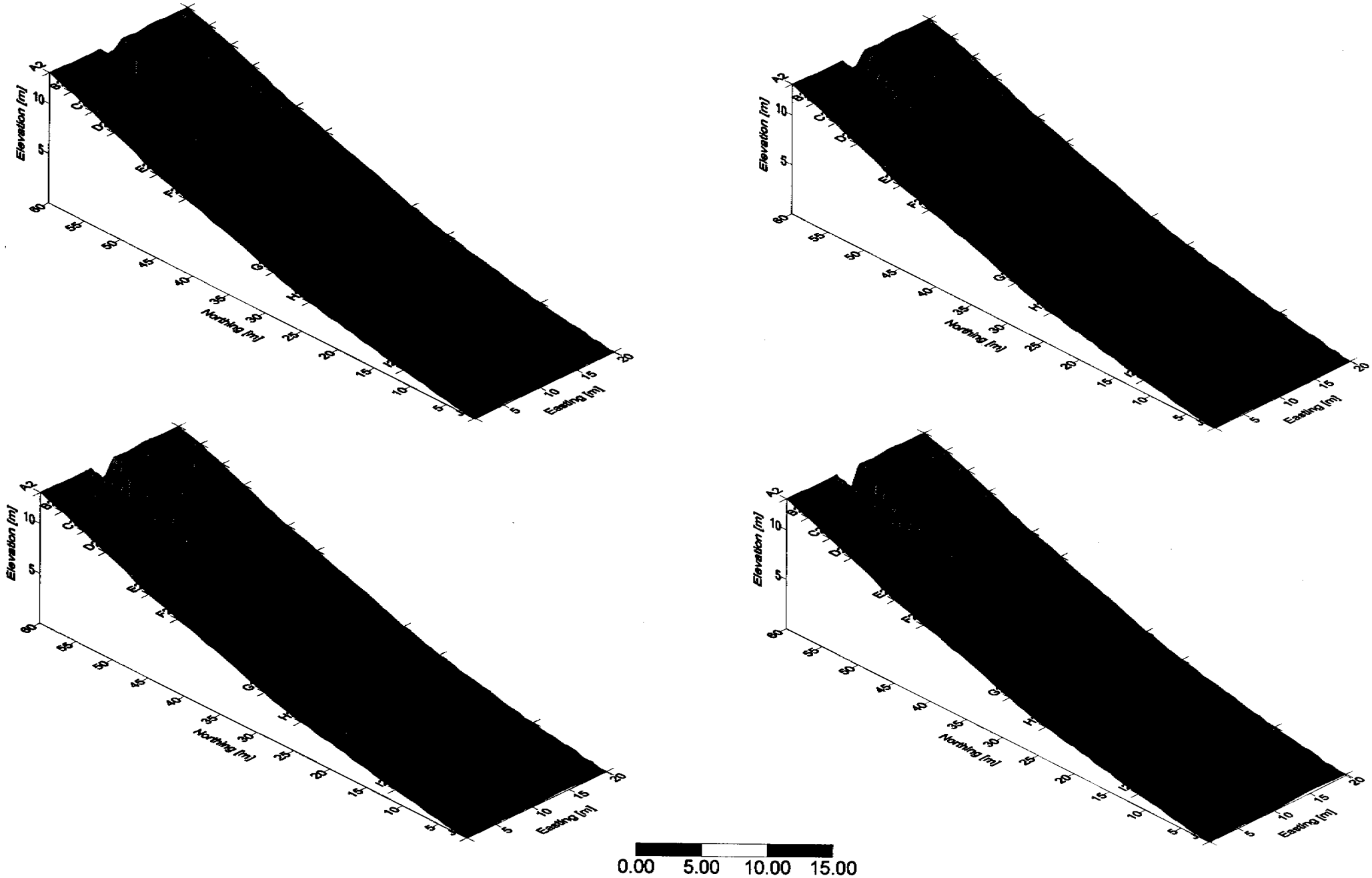

Figure 5.5.1: Simulations for standard batter slope profile with differential erodibility with depth function set at depth coefficient of 2, at a)10 minutes, b) 20 minutes, c) 30 minutes, and d) 1 hour.

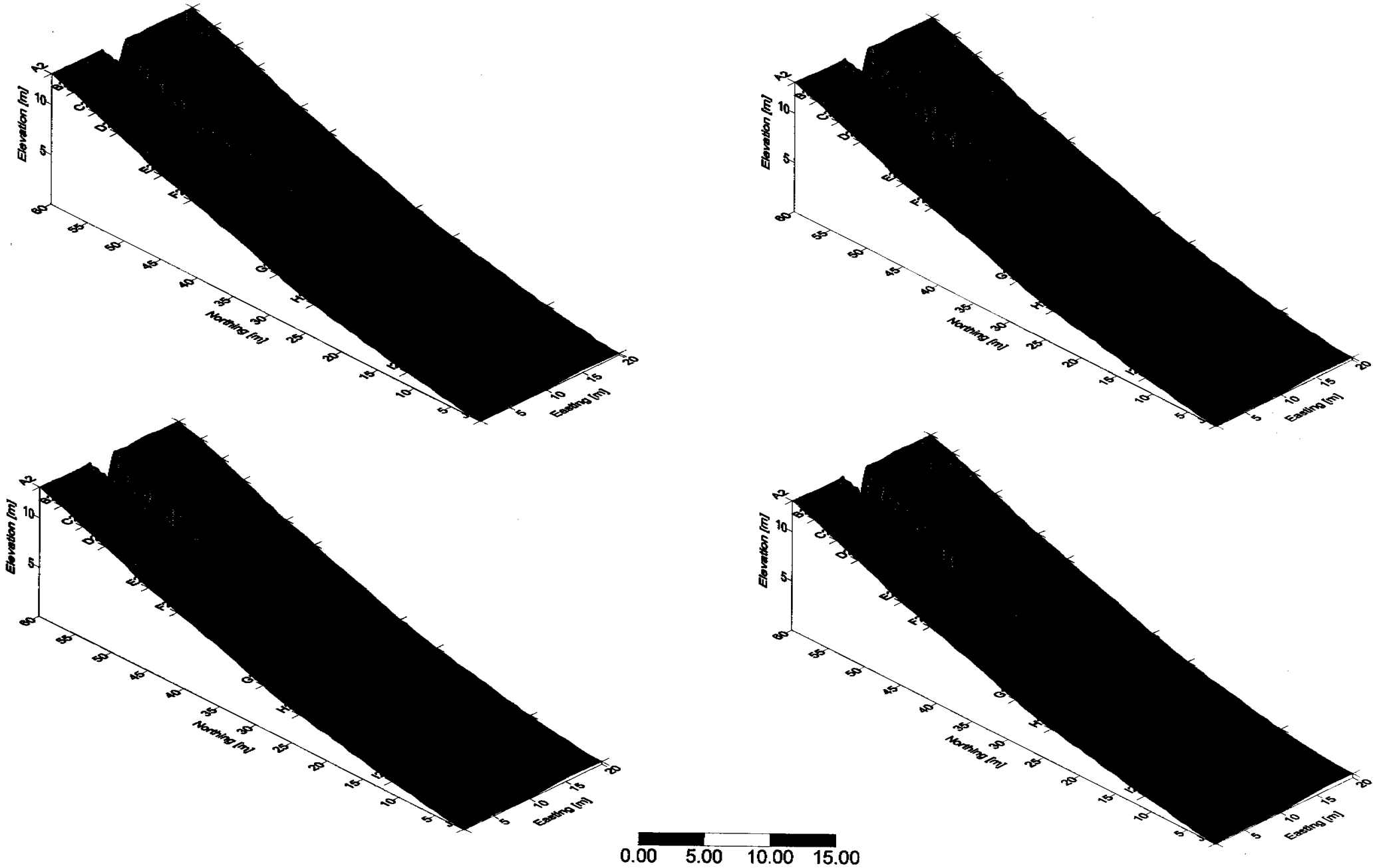

Figure 5.5.2: Simulations for standard batter slope profile with differential erodibility with depth function set at depth coefficient of 2, at a)1.5 hours, b) 2 hours this represents the second storm event, and c) 2.5 hours and d) 3 hours representing the final storm event.

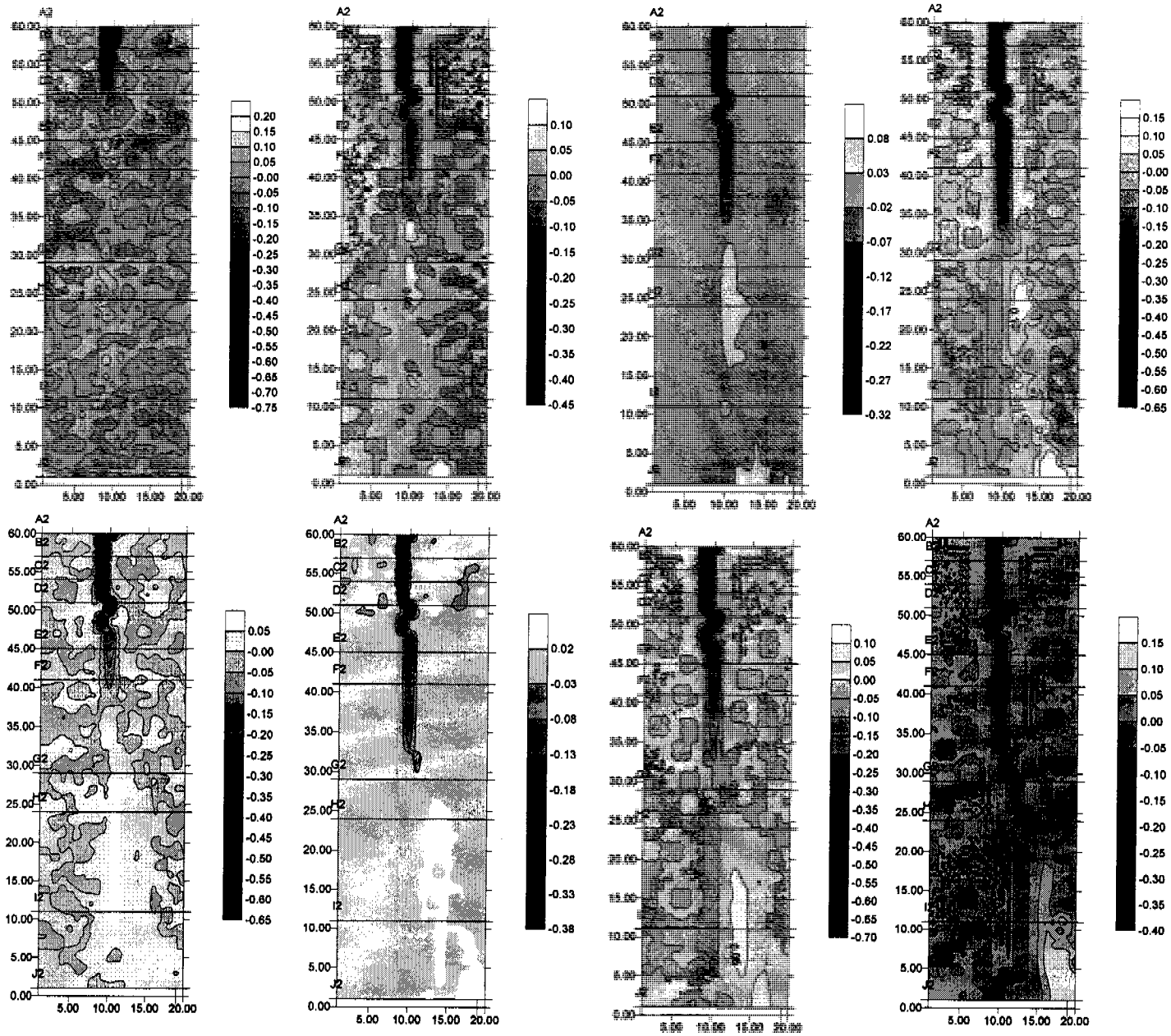

Figure 5.5.3: The morphology contour plots a) initial profile and 10 minutes, b) 10 minutes and 20 minutes, c) 20 minutes and 30 minutes, d) 30 minutes and 1 hour. The difference in elevations are also calculated from the remainder of the simulations with e) difference between 1 hours and 1.5 hours, f) 1.5 and 2 hours, g) 2 and 2.5 hours, and h) 2.5 and 3 hours.

The implementation of a series of three initial surfaces is not considered the usual adaptation for this model, and as such this application would represent an over-prediction of erosion depth for these simulations.

The implementation of the armouring component can be considered at the developmental stage, with a more realistic approximation devised when a depth coefficient of C~15, equating to a reduction factor of 1/30 when adopted. Figure 5.5.4, and Figure 5.5.5 illustrate these simulations, with Figure 5.5.6 highlighting the change in elevations between simulation time periods.

Maximum erosion depth, in this case reaches to only about 2 to 3m, approximately half of that observed in simulations observed in Section 5.1.

The development of the gully is similar between the lower erodibility coefficient and high erodibility coefficient, with more deposition of material with increased erosion associated with reduction factor of 1/10.

This is also verified when compared to the standard scenario Figure 5.1.1, and Figure 5.1.2, where the change in curvature at Row H to Row G is associated with accumulation of material and change in the path of the gully. Once again this behaviour is representative of an alteration in only one component, with the combination of these simulations with inclusion of randomised erodibility considered an even more realistic approximation.

Figure 5.5.7, and Figure 5.5.8 illustrate the effect of reduction of erodibility with depth on the extended batter site (Figure 5.1.4, and Figure 5.1.5). Similarities in development can be observed between these figures, however it is noted that from Figure $5.1.4_d$ compared to Figure $5.5.7_d$, that the gully can be seen to have developed to reach Row G, whereas it has reached only Row E in the earlier simulation. A similar comparison using Figure $5.5.4_d$ and Figure $5.1.1_d$ that although the gully depth of only about 10cm, the formation has reach almost Row I (at 60 minutes). Two explanations for this phenomenon, with reduction in transported sediment equating to a reduction in material deposited at the outlet of the gully resulting in drainage direction at these outlet points not being altered.

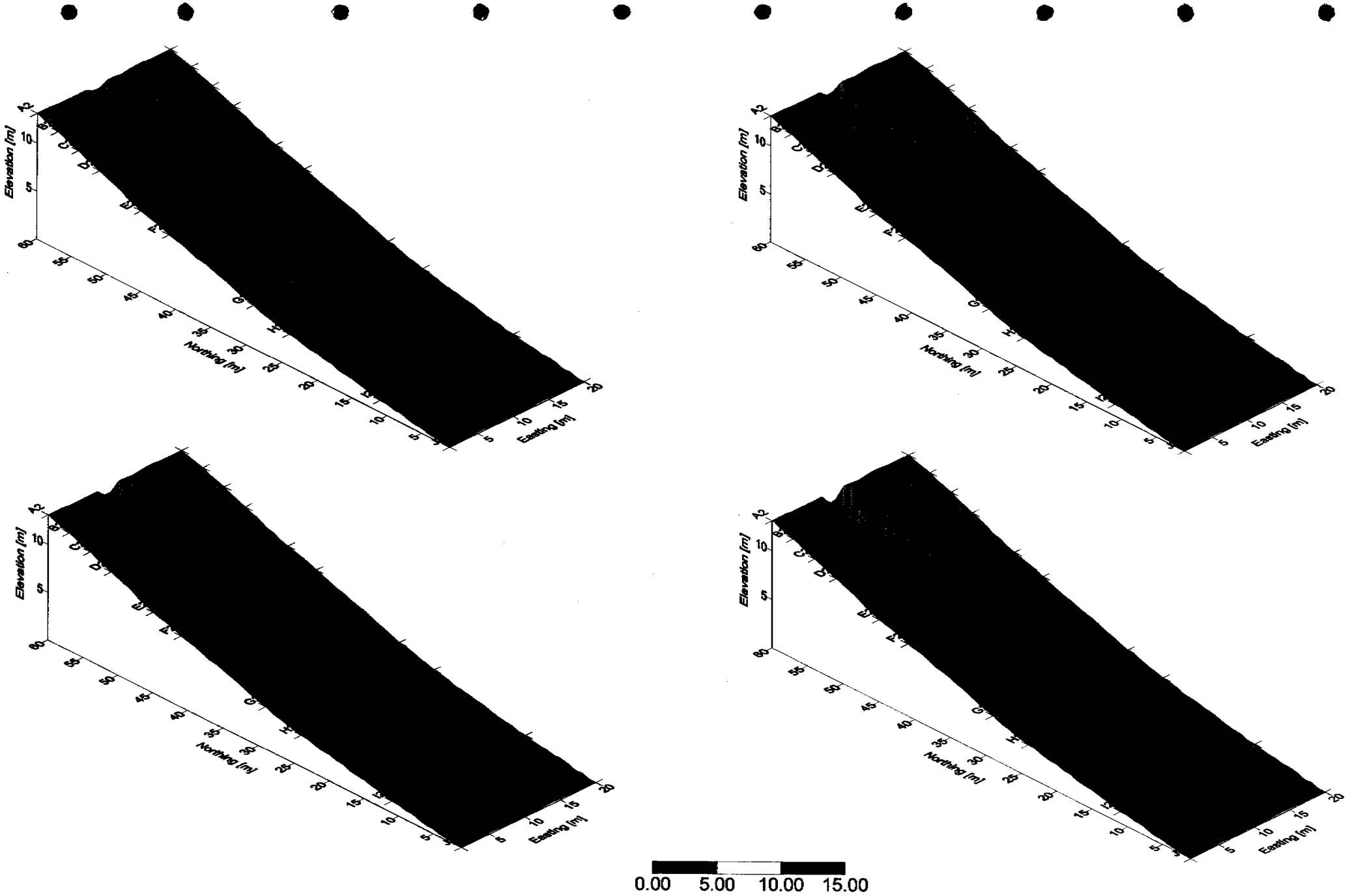

Figure 5.5.4: Simulations for standard batter slope profile with differential erodibility with depth function set at depth coefficient of 15, at a)10 minutes, b) 20 minutes, c) 30 minutes, and d) 1 hour.

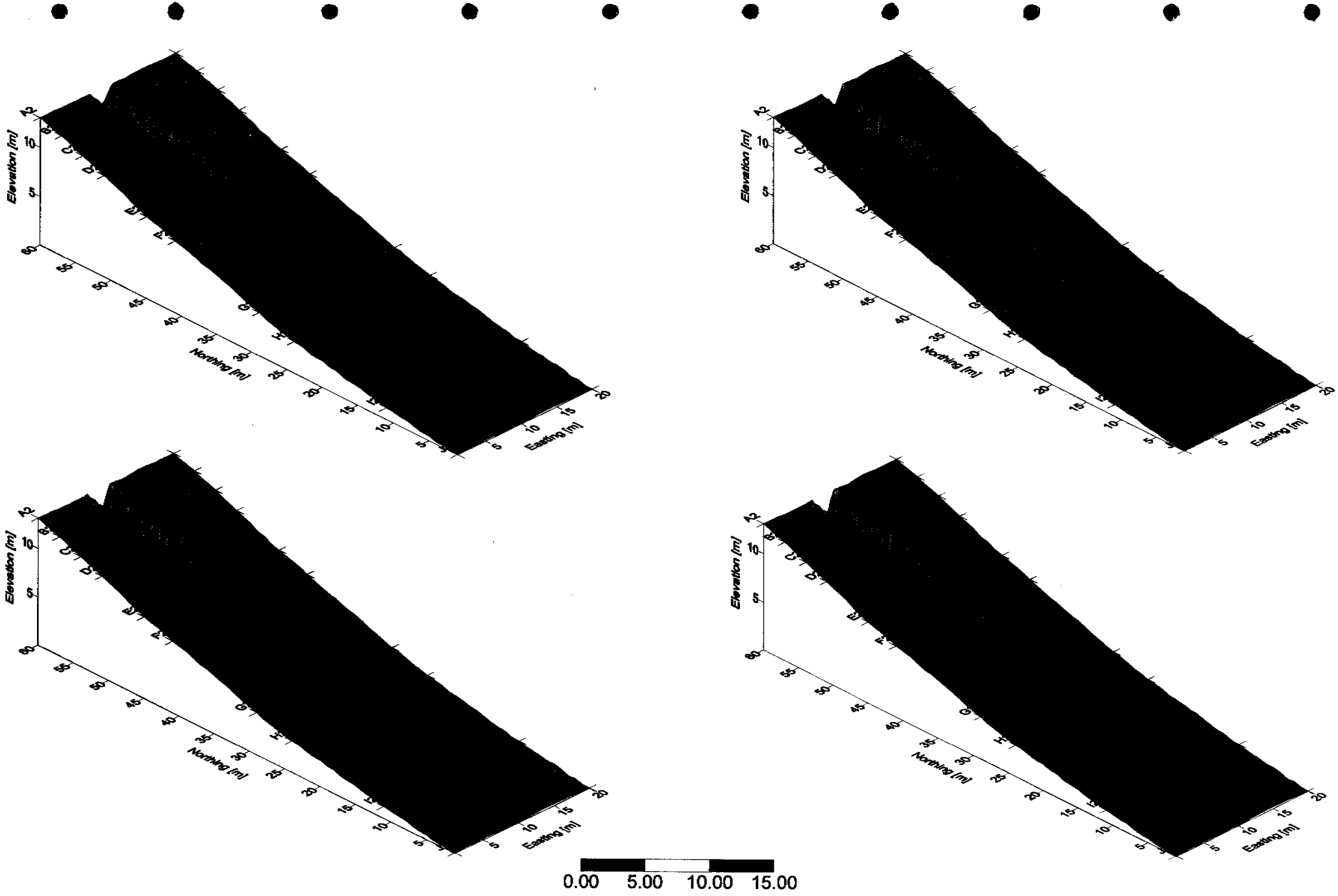

Figure 5.5.5: Simulations for standard batter slope profile with differential erodibility with depth function set at depth coefficient of 15, at a)1.5 hours, b) 2 hours this represents the second storm event, and c) 2.5 hours and d) 3 hours representing the final storm event.

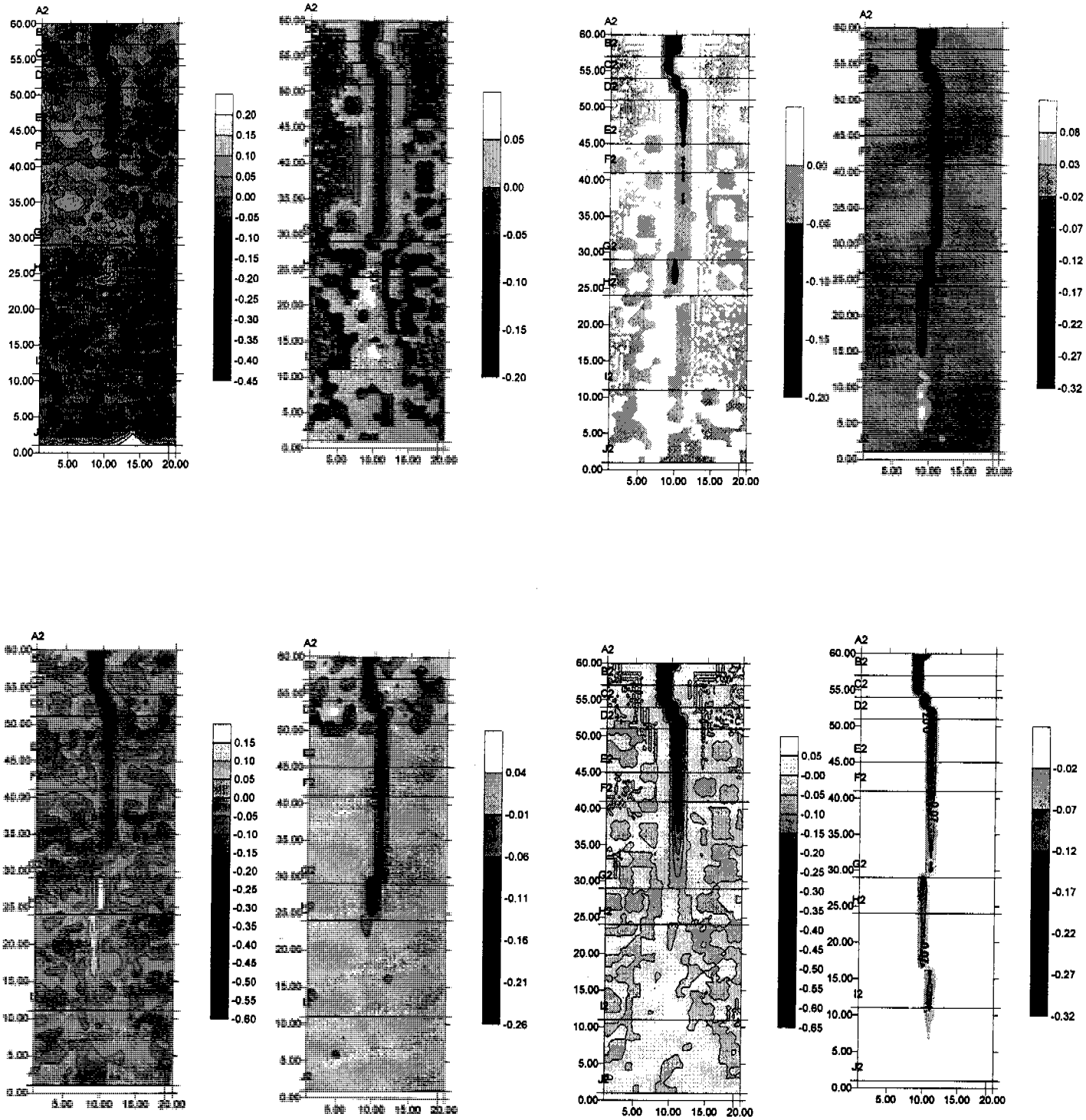

Figure 5.5.6: The morphology contour plots a) initial profile and 10 minutes, b) 10 minutes and 20 minutes, c) 20 minutes and 30 minutes, d) 30 minutes and 1 hour. The difference in elevations are also calculated from the remainder of the simulations with e) difference between 1 hours and 1.5 hours, f) 1.5 and 2 hours, g) 2 and 2.5 hours, and h) 2.5 and 3 hours.

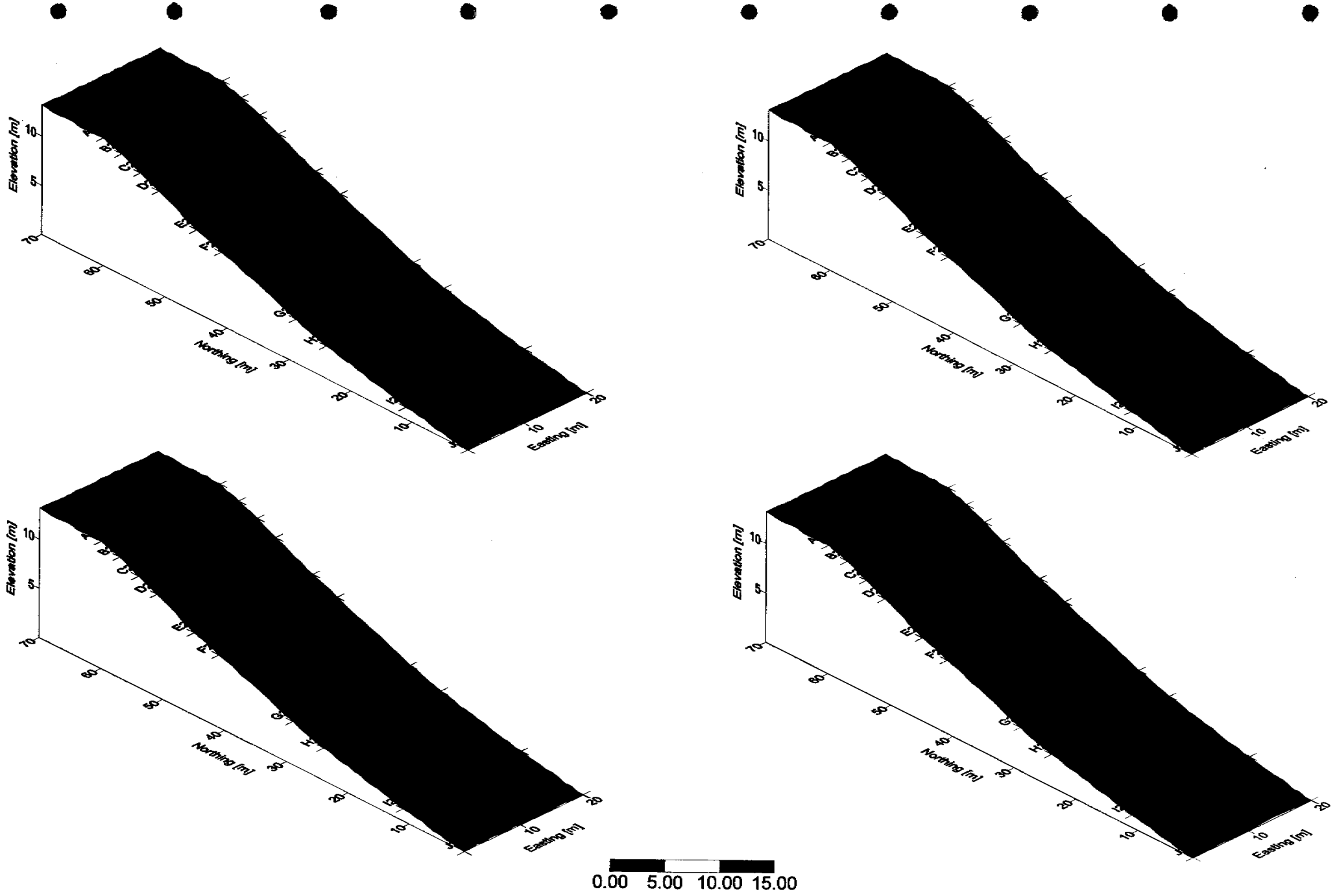

Figure 5.5.7: Simulations for extended batter slope profile with differential erodibility with depth, at a)10 minutes, b) 20 minutes, c) 30 minutes, and d) 1 hour.

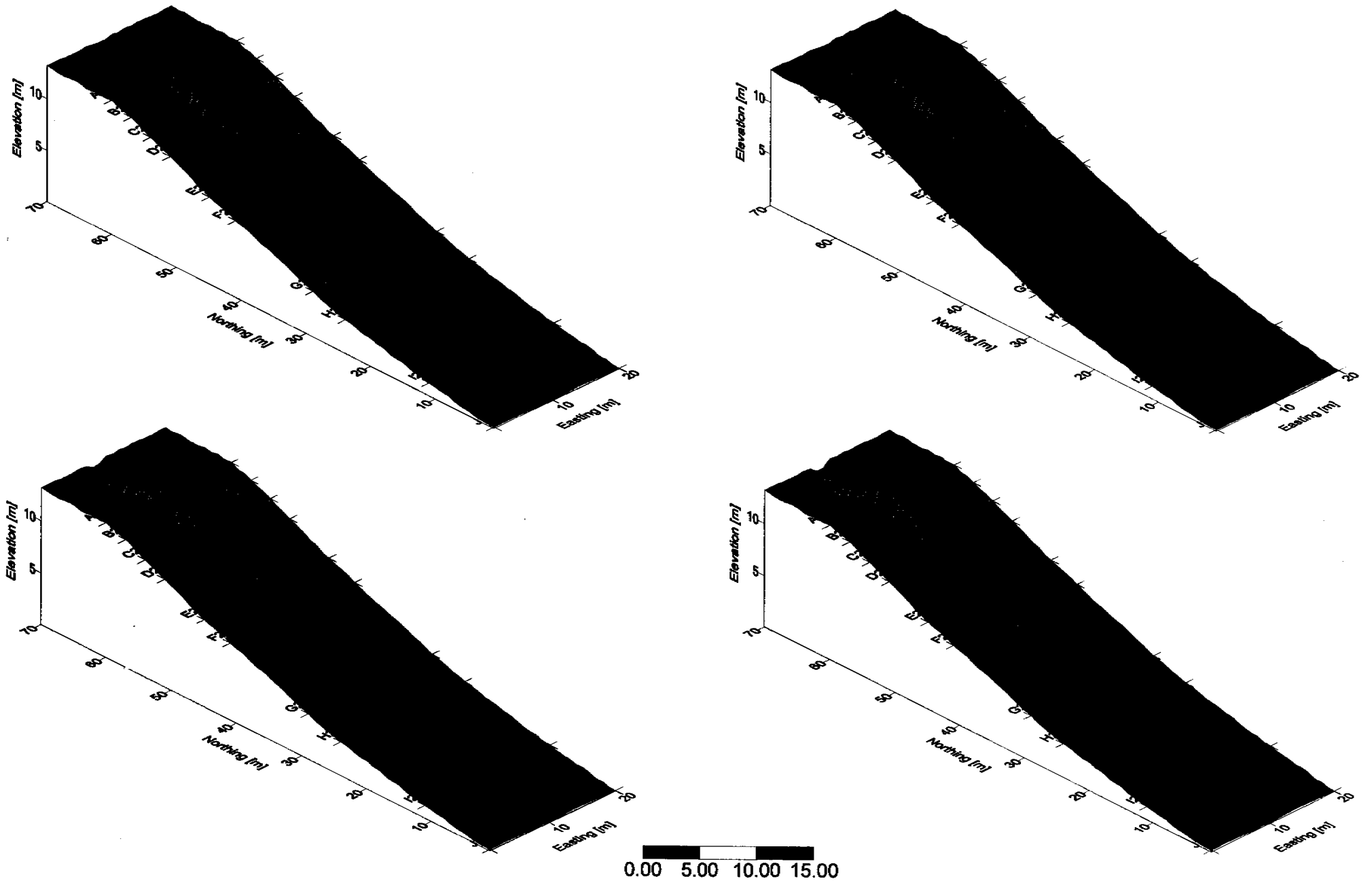

Figure 5.5.8: Simulations for extended batter slope profile with differential erodibility with depth function, at a)1.5 hours, b) 2 hours this represents the second storm event, and c) 2.5 hours and d) 3 hours representing the final storm event.

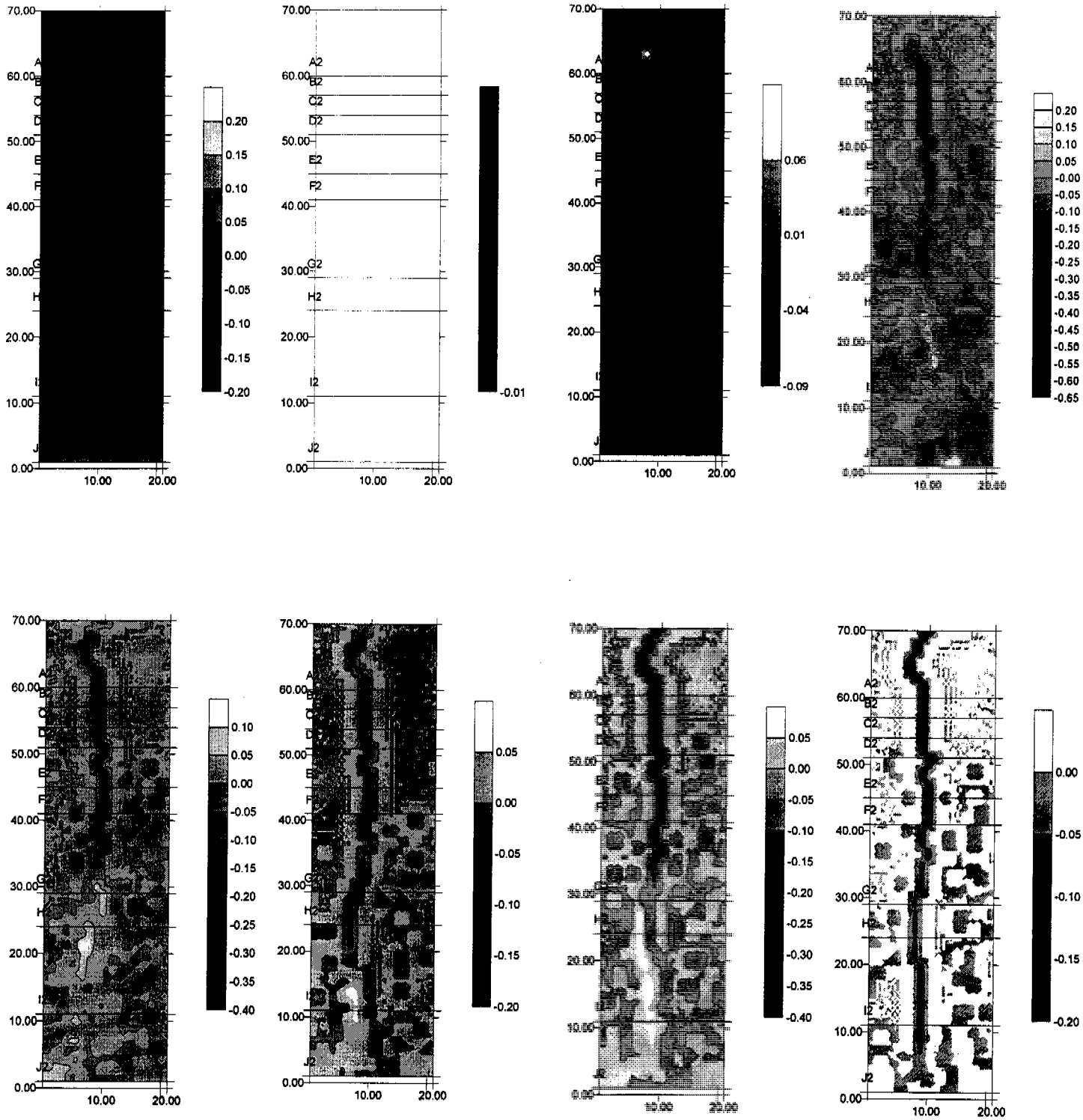

Figure 5.5.9: The morphology contour plots a) initial profile and 10 minutes, b) 10 minutes and 20 minutes, c) 20 minutes and 30 minutes, d) 30 minutes and 1 hour. The difference in elevations are also calculated from the remainder of the simulations with e) difference between 1 hours and 1.5 hours, f) 1.5 and 2 hours, g) 2 and 2.5 hours, and h) 2.5 and 3 hours.

This is observed in Figure $5.1.1_d$ where the gully has developed to beyond Row F, and has incised about 0.5 to 0.8m at this point, whilst the gully in Figure $5.5.4_d$ has developed to Row H with depths of about 40cm at Row F and 10cm noticeable due to the uniform nature of the material. Material deposited at the outlet of the gully in Figure $5.1.1_d$ is not apparent in Figure $5.5.4_d$.

The other observation is made by the comparison between Figure $5.5.4_d$ and $5.5.5_d$ at 60 minutes and 1.5 hours respectively, where material from increased incision of the gully in the upper section smothers the 10cm pathway revealed at the 60 minute time period. This is illustrated in Figure 5.5.6 where about 10 to 15cm of material is deposited over the gully at Row H to Row I. This suggests a change in the overall discharge relationship β_3 from 0.00272 to 0.00199 has an impact on the nature of erosion at these points, with the same observation made comparing Figure $5.5.7_a$ and Figure $5.5.8_a$ with shallow formation at the bottom end of slope smothered by introduction of consequent storm event.

The next considerations were the combination of randomised erodibility and the depth-erodibility coefficient for both the usual cases including increased inlet width, whilst similarities between simulations without inclusion of wide inlet verify previous observations.

The first scenario is illustrated Figure 5.5.10, with Figure 5.5.11 representing the second and third storm events with narrow inlet feed and the combination of characteristics from randomised erodibility and armouring erosion module. Figure 5.5.12 exhibits an obvious combination of characteristics from investigations above. The depth of erosion is similar to that observed in Figure 5.5.4 and Figure 5.5.5, with the nature of pathway being altered due to the randomised erodibility as expected.

The maximum depth of erosion for simulations incorporating the wide inlet point can be considered similar to Figure 5.5.4, and Figure 5.5.5. Below the inlet zone of influence at Row C in Figure 5.5.13, and Figure 5.5.14, the gully congregates into a single flowpath once again with depth of erosion observed to replicate that of comparative figures.

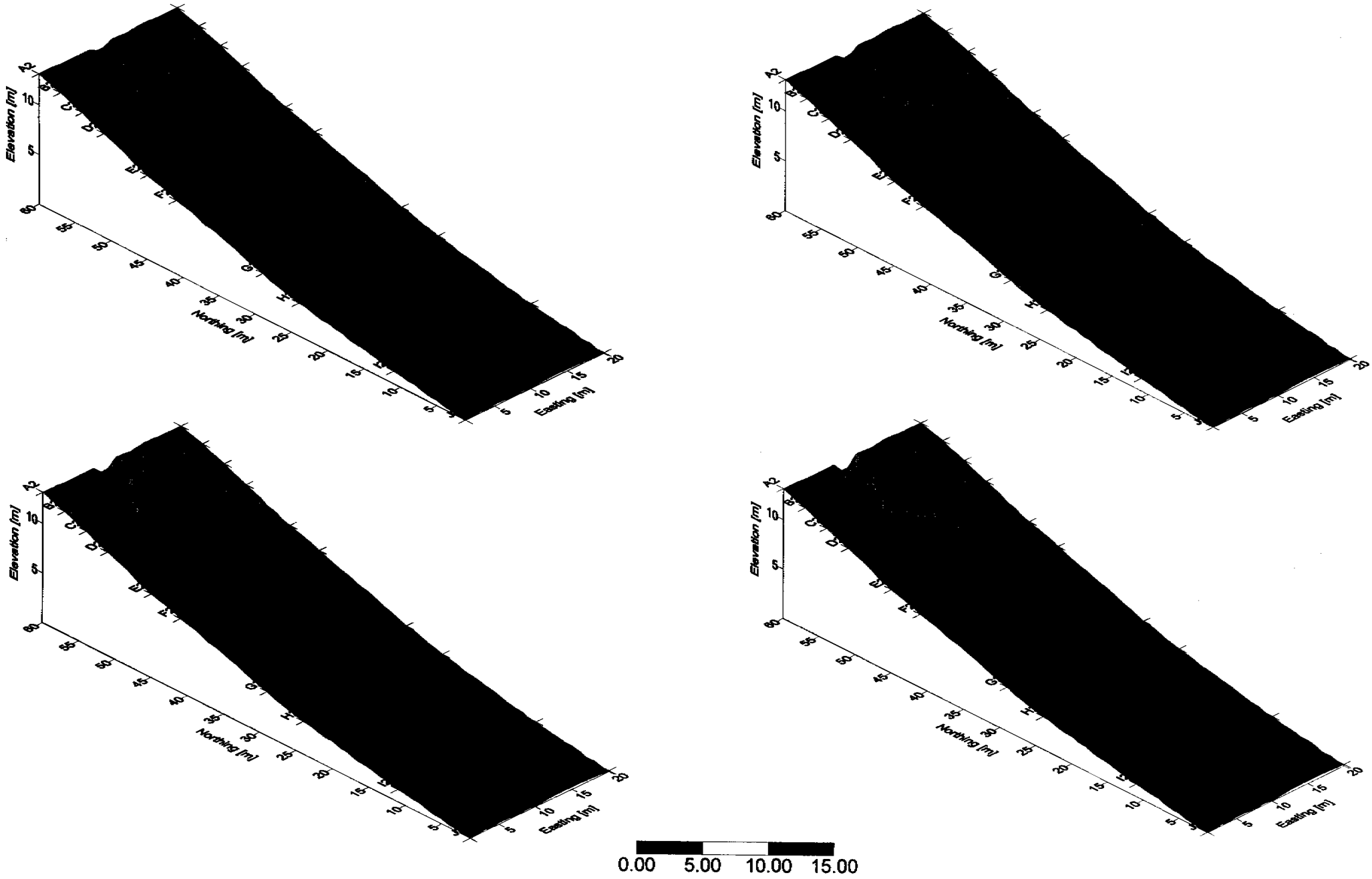

Figure 5.5.10: Simulations for standard batter slope profile with differential erodibility with depth, and randomised erodibility function, at a)10 minutes, b) 20 minutes, c) 30 minutes, and d) 1 hour.

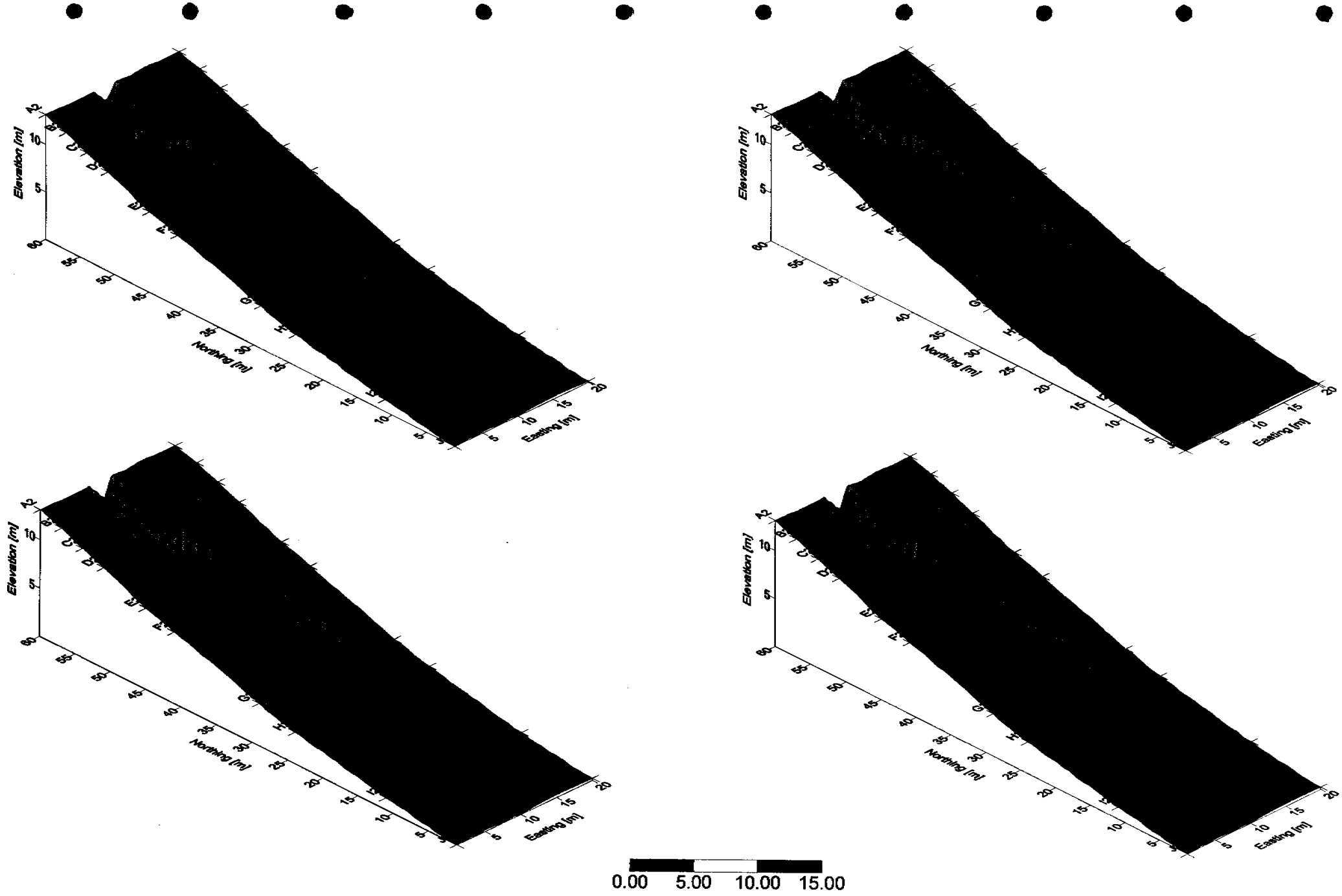

Figure 5.5.11: Simulations standard batter slope profile with differential erodibility with depth, and randomised erodibility function, at a)1.5 hours, b) 2 hours this represents the second storm event, and c) 2.5 hours and d) 3 hours representing the final storm event.

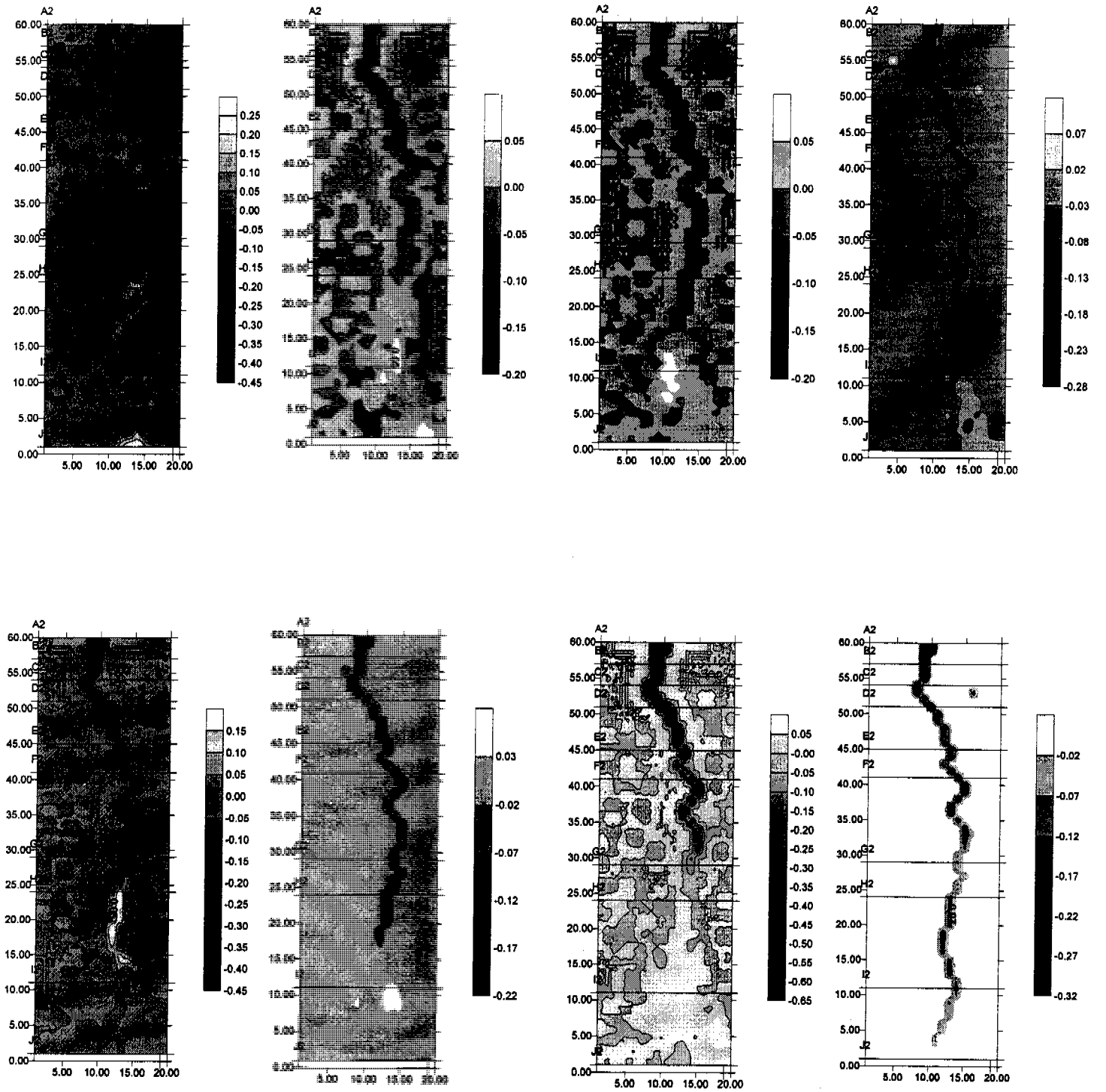

Figure 5.5.12: The morphology contour plots a) initial profile and 10 minutes, b) 10 minutes and 20 minutes, c) 20 minutes and 30 minutes, d) 30 minutes and 1 hour. The difference in elevations are also calculated from the remainder of the simulations with e) difference between 1 hours and 1.5 hours, f) 1.5 and 2 hours, g) 2 and 2.5 hours, and h) 2.5 and 3hours.

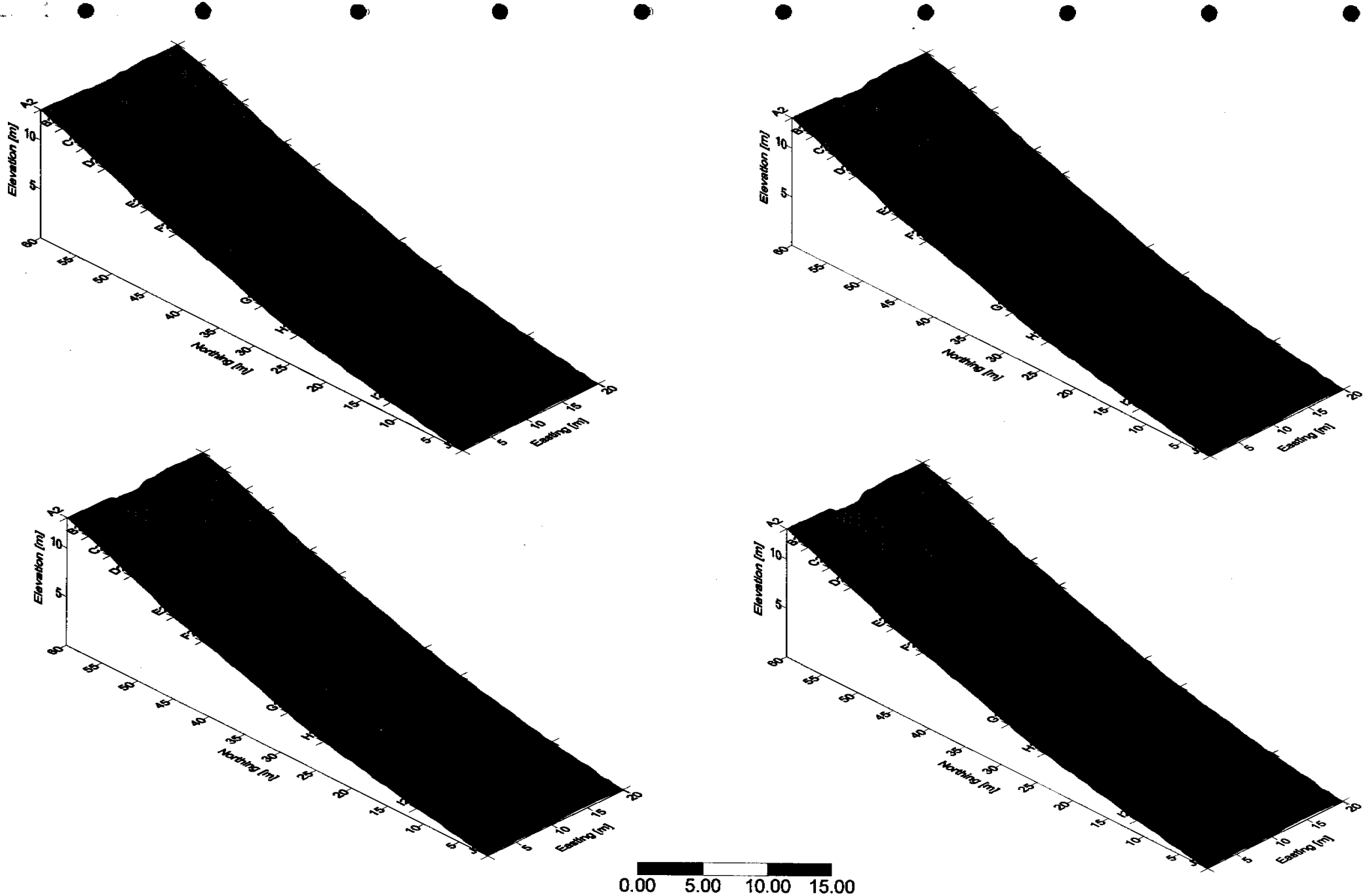

Figure 5.5.13: Simulations for standard batter slope profile with differential erodibility with depth, and randomised erodibility function, as well as wide inlet point, at a)10 minutes, b) 20 minutes, c) 30 minutes, and d) 1 hour.

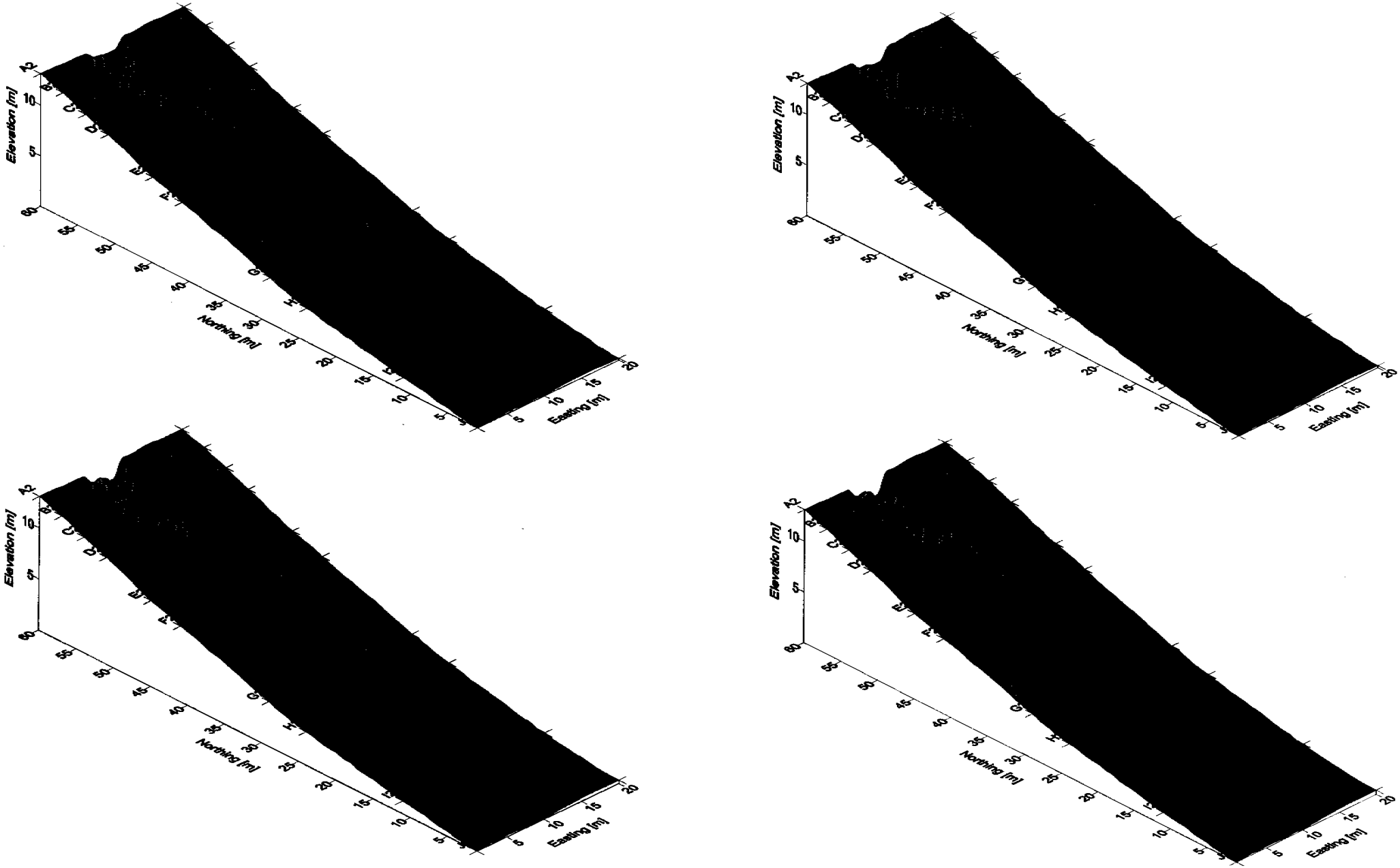

Figure 5.5.14: Simulations standard batter slope profile with differential erodibility with depth, and randomised erodibility function, as well as wide mesh point, at a) 1.5 hours, b) 2 hours this represents the second storm event, and c) 2.5 hours and d) 3 hours representing the final storm event.

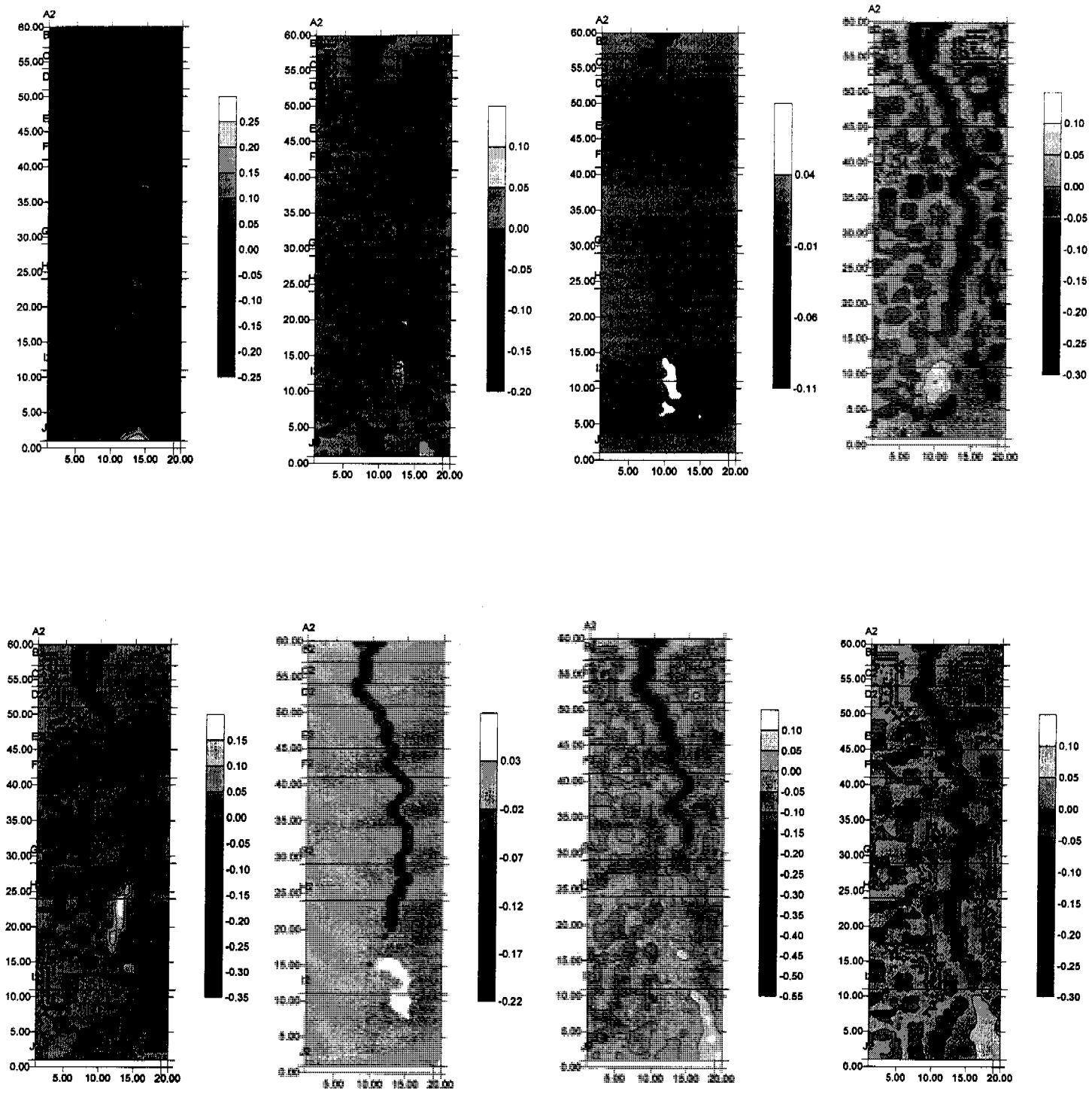

Figure 5.5.15: The morphology contour plots a) initial profile and 10 minutes, b) 10 minutes and 20 minutes, c) 20 minutes and 30 minutes, d) 30 minutes and 1 hour. The difference in elevations are also calculated from the remainder of the simulations with e) difference between 1 hours and 1.5 hours, f) 1.5 and 2 hours, g) 2 and 2.5 hours, and h) 2.5 and 3 hours.

Further investigations consider the same scenarios with the extended batter slope profile, where similar behaviour is exhibited in Figure 5.5.16, Figure 5.5.17 for narrow inlet point, and Figure 5.5.19, and Figure 5.5.20 for wide inlet point respectively.

The gully formation at 60 minutes duration is compared to observations on site in Figure 3.2.6 above, with results of first storm event excavating material between Row B and Row D and gully extending down to Row G. Approximately 40 to 50cm depth of material was transported between Row C to Row D whereas from Figure 5.5.15, a total depth of 60 to 70cm was predicted. It is noted that the initial delay in gully development observed in earlier simulations is repeated in Figure 5.5.19 and Figure 5.5.20 even though final landscapes are of similar extent and magnitude.

The maximum depth of erosion at the head of the gully was 2.2m for the standard case, and 1.9m overall for the extended profile scenario (Figure $5.5.18_d$ and Figure $5.5.20_d$ respectively). This represents an over-prediction with maximum depth observed on site at Row A in the order of 20 to 25cm, however as noted, this transition was considered to be heavily armoured and buffered due to the reservoir.

The formation of shallow tributaries ahead of the main gully was also observed on site, with 10 to 20cm depth seen in Figure 5.5.17d) of comparable magnitude to that seen in Figure 3.2.4, Figure 3.2.5, Figure 3.2.6.

The final landform pictured in Figure $5.5.18_d$ illustrates a few noteworthy characteristics, with depth of gully increasing uniformly in the upper sections of the slope, and movement of the formation down the hillslope, combined with deposition of material observed between Row H to Row I. The development observed on site is comparable, with deposition of material observed between Row H and Row I and excavation of material to a maximum depth of 60 to 70cm at Row G.

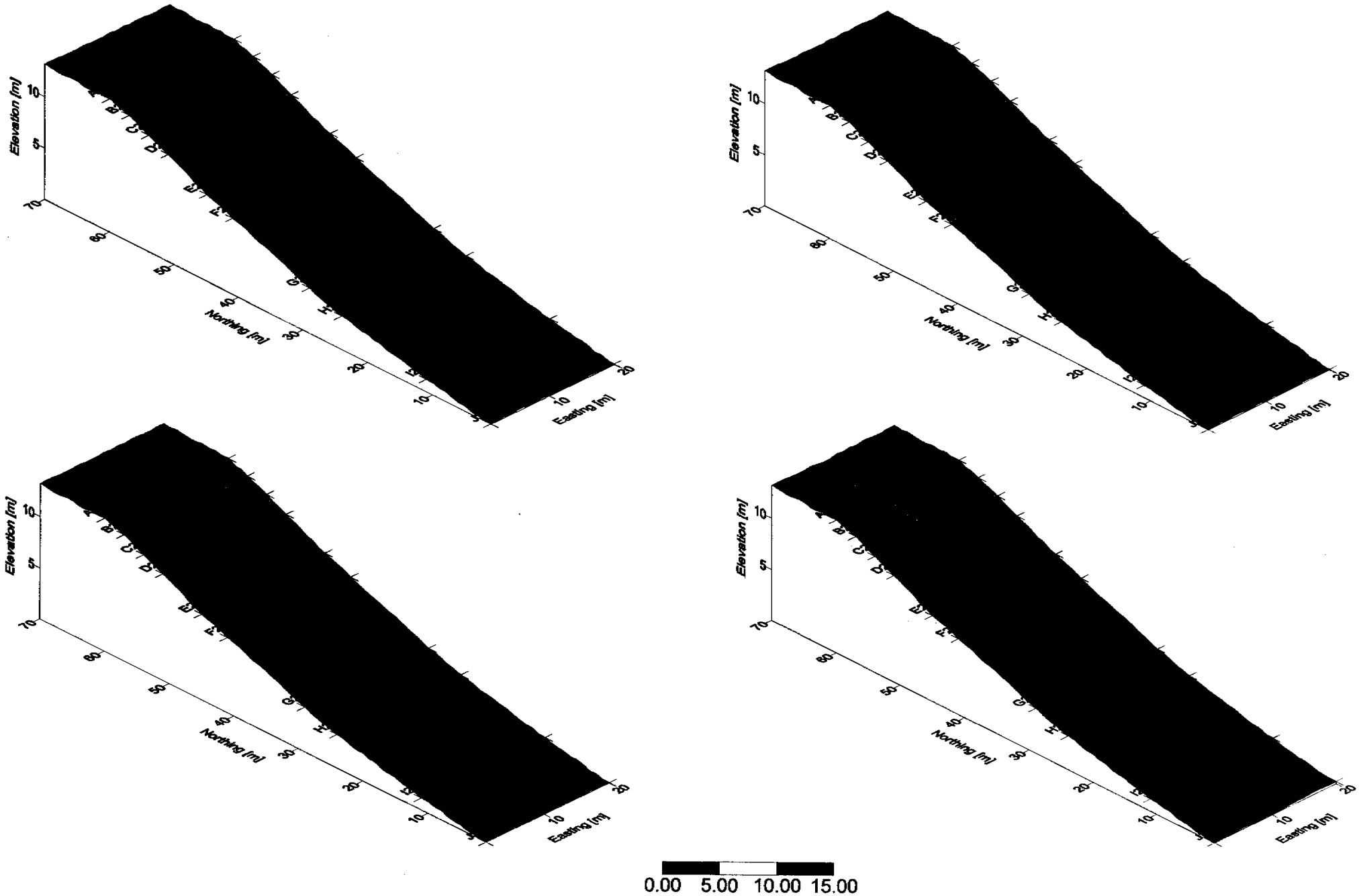

Figure 5.5.16: Simulations for extended batter slope profile with differential erodibility with depth, and randomised erodibility function, at a)10 minutes, b) 20 minutes, c) 30 minutes, and d) 1 hour.

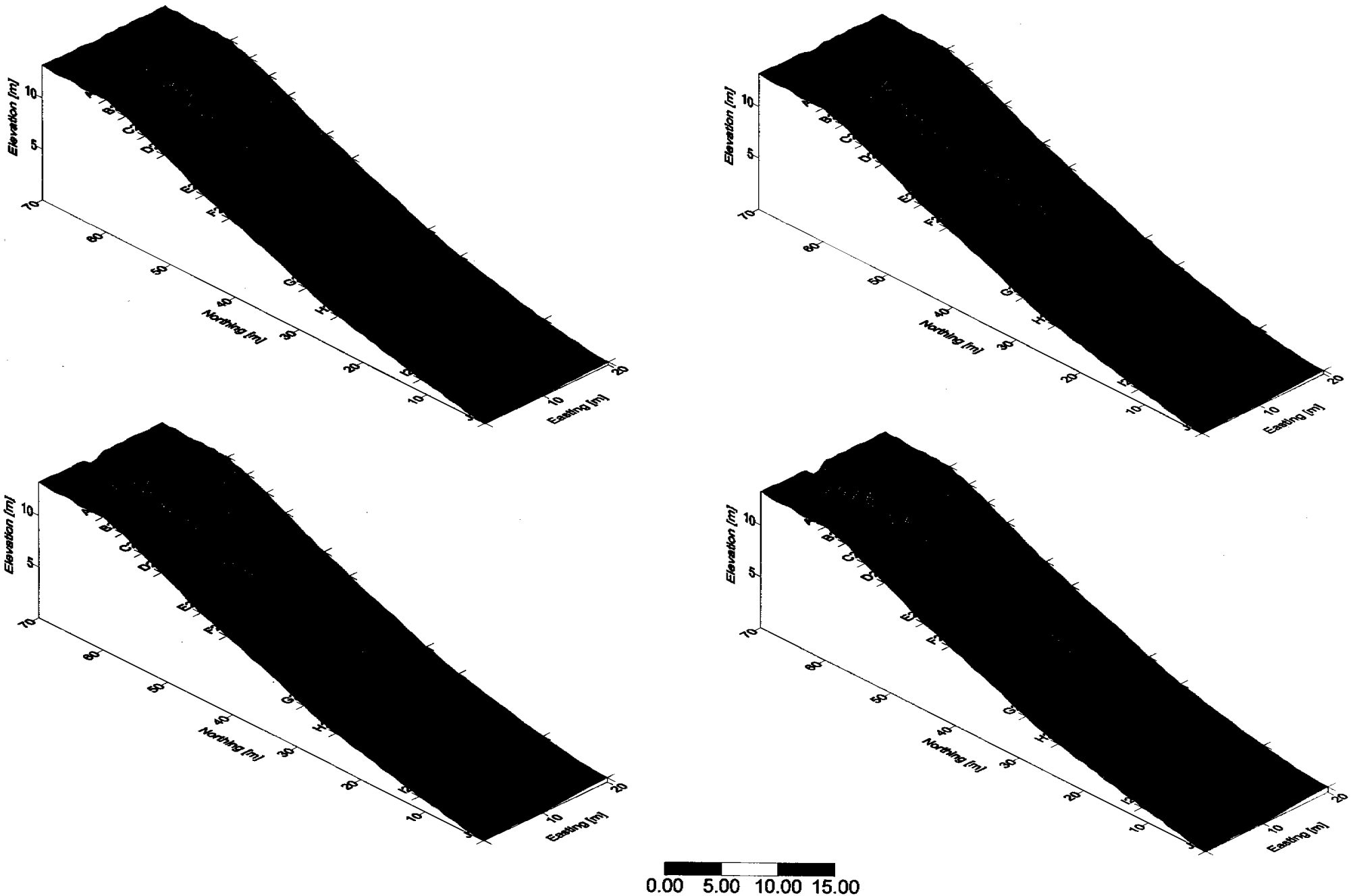

Figure 5.5.17: Simulations extended batter slope profile with differential erodibility with depth, and randomised erodibility function, at a)1.5 hours, b) 2 hours this represents the second storm event, and c) 2.5 hours and d) 3 hours representing the final storm event.

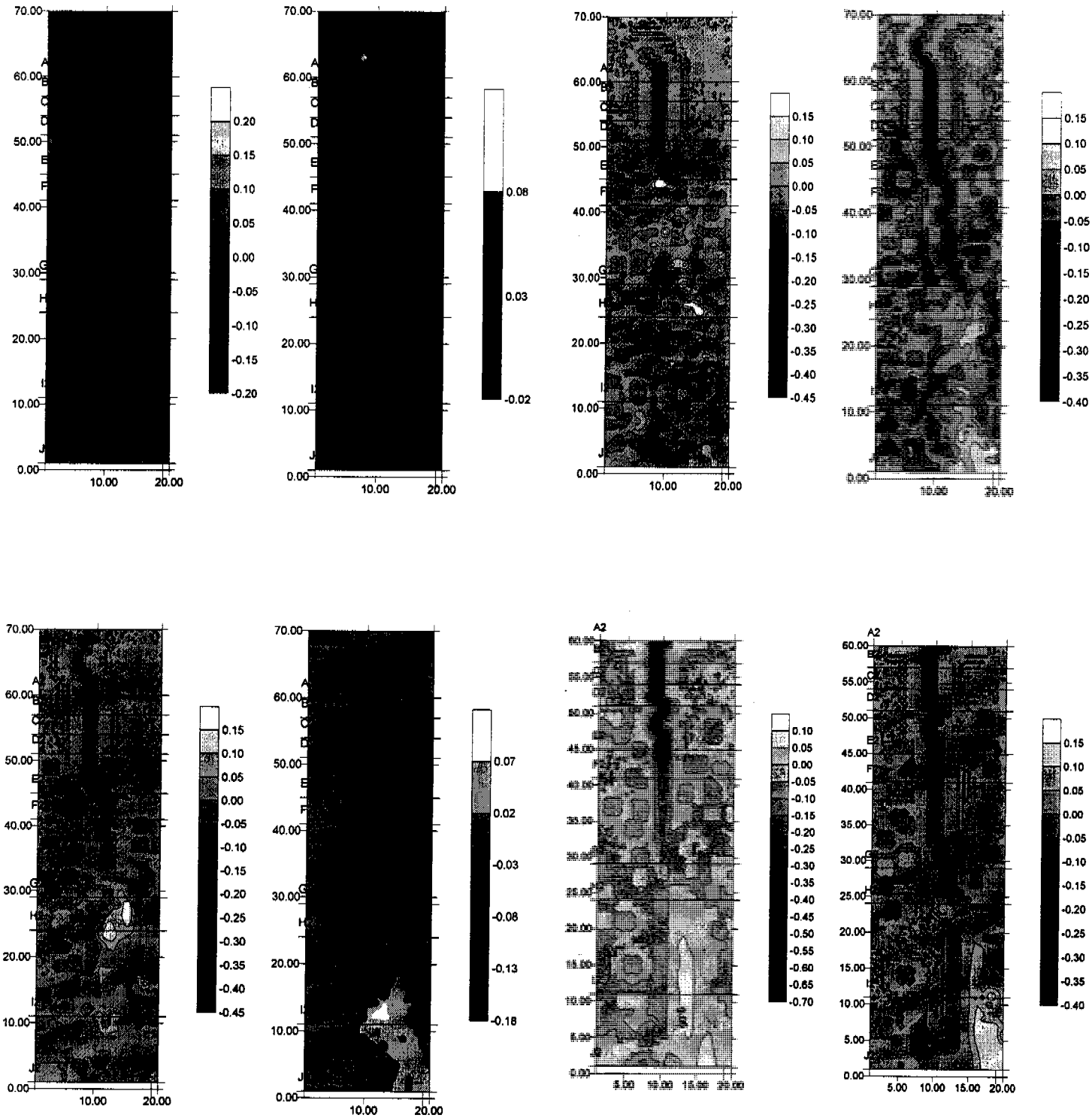

Figure 5.5.18: The morphology contour plots a) initial profile and 10 minutes, b) 10 minutes and 20 minutes, c) 20 minutes and 30 minutes, d) 30 minutes and 1 hour. The difference in elevations are also calculated from the remainder of the simulations with e) difference between 1 hours and 1.5 hours, f) 1.5 and 2 hours, g) 2 and 2.5 hours, and h) 2.5 and 3hours.

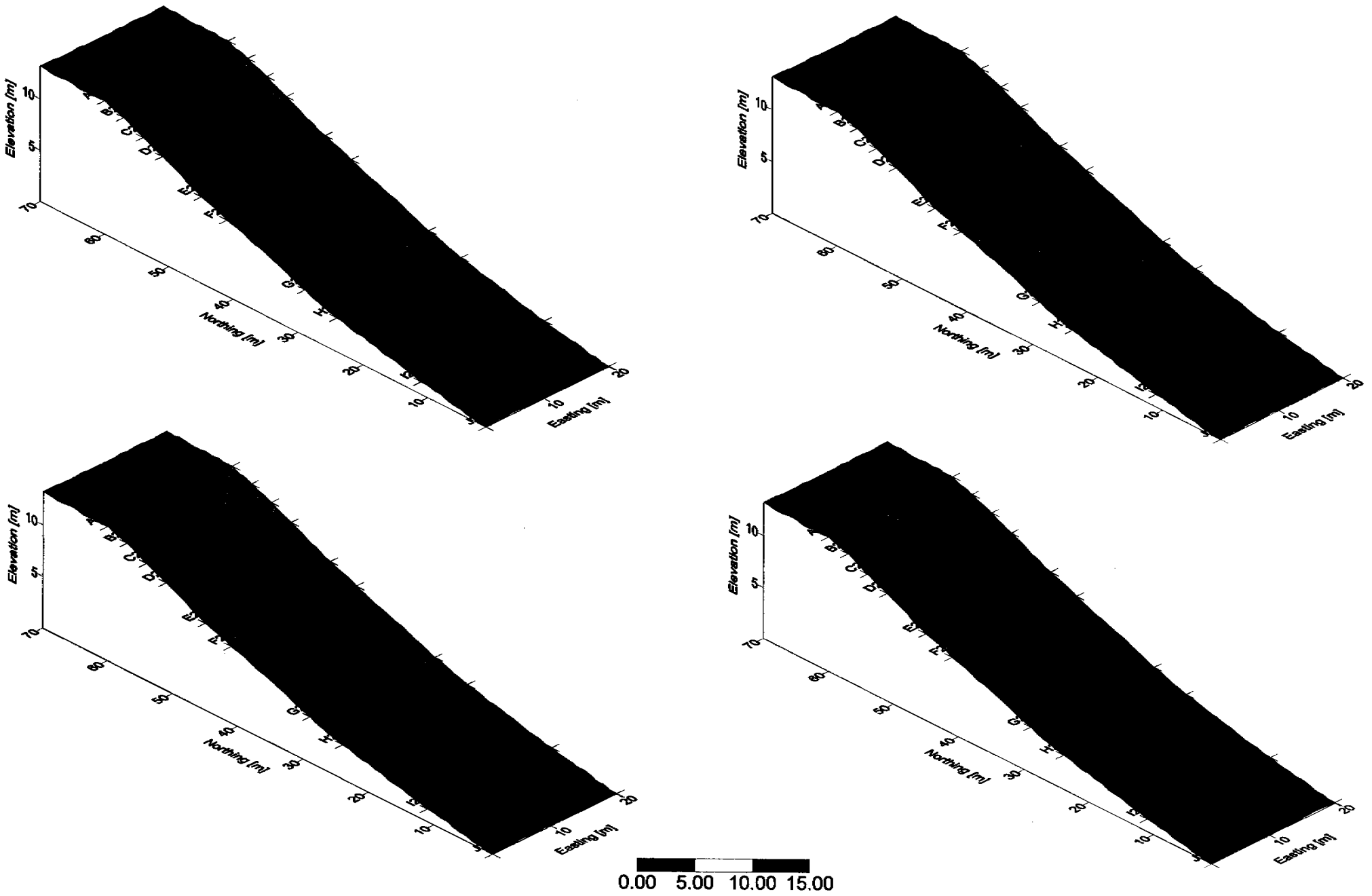

Figure 5.5.19: Simulations for extended batter slope profile with differential erodibility with depth, and randomised erodibility function, as well as wide inlet point, at a)10 minutes, b) 20 minutes, c) 30 minutes, and d) 1 hour.

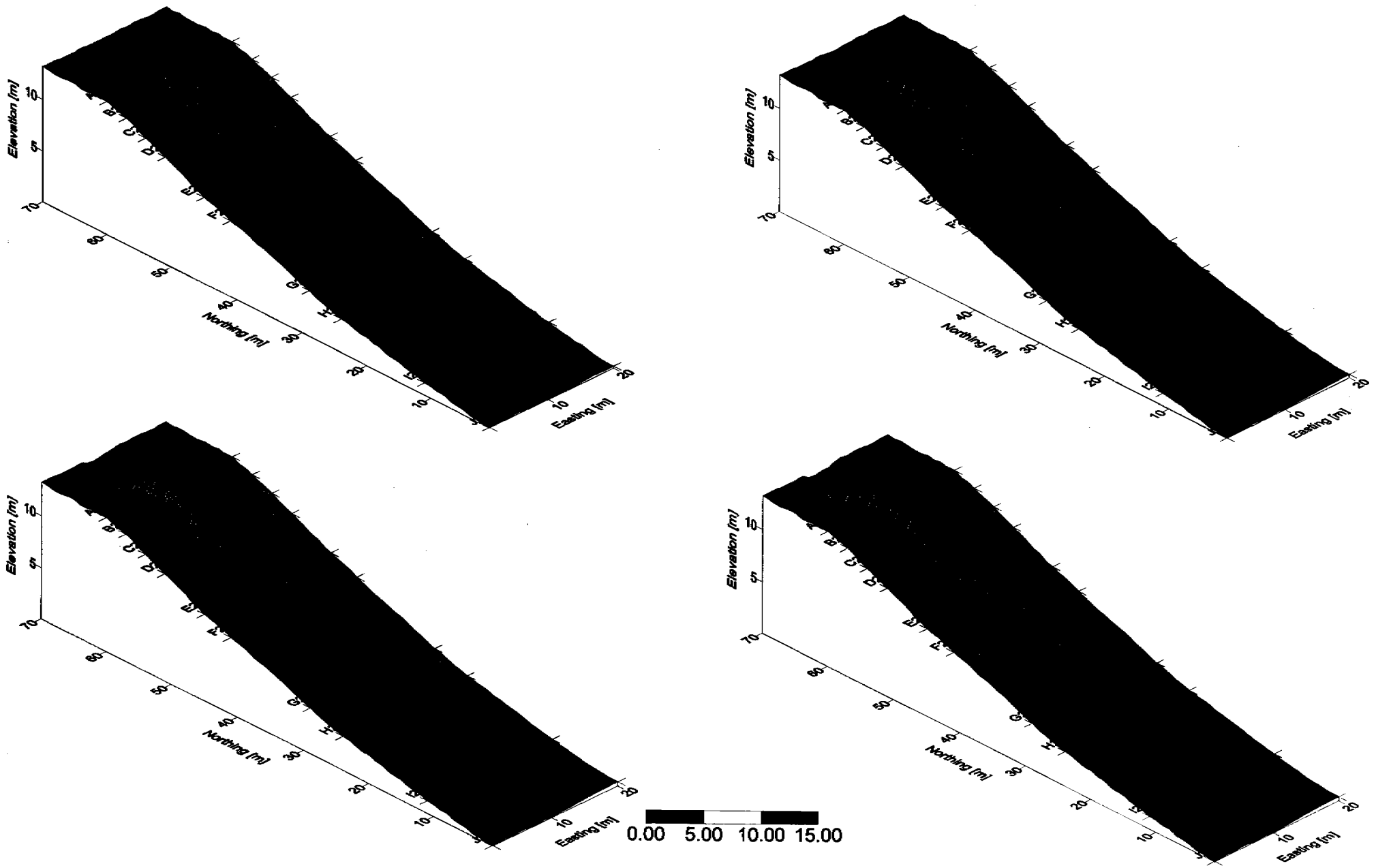

Figure 5.5.20: Simulations extended batter slope profile with differential erodibility with depth, and randomised erodibility function, as well as wide inlet point, at a)1.5 hours, b) 2 hours this represents the second storm event, and c) 2.5 hours and d) 3 hours representing the final storm event.

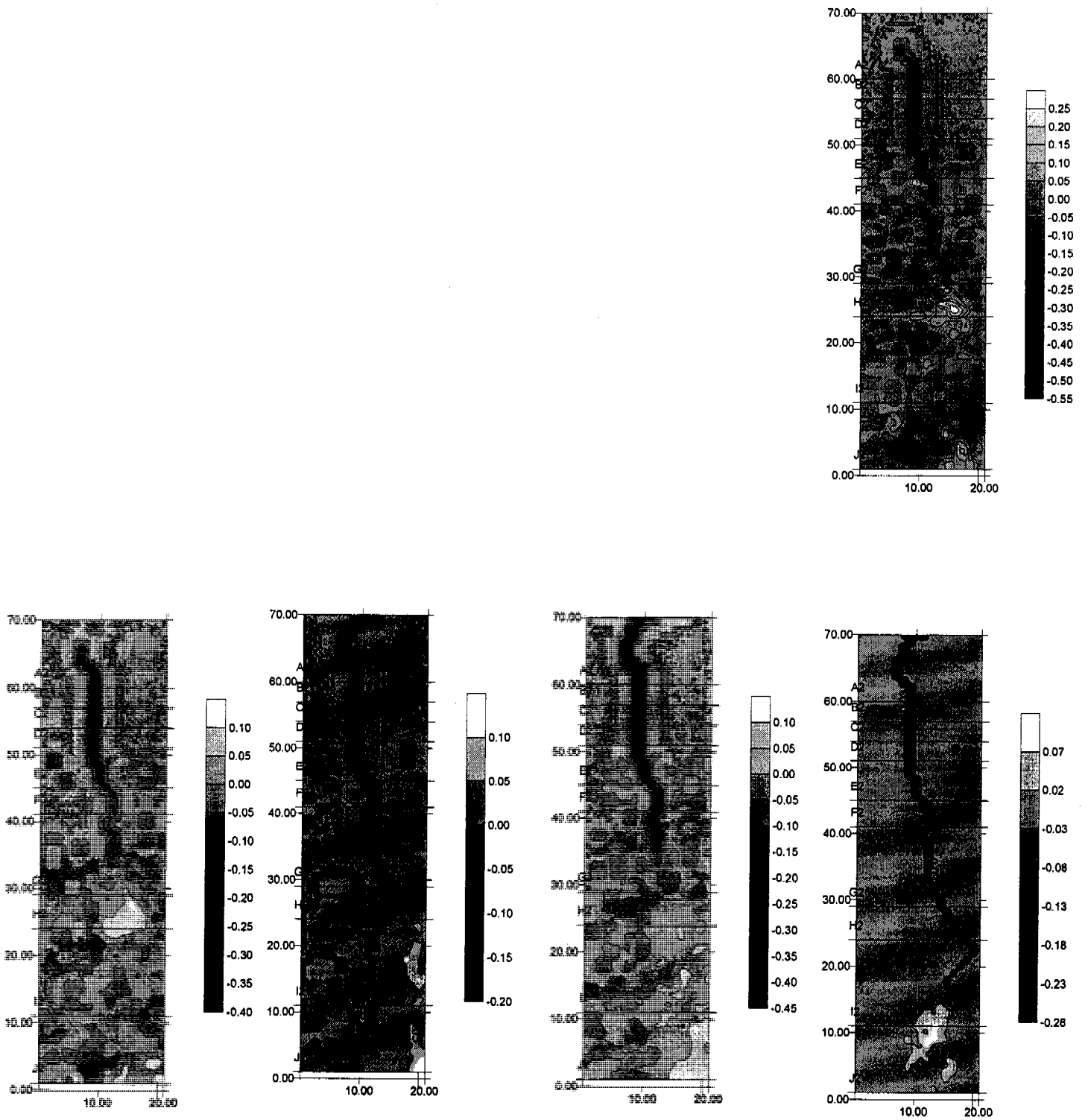

Figure 5.5.21: The morphology contour plots a) initial profile and 10 minutes, b) 10 minutes and 20 minutes, c) 20 minutes and 30 minutes, d) 30 minutes and 1 hour. The difference in elevations are also calculated from the remainder of the simulations with e) difference between 1 hours and 1.5 hours, f) 1.5 and 2 hours, g) 2 and 2.5 hours, and h) 2.5 and 3 hours.

The incision at Row A in Figure 5.5.19, reaches a maximum depth of 1.8m with depth at 60 minutes reaching 60cm. Development of the gully at this point has begun to extend back into the catchment, whilst 20cm shallow tributaries extend down to Row F. Although these figures represent 2 different development scenarios, the overall depth of erosion and extent are similar (Figure 5.5.18, and Figure 5.5.20).

The depth of incision into the catchment reaches 1.5m just before the transition point back to 50cm adjacent to the inlet point, and reflects a similar observation to that seen in Figure 5.1.4 at 60 minute mark. In this figure the pathway adopted is identical, confirming that development follows the same process by extending backward from the incision point. The depth of incision at 60 minutes was only 60cm as stated above, whereas 1.8m was predicted with the standard profile.

These landforms perhaps represent the closest approximation devised from the modelling process, and can be considered a reasonable estimate. Depth within the gully of either of the two important simulations of Figures 5.5.18, or Figure 5.5.20 between 1.8 m and 0.6m for Rows A to Row C with 0.6m gully representing the depth of the secondary tributary observed in Figure 5.5.18.

5.6 Slope Final

The final modelling regime considered was the modification of the exponent on the slope term in the sediment transport equation, n_1. This investigation generated surfaces illustrated in Section 5.2, with none of the additional erosion modules enabled. As noted, the results seen in these figures were considered dramatic with maximum depths of erosion about 11m by end of the monitoring period, with a maximum depth of 5m observed in the extended profile case.

The final model scenarios investigated included all of the erosional modules, with slope exponent n_1 altered from 2.1 to 0.69. The slope exponent n_1 was considered the most sensitive parameter, with field observations indicating a significant change in erodibility with depth. The batter slope profile and extended profile were both investigated, with depths of erosion at the head of the gully reaching 4m, for the standard profile case.

The extended profile, however does not erode significantly, with gully development considerably slower than that observed in previous simulations with inclusion of wide inlet. Maximum depth of erosion, and development behaviour is sporatic, with comparisons favourable between these simulations and observed depths.

Also noted that the gully does not extend from the transition point (Row A) back into the cap site with this simulation, and it is suggested that this is a product of the combination of the armouring component and similar observations in Section 5.3.

As noted, the derivation of this exponent is dependent on mean particle diameter and hence considered subjective. The maximum depth of erosion at the head of the gully was 3 to 4 m, with this prediction greater than that observed in Figure 5.5.14 at about 2 m. owever the depths of erosion below this initial inlet zone, Row C, are comparable, although the rate of development of the gully is much more rapid, with the gully extending to the bottom of the slope within the first storm event. The simulation also exhibits some indication of numerical instability, although for the extended profile, similar behaviour to that observed in Figure 5.2.4, and 5.2.5 where the wide inlet point given the fitted value of n_1 at 0.69 resulted in the gully not developing, as incision at transition point did not occur.

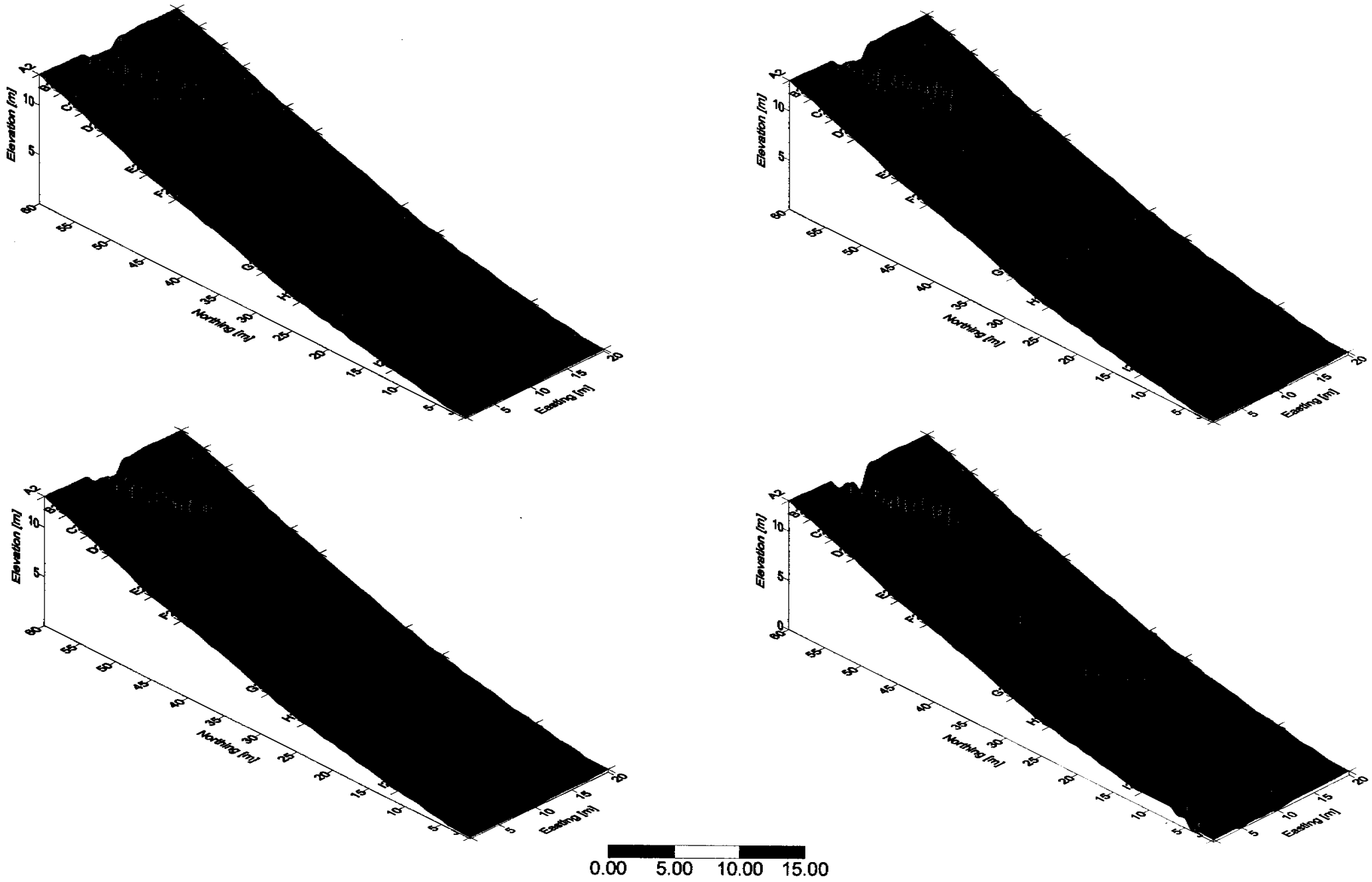

Figure 5.6.1: Simulations for standard batter slope profile with differential erodibility with depth, and randomised erodibility function, together with wide inlet point and n_1 slope exponent at 0.69 instead of 2.1, at a)10 minutes, b) 20 minutes, c) 30 minutes, and d) 1 hour.

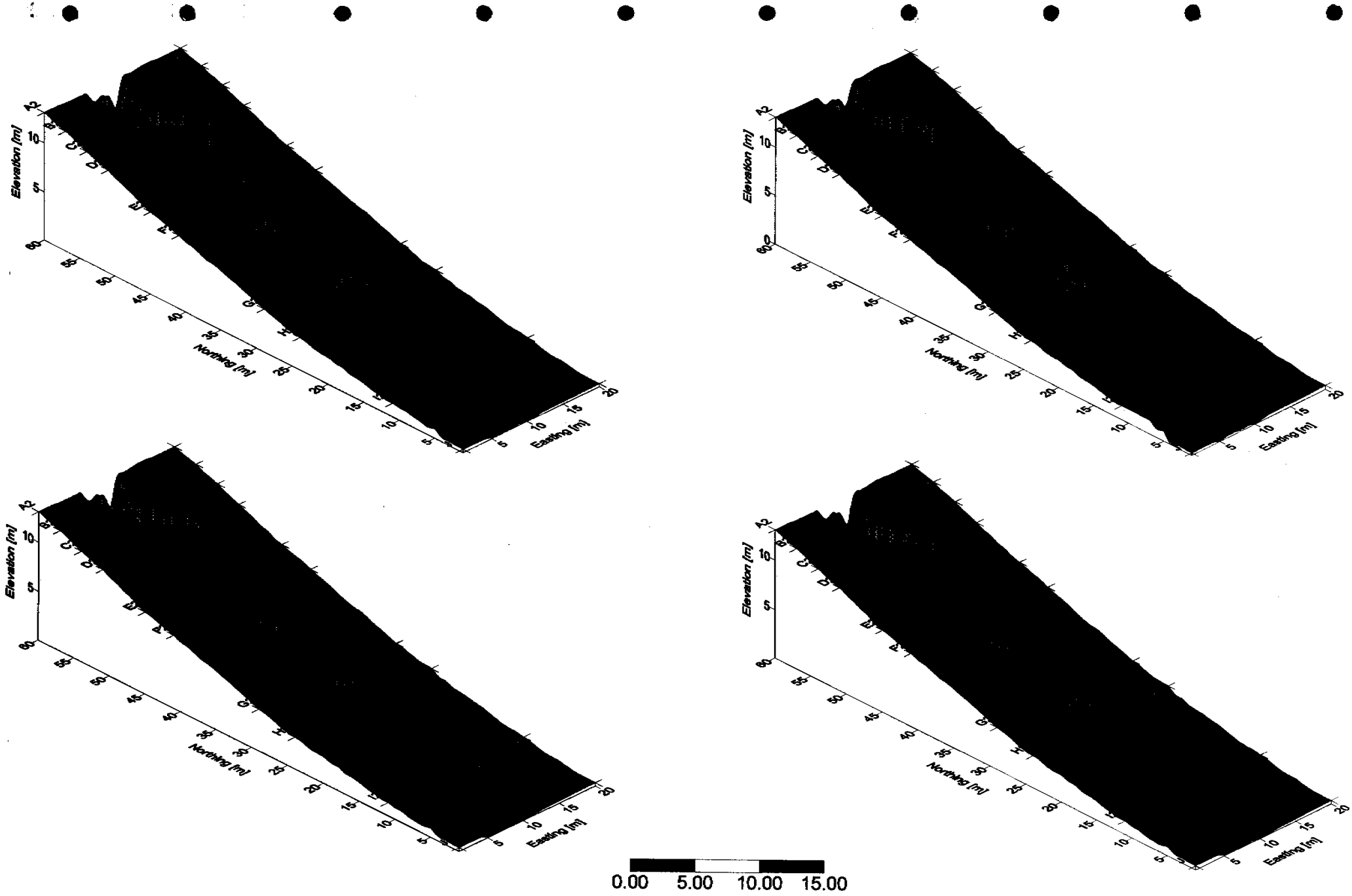

Figure 5.6.2: Simulations standard batter slope profile with differential erodibility with depth, and randomised erodibility function, together with wide inlet point and n_1 slope exponent at 0.69 instead of 2.1, at a)1.5 hours, b) 2 hours this represents the second storm event, and c) 2.5 hours and d) 3 hours representing the final storm event.

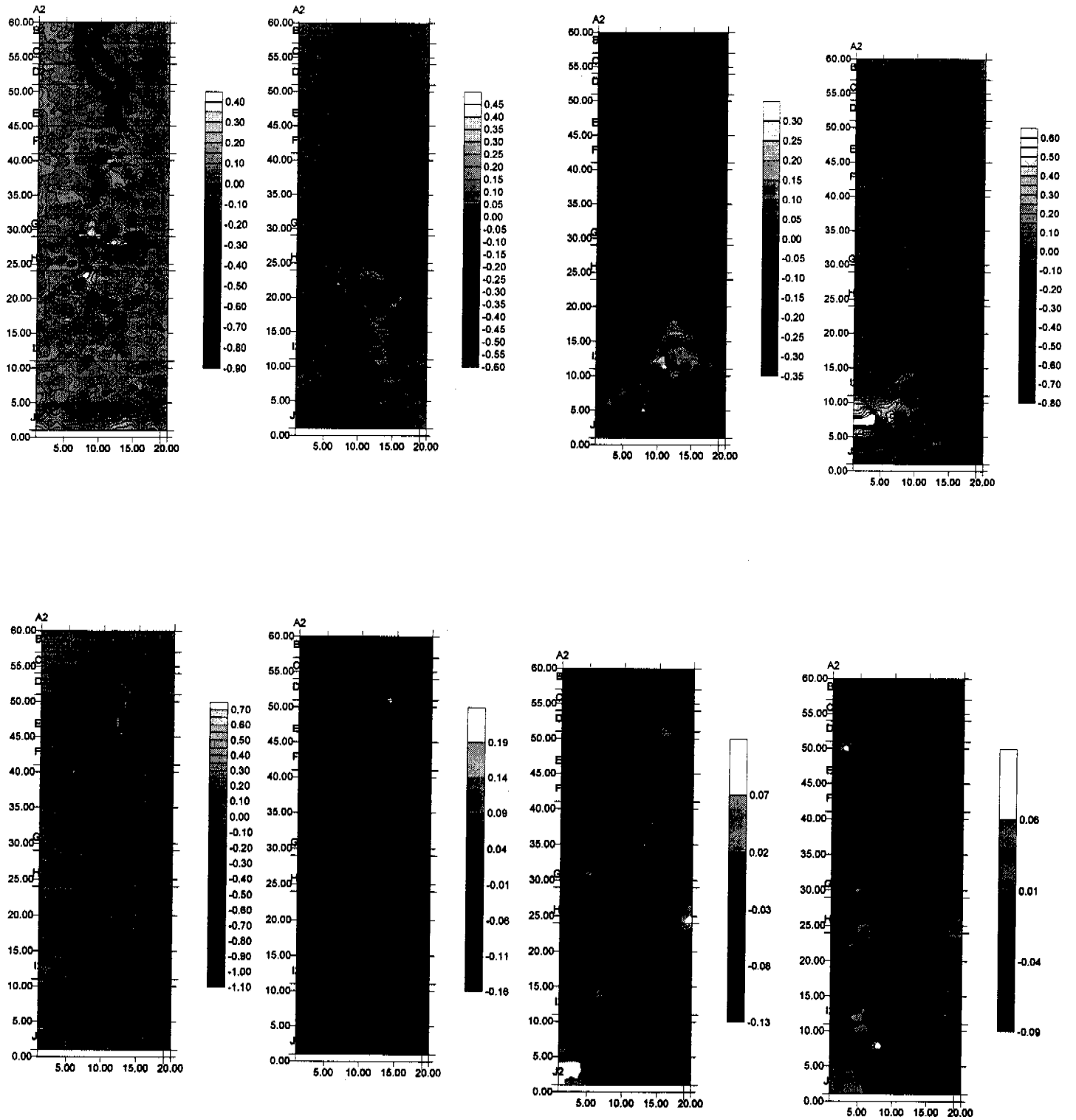

Figure 5.6.3: The morphology contour plots a) initial profile and 10 minutes, b) 10 minutes and 20 minutes, c) 20 minutes and 30 minutes, d) 30 minutes and 1 hour. The difference in elevations are also calculated from the remainder of the simulations with e) difference between 1 hours and 1.5 hours, f) 1.5 and 2 hours, g) 2 and 2.5 hours, and h) 2.5 and 3hours.

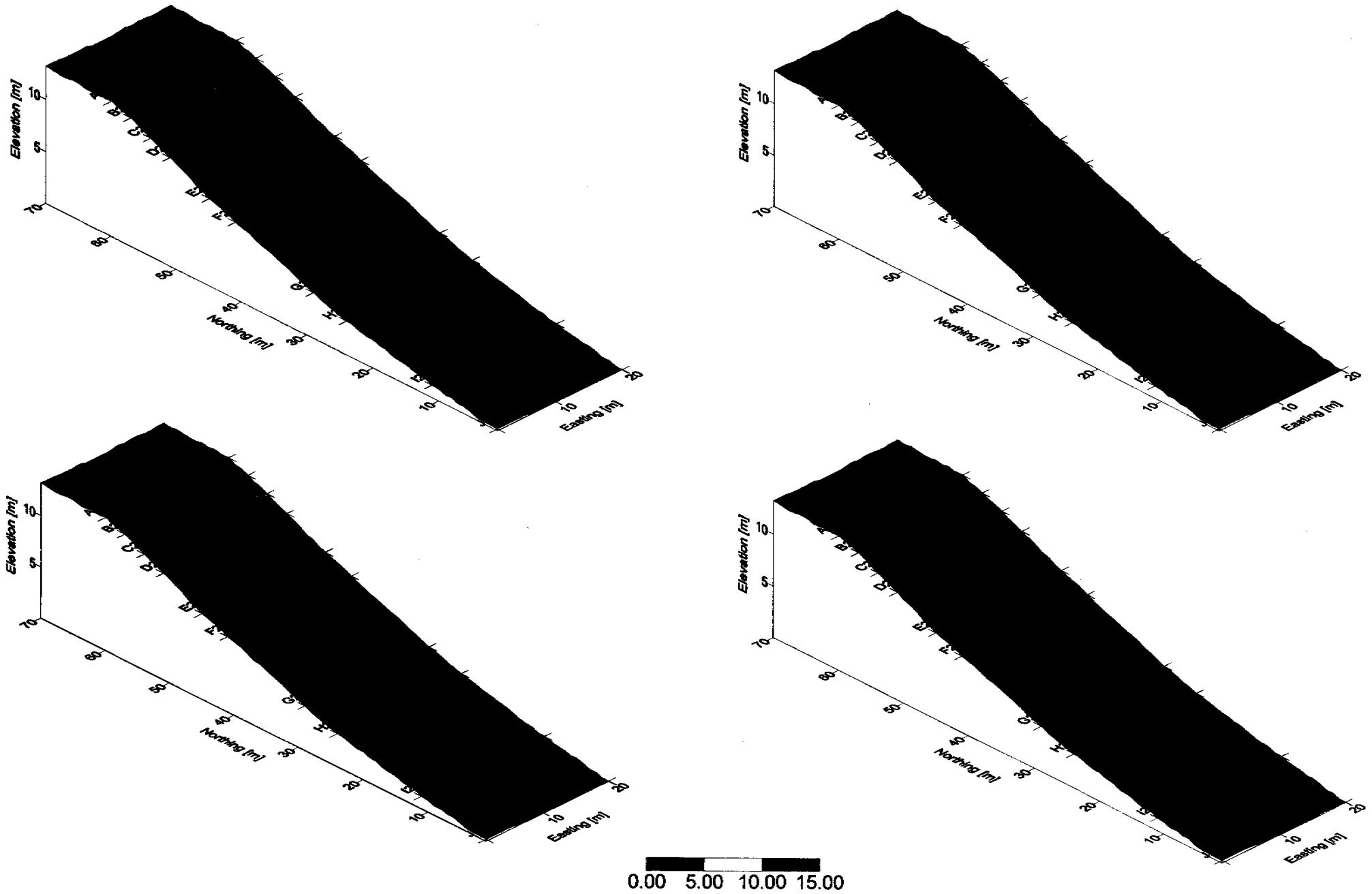

Figure 5.6.4: Simulations for extended batter slope profile with differential erodibility with depth, and randomised erodibility function, together with wide inlet point and n_1 slope exponent at 0.69 instead of 2.1, at a)10 minutes, b) 20 minutes, c) 30 minutes, and d) 1 hour.

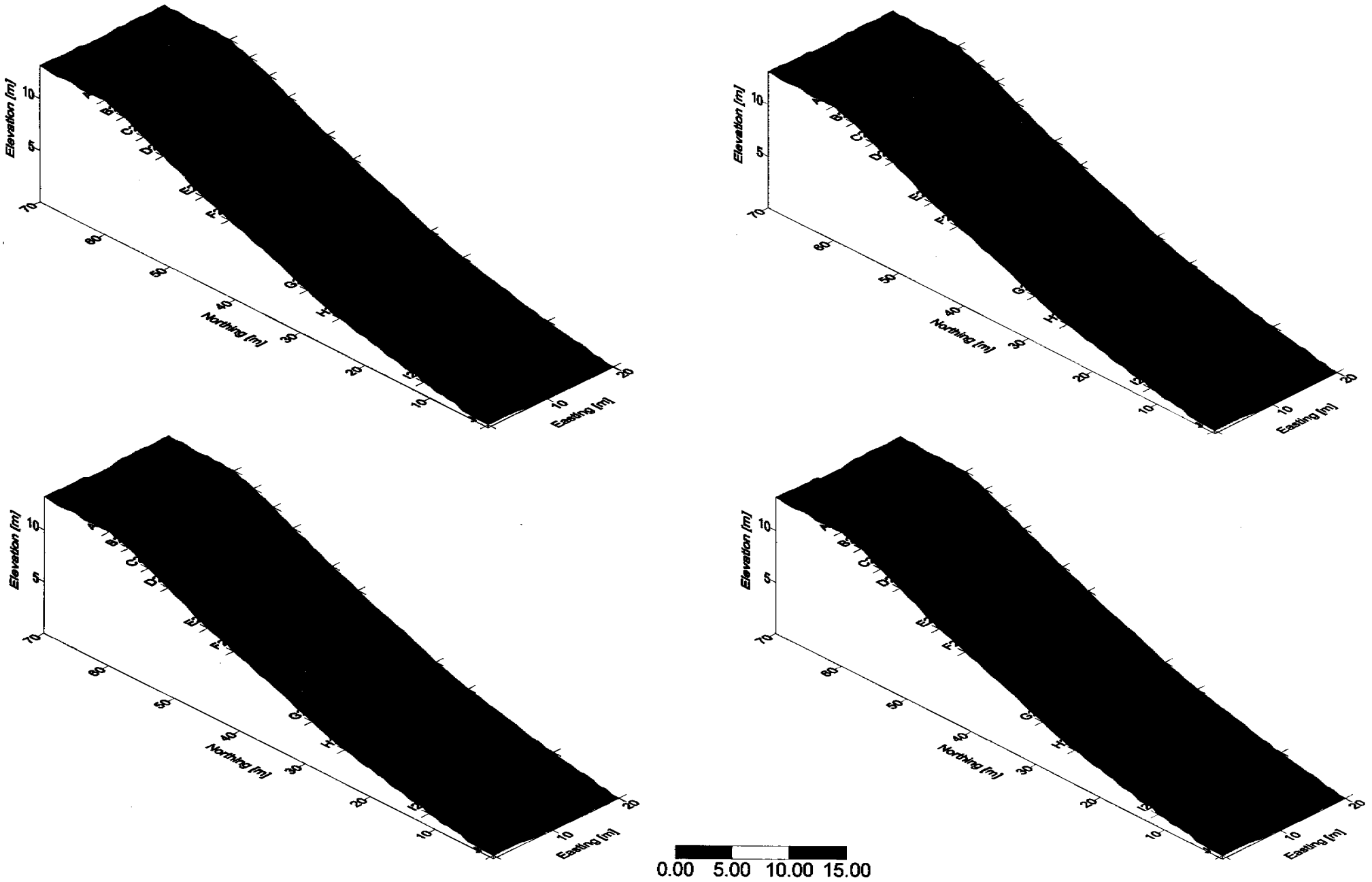

Figure 5.6.5: Simulations extended batter slope profile with differential erodibility with depth, and randomised erodibility function, together with wide inlet point and n_1 slope exponent at 0.69 instead of 2.1, at a)1.5 hours, b) 2 hours this represents the second storm event, and c) 2.5 hours and d) 3 hours representing the final storm event.

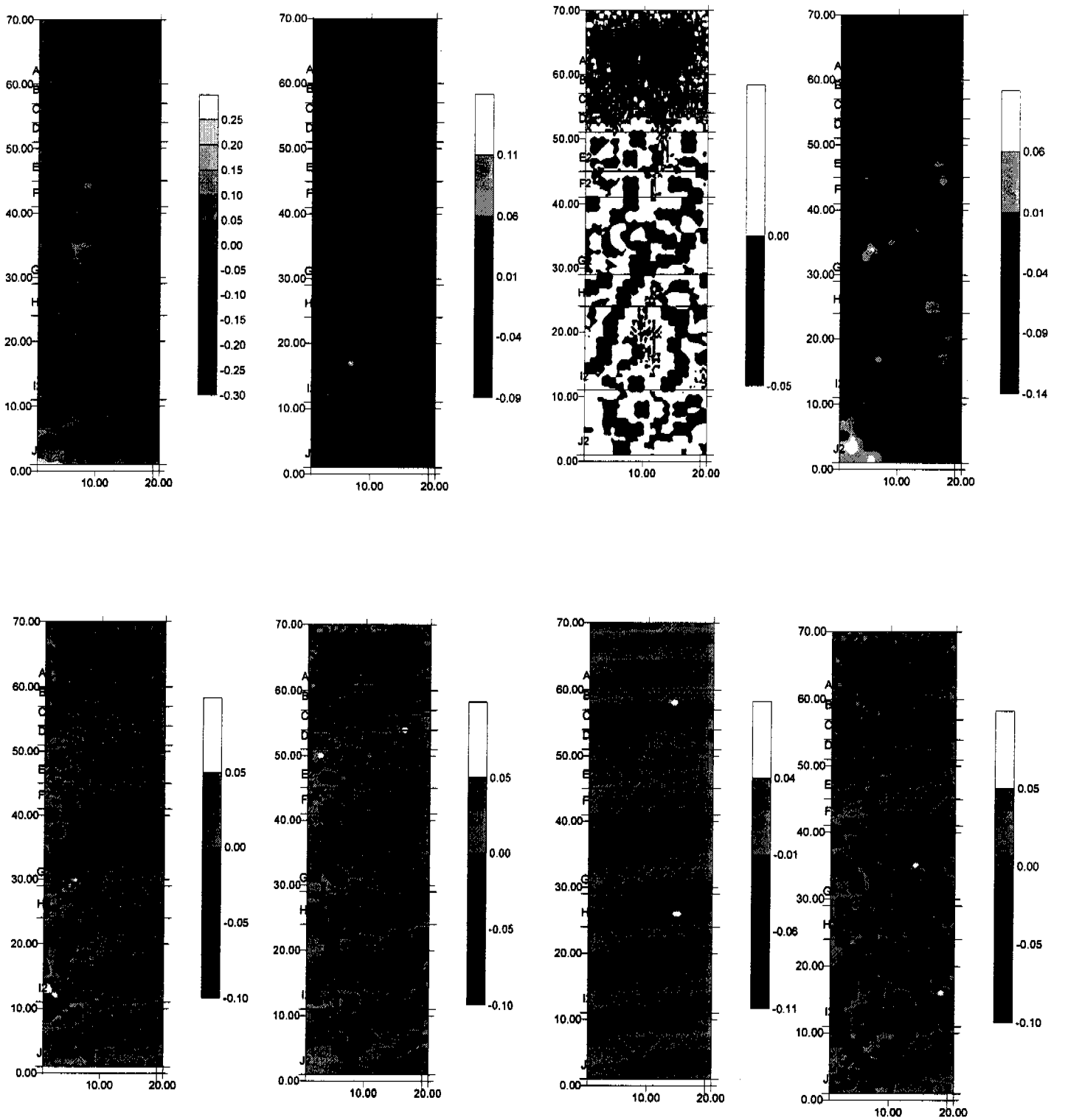

Figure 5.6.6: The morphology contour plots a) initial profile and 10 minutes, b) 10 minutes and 20 minutes, c) 20 minutes and 30 minutes, d) 30 minutes and 1 hour. The difference in elevations are also calculated from the remainder of the simulations with e) difference between 1 hours and 1.5 hours, f) 1.5 and 2 hours, g) 2 and 2.5 hours, and h) 2.5 and 3hours.